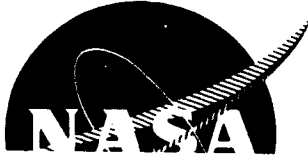NASA CR-54306

R-5947

PRICE $ _____

PRICE(S) $ _____

rd copy (HC) _5.00_

crofiche (MF) _1.00_

uly 65

N65-31951

(ESSION NUMBER)

_168_

(PAGES)

CR 54306

(NASA CR OR TMX OR AD NUMBER)

(THRU)

_1_

(CODE)

_14_

(CATEGORY)

FEASIBILITY STUDY OF RADIATION PYROMETER FOR NUCLEAR ROCKET APPLICATION (U)
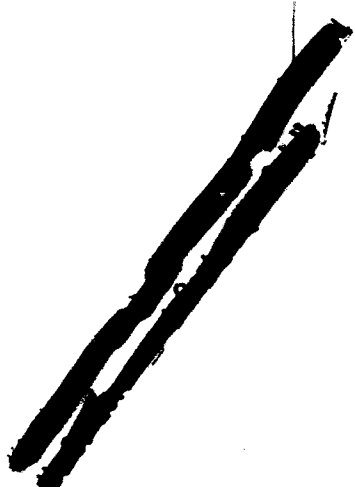
by

J. Perow, B.E. Harper, P.A. Kinzie

prepared for

NATIONAL AERONAUTICS AND SPACE ADMINISTRATION

CONTRACT NAS 3-5213

Declassified by authority of NASA
Classification Change Notices No. 25-1
Dated ** 7-21-65

DOWNGRADED TO UNCL, AUTHORITY:
ATOMIC ENERGY COMMISSION LETTER
DATED JUNE 29, 1965.
SIGNED MR. CHARLES F. KNESEL

ROCKETDYNE

A DIVISION OF NORTH AMERICAN AVIATION, INC.

NOTICE

This report was prepared as an account of Government sponsored
work. Neither the United States, nor the National Aeronautics
and Space Administration (NASA), nor any person acting on
behalf of NASA:

  A.) Makes any warranty or representation, expressed or
      implied, with respect to the accuracy, completeness,
      or usefulness of the information contained in this
      report, or that the use of any information, apparatus,
      method, or process disclosed in this report may not
      infringe privately owned rights; or

  B.) Assumes any liabilities with respect to the use of,
      or for damages resulting from the use of any infor-
      mation, apparatus, method or process disclosed in
      this report.

As used above, "person acting on behalf of NASA" includes
any employee or contractor of NASA, or employee of such con-
tractor, to the extent that such employee or contractor of NASA,
or employee of such contractor prepares, disseminates, or
provides access to, any information pursuant to his employment
or contract with NASA, or his employment with such contractor.

    Requests for copies of this report should be referred to

    National Aeronautics and Space Administration
    Office of Scientific and Technical Information
    Attention: AFSS-A
    Washington, D.C. 20546

FINAL REPORT

FEASIBILITY STUDY OF RADIATION PYROMETER FOR NUCLEAR ROCKET APPLICATION(U)

by

J. Perow, B. E. Harper
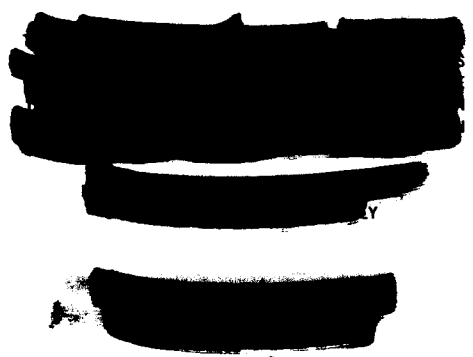P. A. Kinzie

prepared for

NATIONAL AERONAUTICS AND SPACE ADMINISTRATION

October 31, 1964

CONTRACT NAS 3-5213

Technical Management
NASA Lewis Research Center
Cleveland, Ohio
Advanced Development and Evaluation Division
John Reardon

ROCKETDYNE
A DIVISION OF NORTH AMERICAN AVIATION, INC.
6633 Canoga Avenue
Canoga Park, California

ABSTRACT

An analytical study was conducted to determine
the feasibility of developing a radiation pyrometer
to be used as a control instrument for measuring
the temperature of a nuclear rocket core material.
The system recommended for further experimental
study is a device employing a direct viewing
system and a dual foil thermocouple as a sensing
element. Irradiation of selected pyrometer
components is also recommended as a parallel
effort to provide radiation data relative to
the problem areas.

iii

CONTENTS

CONTENTS (CONTINUED)

CONTENTS (CONTINUED)

LIST OF FIGURES

LIST OF TABLES

SUMMARY

An analytical study was performed to determine the feasibility of developing a pyrometer device for continuous measurement of the temperature of a graphite material nuclear propulsion core. The primary use of this device would be for temperature control in a nuclear rocket engine system.

This study included the investigation of all components for sensing core temperature and the components necessary for transmitting the temperature signal to a control device. The primary emphasis was placed on the sensor concepts and the viewing method; the associated components (signal conditioning equipment) were studied briefly to determine availability and limitations of such equipment under the specified environmental conditions.

Three thermal sensor concepts were selected for detail analysis: namely, the foil thermocouple, the eddy current principle (inductance type), and the turbulent flow heat exchanger. The foil thermocouple was selected for this application. The basis for selection was sensitivity, adequate signal to noise ratio, well defined technology and experience in fabrication and testing. The eddy current detector required operation at cryogenic temperatures ($80^{\circ}R$ or less) to preserve the time constant. This resulted in a complex cooling system and fabrication problems. It was also the least sensitive of the three concepts considered. The heat exchanger sensor approached the foil thermocouple in sensitivity but was beyond the present state-of-the-art with respect to availability of conditioning equipment and experimental data.

With regard to the viewing system, there are basically three types: direct viewing with detector exposed to the source, transmission viewing (focus of energy onto detector by lens), and reflection viewing (focus of energy onto detector by mirrors). The direct viewing was the method selected. This selection was based on simplicity, on the energy deposition rate required to operate the detector in a high nuclear radiation environment and on the limitation of the maximum feasible aperture diameter (3/16 inch). (The feasibility of increasing the Rocketdyne nozzle aperture to one inch diameter has been established recently.) The reflection, optics is a more conservative approach to the viewing problem. It has the advantage of permitting simple nuclear shielding for the detector and therefore merits consideration for use in future nuclear rocket engines where the nuclear radiation levels are expected to increase.

Both electrical and pneumatic signal conditioning equipment were investigated. There is a wide choice of electrical equipment available but based on available irradiation data the operational limits of electronic equipment are estimated to be at least one order of magnitude below the integrated dose specified for the study. (Private communication, Z. P. Azary, Edgerton, Germeshausen & Grier, Inc.) Shadow shielding should be considered for reducing the nuclear radiation to an acceptable level; the shielding volume could probably be minimized by using "miniature" tube type conditioning equipment. Electrical cable and connectors have been designed for nuclear application and are recommended by manufacturers for application in the specified environment for short term operation (2 to 3 hours). There is apparently no limitation for pneumatic conditioning equipment in a

nuclear environment but there are problems of interstage coupling and inherent noise in both the transducer and the amplifier which may be limiting factors in design and which require further investigation if this type of system is considered for future application.

The final pyrometer system chosen for further experimental study and development is the electrical instrument employing the foil thermo-couple sensor and the direct viewing system. The problem areas associated with this pyrometer are as follows:

1. Behavior of the foil thermocouple in a nuclear environment.

2. Nature and extent of degradation of mirrors in a radiation environment if an optical funnel is employed in the direct viewing system.

3. Significant influence factors in the measuring system: emissivity of source and view factor.

4. Limitations and possible modification of signal conditioning equipment.

5. Purge system to eliminate chamber gas effect.

In connection with the precision requirements of the pyrometer instrument, the measuring system will not be capable of determining the temperature of the source to within $\pm 50^{\circ}R$ at the low temperature end (less than $2000^{\circ}R$). The limitation in this range is primarily system noise. The estimated measurement precision of the device, excluding conditioning equipment, will be about $\pm 50^{\circ}R$ over the temperature range from $2000^{\circ}R$ to $5000^{\circ}R$.

The emissivity of the specified core surface appears to be non-linear
and is a strong function of source temperature. If the degree of non-
linearity is known and is repeatable then it can be compensated for
in the conditioning equipment. The change in emissivity that may
occur during operation would have to be determined by calibration. A
constant emissivity over the temperature range of interest would of
course eliminate this problem area. (A constant emissivity of 0.85
was used for calculation purposes in this study.)

It should be noted that these estimates are based on the influence
factors considered and the assumptions made in the study. It is
recognized that an experimental study is required to determine the
precision of the pyrometer instrument.

It is recommended that a minimum pyrometer system be fabricated to
demonstrate "proof of principle" of the selected pyrometer system in
a non-nuclear environment. Concurrent with this experimental work
it is suggested that the problem areas be investigated by irradiating
the selected components of the system in the specified nuclear environ-
ment. This would provide the nuclear radiation data needed relative
to the problem areas.

The changes in emissivity and view factor under operating conditions
would require testing the minimum pyrometer system in a nuclear rocket
engine or under simulated conditions.

Upon successful completion of the proof of principle tests and the
irradiation tests, the minimum pyrometer instrument could be tested
in the specified nuclear environment.

INTRODUCTION

There is, at present, no proven and satisfactory method of measuring
the high temperatures encountered in the nuclear rocket core material
which will permit the effective and reliable control of reactor
power. The combined effects of temperature, ranging to $5000^{\circ}R$,
vibration and nuclear radiation create an environment that produces
a degradation effect in most materials and alters the operational
characteristics of control and instrumentation components.

It appeared that this problem could possibly be resolved by a radia-
tion temperature sensing device with compatible support equipment.
Knowledge of current radiation pyrometry technology suggested that a
moderate research and development effort should determine its feasibi-
lity of application to the nuclear rocket. Therefore a three month
analytical study was initiated to determine the feasibility of
developing a pyrometric device for measuring the temperature of a
niobium-carbide coated graphite core material within a reactor.

The task undertaken was to conduct an analytical feasibility study
leading to the development of a pyrometric method for measuring the
temperature of the reactor core material. The study included all
components of the instrument: Radiation sensor and components
necessary for transmitting the sensed information to a control device.
The major effort was devoted to demonstration of adequacy of the
principles involved through theoretical analysis. Two radiation
pyrometer concepts were studied in detail. These were the electrical
pyrometer (foil thermocouple) and the pneumatic pyrometer. The
electrical pyrometer concept is recommended for state-of-the-art
development as a reactor core temperature measuring technique.

Similar work on radiation temperature sensing devices for a nuclear environment has not been found in the open literature. Comments made on conventional radiation pyrometers for nuclear application give size, fragility, environment and inability of detector to view the source temperature as limiting factors.

The material presented herewith indicates that there are problem areas that require investigation before hardware development of the radiation pyrometer can proceed but these do not appear to be insurmountable and they could be investigated as part of the development program. The second phase of the program is intended to demonstrate "proof of principle."

This report summarizes the feasibility study of a radiation pyrometer for nuclear rocket application. The work is discussed in the following sections in the order listed: sensor concepts, sensor analysis, support equipment, optical system concepts, final pyrometer system, problem areas and recommendations.

Acknowledgement is due to G. D. Nutter and S. J. Wode of Atomics International, a Division of North American Aviation, Inc. for valuable help in the analysis and conceptual design of the viewing system.

FUNDAMENTAL CONSIDERATIONS

This study deals with the radiation sensor and support equipment necessary for transmitting the "sensed" information signal to the control device. The detail analysis however emphasizes transducer concepts and viewing methods; the support equipment (amplifiers and associated components) was studied briefly as to availability and limitations of standard components for this application.

The temperature measuring system should be capable of determining core temperatures ranging from $1000^{\circ}R$ to $5000^{\circ}R$ within $\pm 50^{\circ}R$ of the actual temperature. It should be capable of continuous operation over this temperature range for a minimum of 100 hours in a non-nuclear environment and withstand a gas pressure from 0 to 600 psia. The time response of the system should not exceed 0.1 second. The sensor performance should not be decreased by the following environmental conditions.

1. Vibration - 4 g's (RMS) from 10 to 2000 cycles per second
2. Above reactor shield
   a. Neutron flux 2×10^{12} N/cm^2-sec
   b. Gamma flux 5×10^{9} erg/gm (c)-Hr.
   c. Temperature $200^{\circ}R$ to $800^{\circ}R$

3. At the thrust chamber
   a. Neutron flux 5×10^{13} N/cm^2-sec.
   b. Gamma flux 3×10^{11} ergs/gm (c)-Hr.
   c. Temperature   up to $5000^{\circ}R$
   d. Pressure   0 to 600 psia

4. A total neutron dose of 10^{18} NVT will be experienced at the thrust chamber wall.

5. The interior wall temperature of the thrust chamber is approximately $2000°R$.

6. The wall of the thrust chamber is cooled with liquid hydrogen.

7. Thrust chamber gas stream:

   a. Temperature   up to $5000°R$

   b. Velocity   Approximately 800 ft/sec

   c. Pressure   600 psia

8. Noise of the order of 10^{-17} amp/$°R$/ft can exist in the area of the cabling between the sensor and top of core.

The design objectives or goals set for the feasibility study of the radiation temperature measurement instrument were:

Reliability

Performance

Feasibility of fabrication

Feasibility of installation

Availability of equipment

Minimum size and weight

The above objectives together with the customer specifications and required environmental conditions were used as a basis for selecting the pyrometer system for this application.

The nuclear rocket engine environmental conditions and relative location of the radiation pyrometer are shown schematically in figure 1.

NEUTRON FLUX –
2×10^{12} N/CM^2-SEC
GAMMA FLUX –
5×10^{9} ERGS/GM(C)-HR
TEMPERATURE 200°-800°R

SHIELD

CORE MATERIAL

RADIATION
PYROMETER
TRANSDUCER

NEUTRON FLUX –
5×10^{13} N/CM^2-SEC
GAMMA FLUX –
3×10^{11} ERGS/GM(C)-HR

THRUST CHAMBER TEMPERA-
TURE TO 5000°R
PRESSURE – 0 TO 600 PSIA
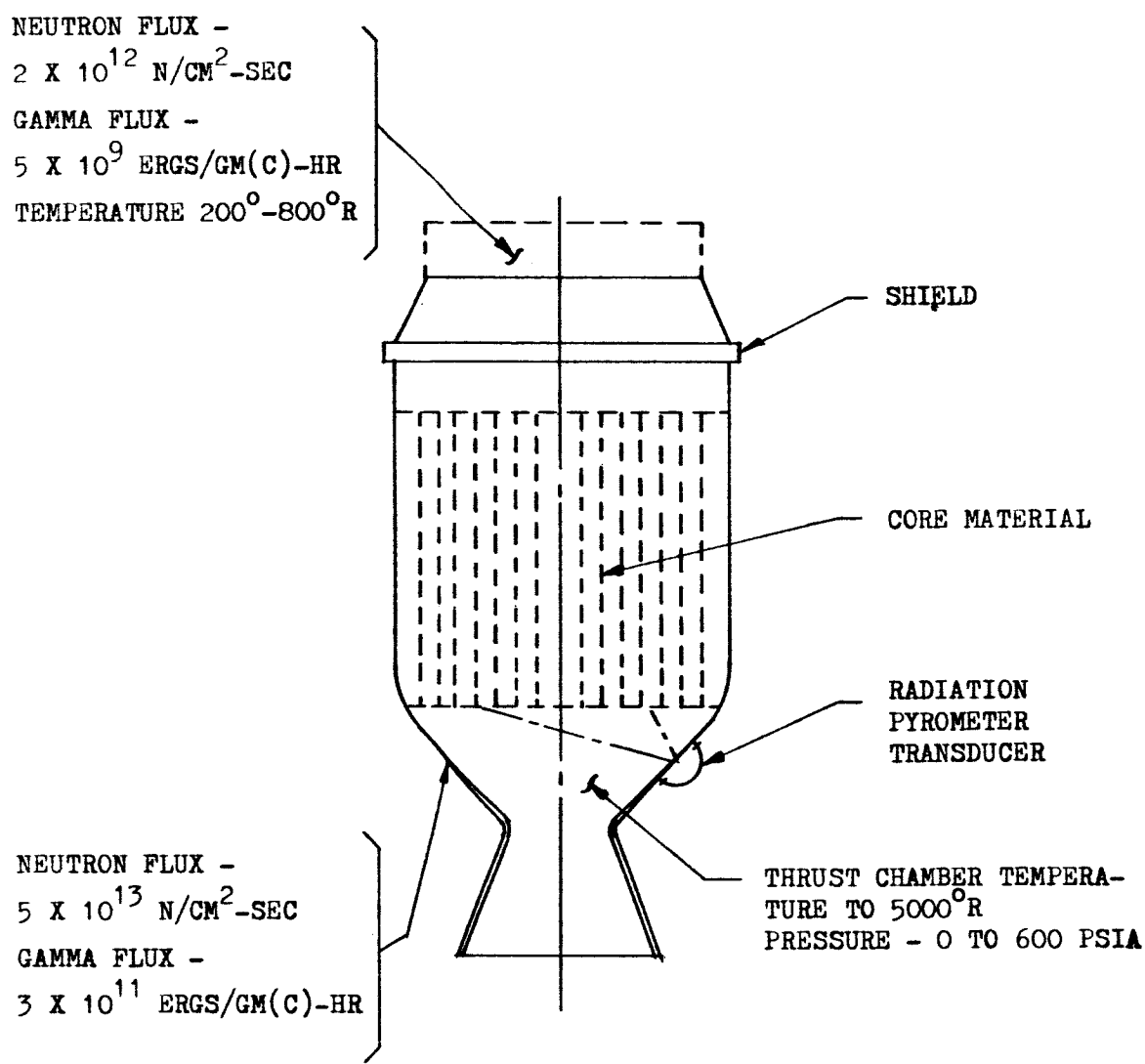
FIG. 1

NUCLEAR ROCKET ENGINE – ENVIRONMENTAL
CONDITIONS AND RELATIVE LOCATION OF
PYROMETER INSTRUMENT

9

SENSOR CONCEPTS

The techniques of sensing temperature are numerous and are limited only by temperature-dependent properties of materials. No attempt was made to categorize these techniques, only those which appeared applicable and which did not require an extensive research effort were considered. For the purpose of this study temperature sensors were classified into two general classes: thermal detectors and direct energy conversion detectors. The absorption of photon energy by a thermal detector results in a rise in detector temperature. The direct energy conversion detector on the other hand does not rely on diffusion of energy but the radiation absorbed by the detector changes the detector properties such as a change in electrical properties (resistance) or photo sensitive properties. These changes may or may not be accompanied by a temperature rise.

It should be noted that for the purpose of this study, a lensless system was considered because the experimental data available did not give reasonable assurance that lenses of any type would withstand satisfactorily the nuclear environment described in the section on fundamental considerations. (1, 2, 3, 4, 5)

In the absence of a spectrally selective filter, a total radiation sensor should be chosen such that, among other properties, its responsivity as a function of wavelength is as nearly relatively constant as possible. This property should be preserved during nuclear irradiation, even though it is not an absolute constant. The class of radiation detectors called "thermal" detectors is the only one which approximates this condition. It should be realized however, that the responsivity of thermal detectors is not

independent of wavelength as is popularly claimed in much of the
literature, but usually varies at least by several percent. This
variation is caused by the corresponding variation in the spectral
absorptance of the "black" coating on the detector. The relative
spectral distribution of black body radiation for two different
temperatures ($1260^{\circ}R$ and $4680^{\circ}R$) are shown in figure 3.

The thermal detectors considered for this application were:
1. Foil thermocouple
2. Eddy current (Inductance type)
3. Turbulent flow heat exchanger
4. Solid disc concept
5. Liquid metal expansion
6. Pyroelectric principle

FOIL THERMOCOUPLE

The foil radiometer described by Gardon (6) is a thermocouple device
that operates on a temperature increment which results from a pre-
ferential heat conduction path. A circular foil-type radiometer is
shown schematically in Figure 2.
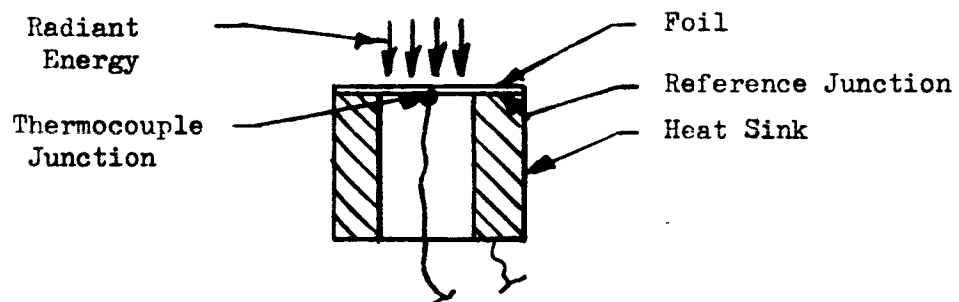
SCHEMATIC DIAGRAM, CIRCULAR FOIL THERMOCOUPLE
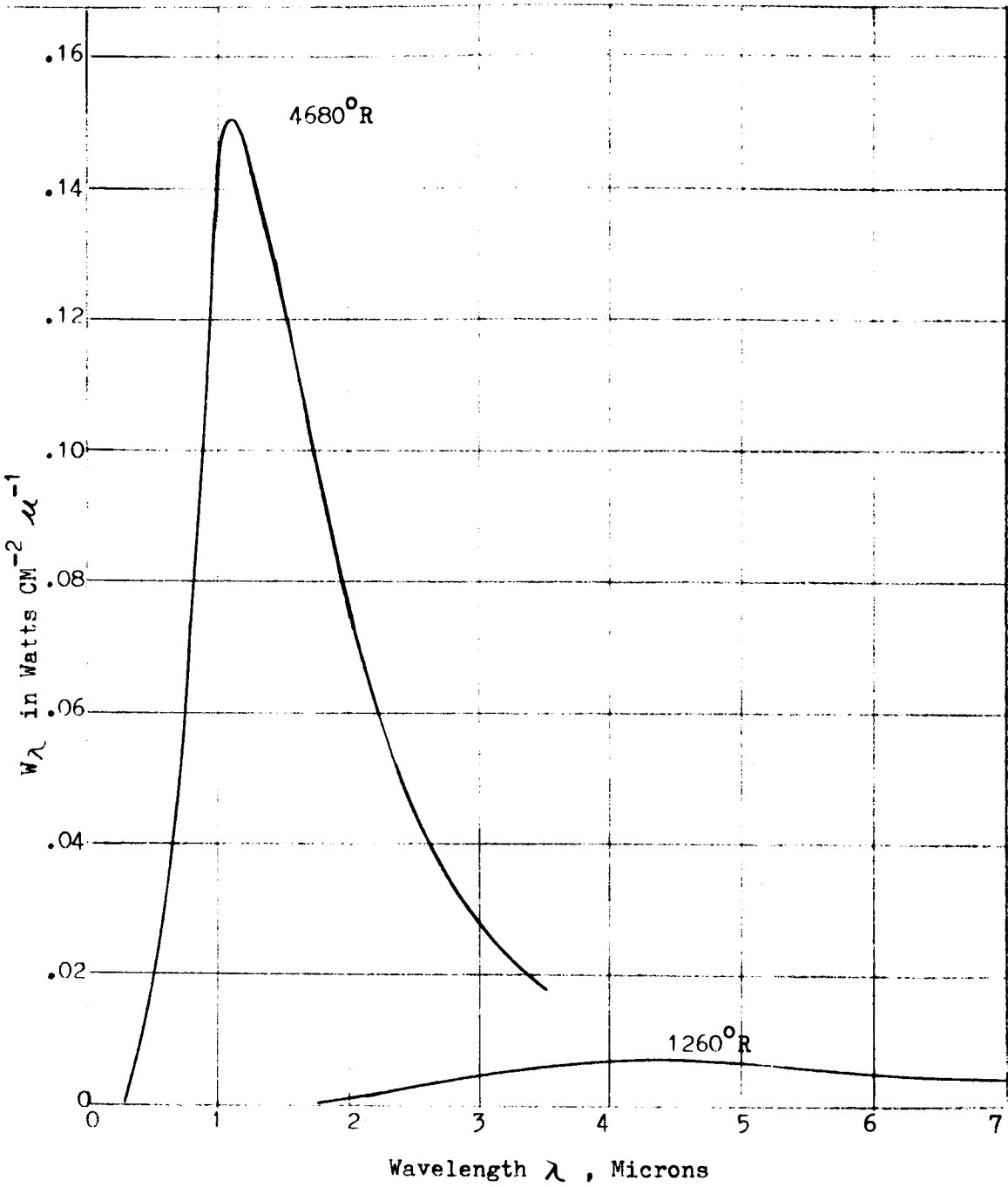
FIGURE 2

FIGURE 3. RELATIVE SPECTRAL DISTRIBUTION OF BLACK BODY
RADIATION (7)

The sensitivity of such a sensor depends on the dimensions and materials chosen, but generally can be increased only at the expense of increased time constant.

If the dominant losses are via conduction to a constant temperature heat sink, the sensor is relatively independent of temperature variations of its other surroundings and detects only the source energy supplied to the target. Response time is usually rapid due to the relatively low thermal resistance path from the target to the heat sink. The Gardon radiometer typifies this approach with its target disk, rimmed by the heat sink and a difference thermocouple circuit between the center of the target disk and the rim.

EDDY CURRENT (INDUCTANCE TYPE)

The operation of a simplified eddy current transducer is presented schematically in Figure 4.
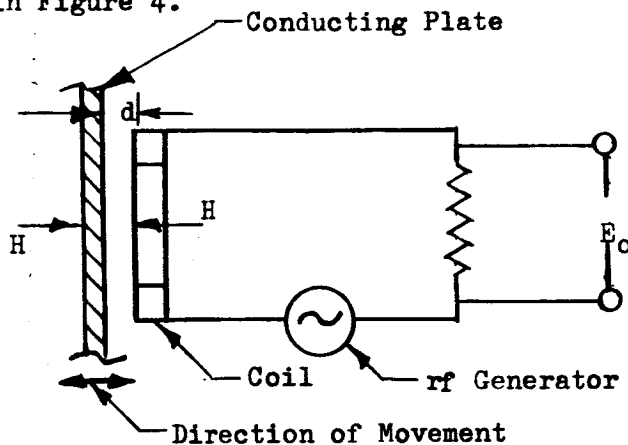
SCHEMATIC DIAGRAM, EDDY CURRENT DISPLACEMENT SENSOR

FIGURE 4

The coil is energized by an rf generator as shown which creates a magnetic field H and generates eddy currents in the conductive plate. The eddy currents cause a magnetic field H' in a direction which reduces the effective inductance of the coil. The net resultant force of the two fields causes a variation of the magnitude and phase of the current which appears as a change in voltage output.

The eddy currents generated in a conductive material are a function of the electrical properties of the metal, resistivity, permeability and the frequency. For an actual eddy current sensor the voltage output is a function of these characteristics as well as dimensional changes or movement of the conducting plate with respect to the coil. Based on actual test data (8), the effect due to dimensional change is several orders of magnitude greater than that due to the electrical characteristics of the conducting plate.

An analytical model of the eddy current sensor considered in this study is shown in figure 5 . It is comprised of a metal expansion cone, conductive plate, conduction controlled heat sink and associated cooling system, an eddy current coil and suitable a.c. conditioning equipment which is not shown. The base or fixed end of the cone is attached to the nozzle wall where it receives radiant energy from the core surface through a fixed aperture. The conducting plate is attached to the convergent or "free end" of the cone and the eddy current probe is set a given distance (on the order of 5 mils) from the conducting plate. When radiant energy is incident on the inside surface of the cone, the cone will expand and contract as a function of temperature, thus changing the "x" distance noted in figure 5 with respect to the eddy current coil. This distance
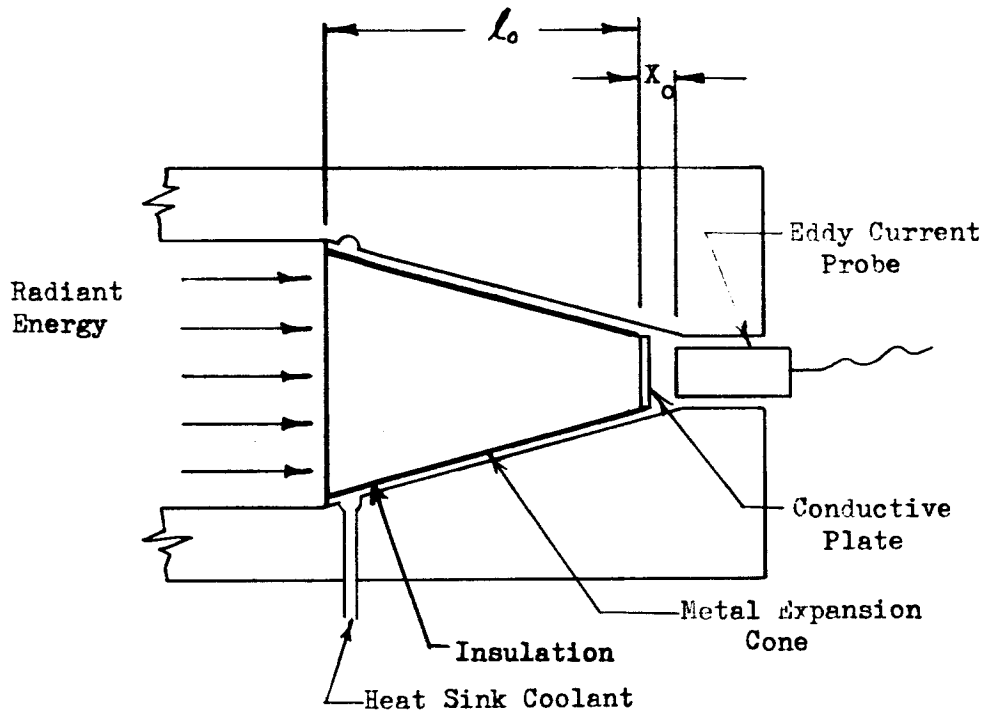
FIGURE 5

ANALYTICAL MODEL OF EDDY
CURRENT SENSOR

15

variation will produce a change in the circuit inductance which causes a voltage change in the output electrical circuit.

TURBULENT FLOW HEAT EXCHANGER

This sensor concept involves a turbulent flow process and is presented schematically in figure 6. A gas from a constant pressure supply is passed through a choked orifice at constant temperature. This assures a constant mass flow rate to the preheater and the thermal radiation-convection heat exchanger. The fluid is heated first in the preheater and then in the heat exchanger. It then flows through a second choked orifice and the output signal is taken off between the heat exchanger and the choked orifice. The output pressure signal is related to the temperature out of the radiation-convection heat exchanger by the expression

$$P_2 = (\dot{m}/Kc) \sqrt{T} \qquad \text{(refer to Appendix E)}$$

The gas is then either exhausted or returned to the secondary side of the heat exchanger depending upon the position of the preheater by-pass valve.

A preheater was chosen as a means of improving the sensitivity of the instrument at the low end of the temperature range. The fluid upon being heated in the radiation-convection heat exchanger flows through the second choked orifice and is then passed through the secondary side of a preheater which raises the temperature of the fluid going into the heat exchanger. This arrangement allows considerable increase in sensitivity at the low end of the range and with proper bypass flow to the preheater it also improves the linearity of the output signal pressure as a function of source temperature. Good sensitivity is already available at the high

---

* Symbols Defined in Appendix **A**
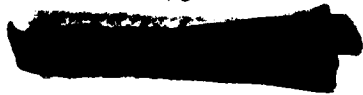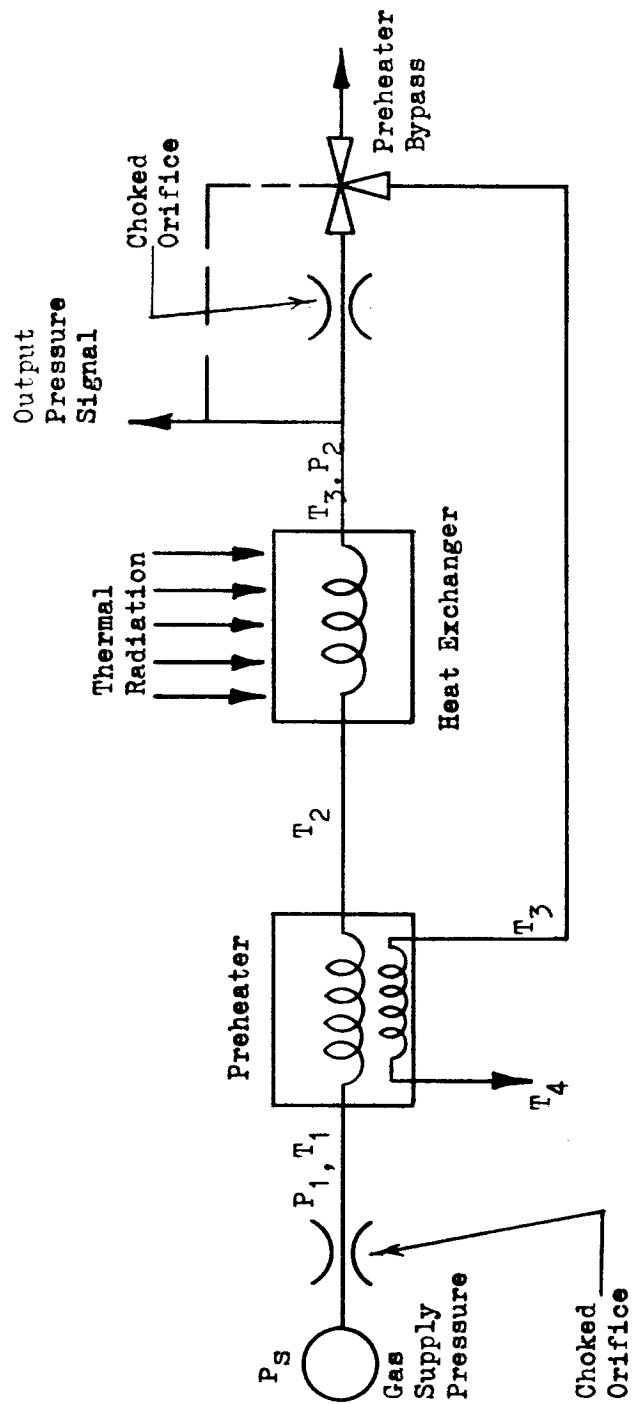
FIGURE 6

PNEUMATIC HEAT EXCHANGER SENSOR

end of the operating range therefore bypass flow is not required; by-pass flow at the intermediate operating points varies inversely as the differential output pressure. This device can be designed to operate with existing fluid amplifiers and to meet the specifications on vibration and nuclear radiation.

SOLID DISC CONCEPT

A problem in radiation pyrometry is that of eliminating emissivity errors between the core and detector. One approach is to have a heated element in thermal equilibrium with core temperature. A candidate for a sensor of this type could be a solid disk coated with the same cladding material as the core. Then the emissivity of both detector and core would be essentially the same.

An electrical sensor concept was considered where the sensor is a refractory metal disc coated with a material which has the same emissivity characteristics as the surface area of the source temperature.
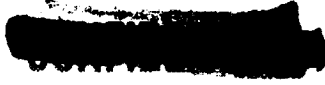
A block diagram representing such a system is shown in figure 7 below.
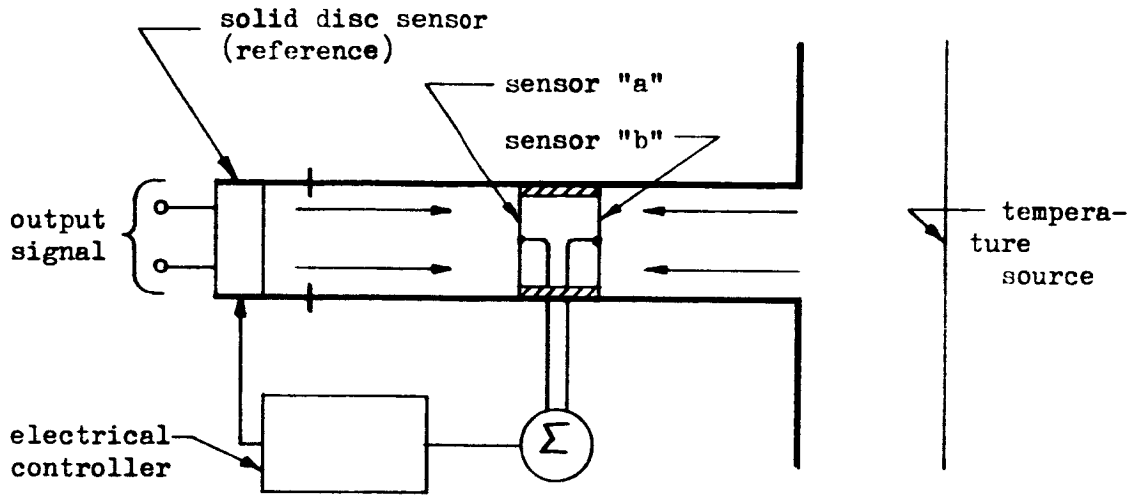
ΔE
FIGURE 7
SCHEMATIC DIAGRAM, SOLID DISC SENSOR CONCEPT

The two sensors ("a" and "b") are connected in a bridge configuration and receive radiant energy from the temperature source (core surface) and from an external electrical source (reference) respectively as indicated by the arrows in figure 7 . An electrical feedback network is provided as part of the instrument which controls the electrical energy to the reference. The viewing system and the area of the electrical source are designed such that when the output at the summing point is zero the radiant energy emitted from the external source is equal to that of the core surface and therefore the temperatures of both emitters are equal because their emissivities are chosen identical. The temperature of the refractory metal disc can be measured either by means of another radiation device or a direct contact sensor (thermocouple). The two sensors

a & b could be foil thermocouples.

The defining equations for this system are as follows:

$$q_{source} = F_S A_S \epsilon_S \sigma T_S^4$$

where subscript "S" refers to temperature source

$$q_{Reference} = F_R A_R \epsilon_R \sigma T_R^4$$

where subscript "R" refers to temperature reference or (solid disc sensor)

$$q_{Source} = q_{Reference} \text{ when net output} = 0$$

$$\therefore F_S A_S \epsilon_S \sigma T_S^4 = F_R A_R \epsilon_R \sigma T_R^4$$

and since by design

$$F_S A_S = F_R A_R$$

then

$$T_{Source} = T_{Reference}$$

Hence the reference body is at the same temperature as the source body. And in measuring the temperature of the back side of the reference body it can be made to appear as a black body if a radiant measurement is made. The foregoing approach thus eliminates the possibility of unknown emissivity detracting from the accuracy of radiant temperature measurement.

LIQUID METAL EXPANSION

The expansion of a confined liquid metal in a conduit can be used to
detect a temperature change. As the liquid metal is heated, its
expansion can actuate a pressure transducer or a bourdon-type move-
ment can move a flapper valve which allows flow into a fluid ampli-
fier circuit. The conduit containing the liquid metal, (the
detector) can be arranged at the end of a collimating tube to
receive directly the radiant energy of the core. The time constant
of the detector can be minimized by using multiple parallel conduits
of small diameter, and a suitable heat rejection scheme. The out-
put can be an electrical signal if a pressure transducer is used or
a pneumatic one if fluid amplifiers are used. The range of detector
temperature depends primarily upon the conduit strength at given
temperatures and the liquid metal temperature expansion relationship.

PYROELECTRIC CRYSTAL

A pyroelectric crystal gives an output current for a rate of change
of crystal temperature (9). The pyroelectric material undergoes an
electrical polarization change when heat is absorbed in the material.
When a pyroelectric ceramic is connected in a current measuring
circuit the current generated is proportional to the rate of change
of charge generated.

After a preliminary analysis three of the thermal detectors; namely,
the pyroelectric device, the solid disc expansion principle, and
the liquid metal expansion principle were eliminated from further
consideration due primarily to one or more of the following factors

or conditions:

1. Excessive radiation heating due to size
2. Heat rejection problems
3. Time response
4. Responds to transients only (pyroelectric sensor)

The pyroelectric detector would follow the core temperature change without a time lag but because the crystal output is zero for a non-changing core temperature, it would present a problem when used in a closed loop in that some other device would have to be used to sense steady state error. The pyroelectric crystal would provide a good feedback signal during the transient but could not be used to indicate the core temperature without integration. Since integrating or differentiating features are not permitted as part of the conditioning equipment, the pyroelectric transducer does not qualify as a detector.

The solid disc expansion principle (all-electrical) was investigated. This device would require a supplemental heat source to heat the disc to the same temperature as the reactor core surface.

Heating a metal disc with coating similar to that of the core to the same temperature as the source will eliminate emissivity errors; however, this approach introduces other problems which are associated with high temperature operation. It becomes difficult to control heat dissipation from the disc, it requires subjecting the disc to high temperatures thus creating problems that affect material stability, processing and fabrication. A sensor required for monitoring the temperature of the disc would have similar materials problems.

Finally the liquid metal sensor was not applicable because of the poor time response due to the extra mass as compared to the heat exchanger probe.

Upon completion of the preliminary analysis it became evident that three sensor concepts were likely candidates for this application: the foil thermocouple, the eddy current sensor and the turbulent flow heat exchanger. Analytical work was continued on these three concepts to determine feasibility of application in the nuclear rocket.

SENSOR ANALYSIS

This section deals with the detail analytical study of the three sensors concepts (foil thermocouple, eddy current, and turbulent flow heat exchanger) and related support equipment characteristics over the range from $1000^{\circ}R$ to $5000^{\circ}R$. In each case a simple model was developed to represent the sensor. These are presented in figures 5 , 8 , and 9 for the three sensors. The models are not an exact representation but are used as lumped parameter analogs. This approach provides a good analytical estimate of performance and will permit the selection of the best general design; it can also be used as a guide for the design of a practical system. The basic equations and derivations used in this analysis are presented in the appendix under appropriate headings; the symbols or nomenclature are also given in the appendix.

The specific items covered in this section are

    1. Time response

    2. Random noise and gamma heating

    3. Sensitivity

    4. Typical design parameters

TIME CONSTANT

The time response of the pyrometer system specified in the work statement has been interpreted as referring to the system time constant. For each transducer considered it is a pre-determined value which is a function of materials, model geometry and the viewing system.

Target at Temp. T_t" Exposed to
Nuclear Radiation Only

Target at Temp. T_t Exposed to
Combined Heating

Radiat
Energy

Heat Sink
Reference
Temp. T_r

$T_t - T_t$"

Thermal Path $\delta\ell$ with
Conductivity K

A_t Target Area

A Thermal Path
Cross Section Area

y

$\delta\ell$

Detail of Target

FIGURE 8

ANALYTICAL MODEL OF FOIL
THERMOCOUPLE

25
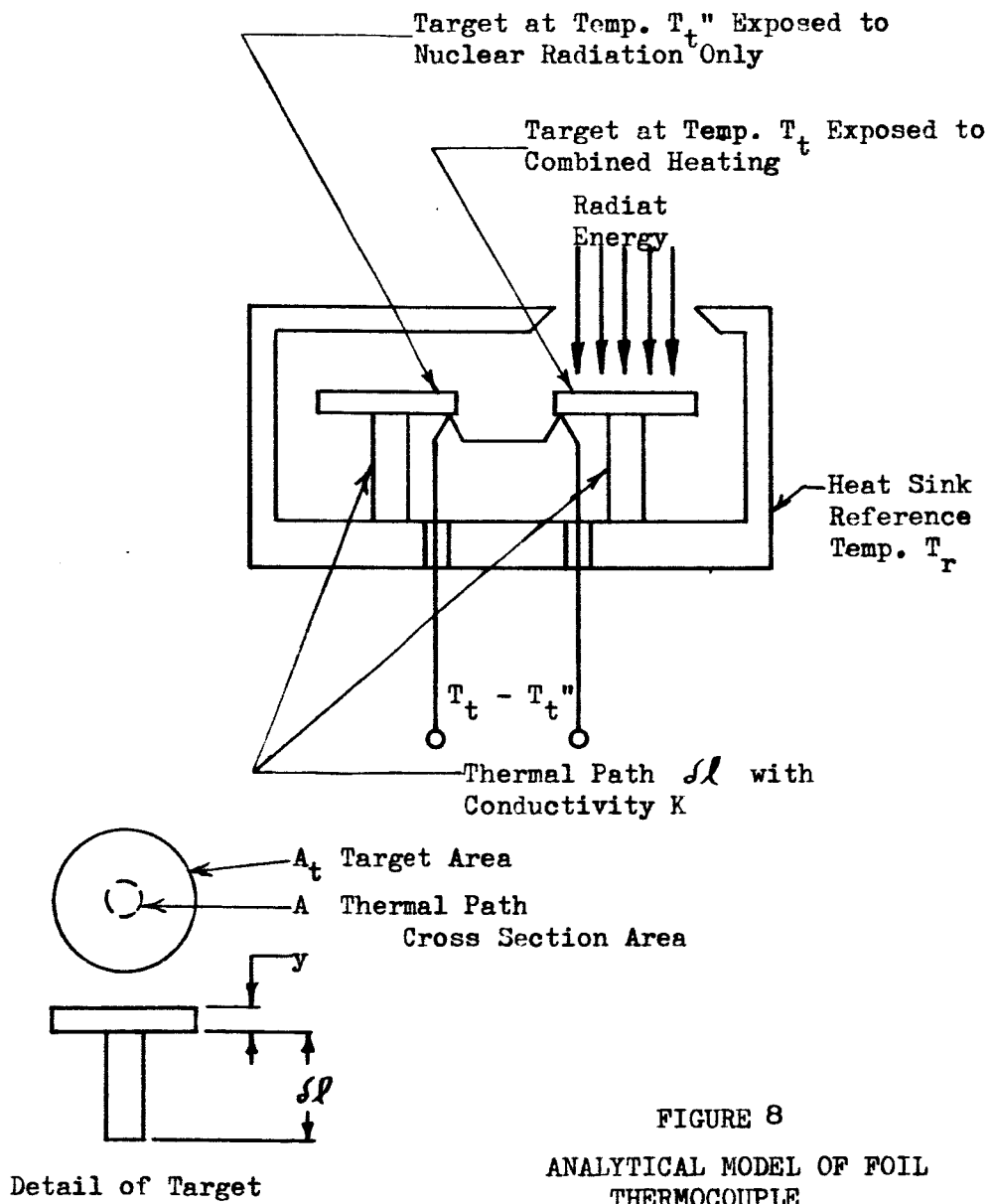
NOMINAL VALUES for H_2 GAS

P_s = 106 psia
T_s = 60°R
P_1 = 47 psia
T_1 = 70°R
$T_3 - T_2 = \Delta T_m = 50°R$
P_2 = 32 to 42 psia

P_s, T_s

Gas Supply Pressure

Choked Orifice

P_1, T_1

Preheater

T_4

T_3

T_2

Thermal Radiation

Heat Exchanger

T_3, P_2

$\dot{m} = \dfrac{1}{\Delta P_2}$

Output Pressure Signal

Choked Orifice

Choked Orifice

Preheater Bypass
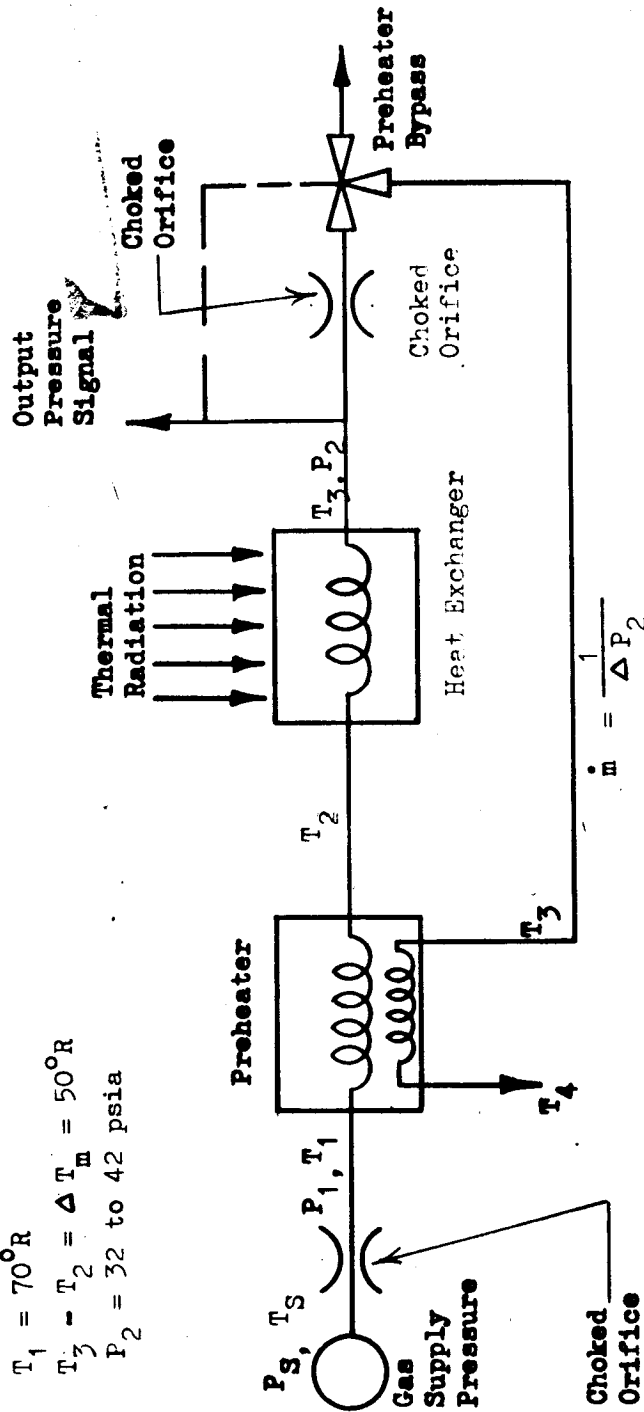
FIGURE 9

ANALYTICAL MODEL PNEUMATIC HEAT EXCHANGER SENSOR
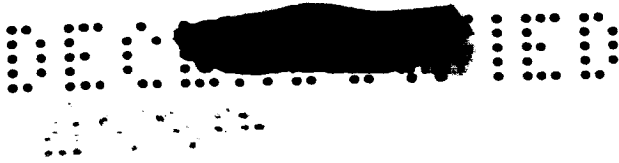
Time response was investigated for all three transducers over a wide band of reference temperatures, ranging from 70°R to 500°R. The calculations were based on absorbed heat flow by the sensor of the order of 10^{-2} BTU/SEC (Appendix B). For the eddy current configuration selected it required operating the reference or heat sink temperature at a cryogenic value in order to preserve the time constant, although the reference temperature could be increased if the cone thickness were reduced to less than 3 mils. The time response for this sensor is given by the expression $\tau = \dfrac{m c_{\rho}}{k A / \tau_{\mu}}$ (Appendix D); therefore, its value can be fixed by trade-offs among these variables: mass, specific heat, conductivity, detector area, and insulation thickness. (10,11)

The time constant of the foil thermocouple is dependent essentially on conducting heat path length and the foil diameter and thickness. Calculations indicate that the 0.1 inch diameter foil and .001 inch thickness will meet the time constant requirement with a reference temperature of 500°R; with the same foil thickness it is possible to increase the diameter of the foil to 0.3 inches by reducing the reference temperature to 80°R. (10,12) Although the larger sensing element requires a cryogenic reference temperature it is most compatible with the reflection optics viewing system because the radiant energy entering the optical system can be focused onto a minimum diameter of 0.5 inch using a single mirror. (Refer to "Basic Consideration for Viewing System.") The smaller sensing element (0.1 inch diameter) on the other hand has a more desirable reference temperature (500°R) but the total radiant energy must be concentrated on a smaller surface area by an additional high reflectance optical cone or funnel (refer to figure 11). This aspect is discussed further in connection with the final pyrometer system.

The pneumatic probe will meet the time response requirements operating over the temperature range from $70^{\circ}R$ to at least room temperature. At the lower temperature limit the time response is approximately 0.019 seconds and is less than 0.100 seconds at the high temperature end. However, the cryogenic reference point will result in a larger ΔP range. (10, 12)

RANDOM NOISE AND GAMMA HEATING

Random Noise

Sensor - Since the random noise estimates are difficult to calculate, an effort was made to obtain experimental data in lieu of analysis. For the foil thermocouple Rocketdyne experience indicates values of 200:1 for the signal to noise ratio.

For the eddy current detector, an estimate of 200:1 was obtained from a local vendor for a typical commercial unit (private communication, D. E. Bently, Bently Nevada Corp.)

An estimate of the signal to noise ratio was made for the pneumatic sensor by assuming that the noise would be generated at the detector pressure pickup point of the detector and transmitted to the first fluid amplifier stage. For this condition the Rocketdyne pneumatics experience indicated that a signal to noise ratio of 100 to 150:1 seemed reasonable.

From the foregoing data, it is recognized that the signal to noise ratio is below the operating range (625:1); however, the information bandwidth required is narrow and the noise (frequency) noted in

nuclear rocket testing is above 400 cps. It should therefore be
possible to improve the signal range by as much as an order of
magnitude by restricting the bandwidth and by filtering out the
high frequencies. Noise should not be a problem when operating in
temperature range of interest for control purposes, 2000°R to
5000°R.

Support Equipment – The noise factor of support equipment as it
relates to the sensors has also been considered. There is a
potential problem with the foil thermocouple if its amplification
equipment is located above the reactor shield, about eight feet
from the point of measurement. There has been evidence of a-c pick-
up occurring in signal transmission lines from direct radiation during
full power runs of the KIWI Reactor experiments but the pickup was
not sufficiently large to require correction in this case. It
consisted of a distribution of discrete frequencies occurring in the
range from 400 cycles to 18 KC. (Private communication, B. J. Brett-
ler, Edgerton, Germeshausen & Grier, Inc.) This is considerably
above the range of interest but it does point out an area that should
be considered.

The eddy current system, which has a higher output voltage range
of the order of 500 millivolts, should be significantly less
sensitive to signal transmission error.

Noise limitations, and impedance matching for the pneumatic probe
have been partially answered by the suppliers of this type of equip-

ment. According to the component suppliers, the predominant part of the noise spectrum is at 6000 cps and is generated in the control line, amplifier cavity and exhaust ports. There is no significant contribution from the input lines. A low frequency noise on the order of a few cycles per second could also exist due to impedance mismatch in the interstage coupling. This noise results from inter-stage capacitance and inductance effects. (Private communication, Bob Bellman, Fluid Amplifier Dept., Corning Glass Works). A precise noise spectrum is not available at this time but it can be determined experimentally for a particular sensor design.

The estimated signal to noise ratio specified for fluid amplifiers was 200:1. However it is believed that the high frequency noise, (6000 cps) can be filtered out to yield a signal to noise ratio of several hundred to one. The same possibility exists for the pneumatic radiation detector also and should be an area for investigation in future pneumatic sensor studies.

Gamma Heating

The energy produced by gamma radiation in each of the three detectors was calculated and compared with the thermal radiation heating. These data are summarized in Table 1. (Refer to Appendix C for gamma heating calculations)

The values for attenuated gamma heating in the table were obtained by considering a typical high energy distribution of gamma radiation as being attenuated by a lead shadow shield. This shield will reduce line of sight gamma-radiation from the reactor face to the detector. The

TABLE 1 — GAMMA HEATING EFFECTS[a] (Single Sensor)

SENSOR	GAMMA HEATING	THERMAL/GAMMA HEATING 5000°R	THERMAL/GAMMA HEATING 1000°R
(Gamma Heating Attenuated by Two Inches of Lead Shielding, Attenuation Factor = 76)			
Foil Thermocouple	$.1978 \times 10^{-6}$ BTU/SEC	16,600	320
Eddy Current	3.83×10^{-6} BTU/SEC	2,610	50
Pneumatic Probe	$.0337 \times 10^{-6}$ BTU/SEC	2,970	57
(Gamma Heating, Without Attenuation)			
Foil Thermocouple	15.01×10^{-6} BTU/SEC	218	4.21
Eddy Current	292×10^{-6} BTU/SEC	34.5	.658
Pneumatic Probe	2.56×10^{-6} BTU/SEC	39.1	.75

[a]Based on Unshielded Gamma Heating Rate of 1 BTU/lb/Sec

attenuation was calculated by ratioing the gamma flux at $X = 0$ and $X = \ell$ where X is the distance into the material. Using the expression for gamma flux level (13) (14)

$$\phi = \frac{B \, S_A}{2} \, E_1(b)$$

where

S_A = source strength $(cm^{-2} - sec^{-1})$

B = buildup factor

b = $\mu_1 \ell$

μ_1 = attenuation coefficient

ℓ = distance into material

$E_1(b)$= exponential integral

The approximate configuration of the gamma shield required is shown in the pyrometer design, figure 20 .

It should be noted that heating by gamma irradiation is also expected to be significant in the temperature transducer (sensor and optical components). Such heating introduces error into the measurement when the thermal radiation originating in the component and incident on the transducer is a significant fraction of that received from the source. It is therefore necessary that all components, unless other- wise specified, be maintained at temperatures below $300^{\circ}R$ for satis- factory sensing of temperature down to $2000^{\circ}R$. In comparing random noise and gamma heating effects, Table 1, for the three transducers, it is seen that noise is the limiting factor for the foil thermo- couple while gamma heating is limiting for the eddy current and the pneumatic detectors. The gamma signal can be nulled out by using two detectors in opposition, one of which sees gamma plus thermal

energy and the other sees gamma only (refer to figure 8). If the use of a single sensor were feasible then an alternate approach would be to provide gamma shielding for the detector. Random noise is an inherent characteristic of the detector but it can be held to a minimum value through careful design. Although the signal to noise ratio is low at the low end of the temperature range (1000°R), the temperature range of interest for control purposes is above 2000°R, thus from this standpoint, all three transducers are acceptable.

SENSITIVITY

For the three detectors, sensitivity is defined in terms of output voltage or pressure and power input to the detector

$$* S = \frac{\Delta E/E}{\Delta \dot{q}/\dot{q}} \quad \text{or} \quad \frac{\Delta P/P}{\Delta \dot{q}/\dot{q}}$$

The expression for the sensitivity of each sensor is derived in the Appendices. The equations used for calculating the sensitivity are as follows:

Foil Thermocouple

$$\frac{\Delta E/E}{\Delta \dot{q}/\dot{q}} = \frac{\dot{q}/\dot{q}_m}{T_r/\Delta T_m + \dot{q}/\dot{q}_m} \qquad \text{(refer to Appendix C)}$$

*Variables defined in Appendix A
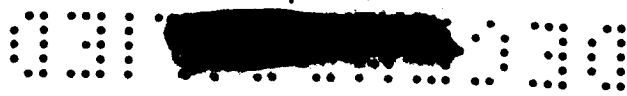
Eddy Current

$$\frac{\Delta E/E}{\Delta q/q} = \frac{q/q_m}{\dfrac{x_0}{\ell_0 \alpha \Delta T_m} + q/q_m} \qquad \text{(refer to Appendix D)}$$

Pneumatic Transducer

$$\frac{\Delta P/P}{\Delta q/q} = \frac{1}{2} \cdot \frac{q/q_m}{T_r/\Delta T_m + q/q_m} \qquad \text{(refer to Appendix E)}$$

If a preheater is added to the heat exchanger for increased pressure gain then the expression becomes

$$\frac{\Delta P/P}{\Delta q/q} = \frac{1}{2} \frac{q/q_m}{\dfrac{T_r(1-\eta)}{\Delta T_m} + q/q_m} \qquad \text{(refer to Appendix E)}$$

where η is the effectiveness of the preheater.

It should be noted from the foregoing equations that source temperature could have been used instead of energy input. The relationship between these two quantities differs by a factor of 4 if radiant energy varies as the fourth power of temperature.

$$\frac{dq}{q} = \frac{d\left(\sigma \overline{\epsilon F A} \, T_s^4\right)}{\sigma \overline{\epsilon F A} \, T_s^4} = \frac{4 T_s^3 \, dT_s}{T_s^4} = 4 \frac{dT_s}{T_s}$$
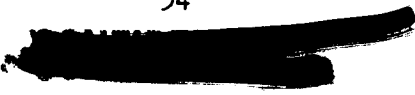
Therefore if $\left(\Delta E/E \Big/ \Delta T_s \Big/ T_s \right)$ is desired, the preceding sensitivity expressions can be presented in terms of source temperature.

Table 2 shows the detector design parameters used in this analysis; Table 3 is a comparison of the detector sensitivites. This comparison indicates that the foil thermocouple is the most sensitive device although its full scale output is about 6.6 millivolts whereas the eddy current output is 10 volts with a voltage swing of 500 millivolts. The large difference in voltage output and sensitivity for these two devices can be explained by considering the basic phenomena. Both detectors are total radiation (spectrally integrated illuminations) energy absorbing devices with conduction controlled heat rejection to a heat sink. Thus it would be expected that the detector temperature change for a given source temperature change would be the same for both devices. Target sensitivity per degree of source temperature change is plotted in figure 10 and is found to be the same for both devices. However the dimensionless sensitivities shown are different because the temperature change in the foil thermocouple produces a thermoelectric effect while in the eddy current sensor the temperature rise results in thermal expansion plus an eddy current effect which produces an output voltage. In each case there is a different gain factor involved. For the foil thermocouple it is the dimensionless term $\left(T_r / \Delta T_m \right)$ and in the eddy current the corresponding term is $\left(X_o / \ell_o \propto \Delta T_m \right)$. This argument is also valid for the pneumatic probe.

TABLE 2

DETECTOR DESIGN PARAMETERS

Item	Foil Thermocouple Figure 8	Eddy Current Figure 5	Pneumatic Figure 9
Reference temp. °R	500	100	70
Differential temp. °R	752	50	50
Foil dia. (in.)	0.1		
Foil thickness (in)	0.001		
Tab length (in)	0.010		
Tab width (in)	0.026		
Displacement (in)		.005	
Coeff. of thermal expansion °R		$.05 \times 10^{-5}$	
Length of cone (in)		1.0	
Cone diameter (in)		1.0	
Heat exchanger length (in)			8.0
Heat exchange O.D.(in)			.035
Preheater length (in)			16.0
Preheater O.D. (in)			.035

TABLE 3

DETECTOR SENSITIVITY

q/q_m	Foil Thermocouple (Fig. 8)	Eddy Current (Fig. 5)	Pneumatic (Fig. 9)
0	0	0	0
.001	.0015	0.0000524	0.0035
.01	.0149	0.000523	0.033
.1	.1315	0.00521	0.208
1.0	.603	0.0498	0.439
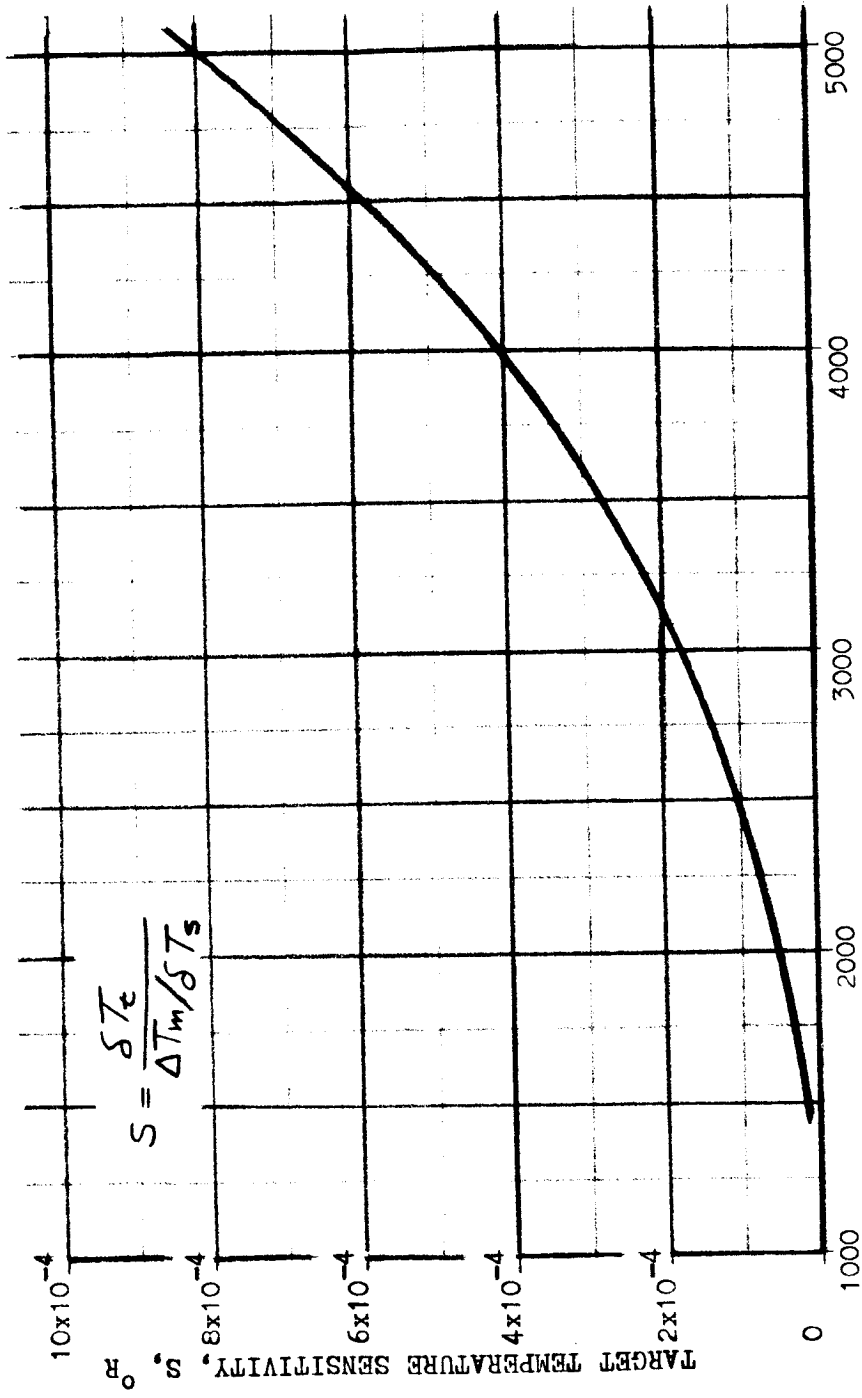
FIGURE 10, TARGET TEMPERATURE CHANGE FOR A
GIVEN SOURCE TEMPERATURE CHANGE

$$S = \frac{\delta T_t}{\Delta T_m / \delta T_s}$$
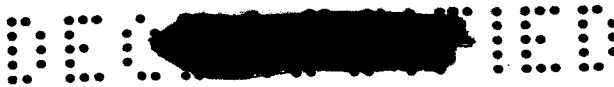
It should be pointed out that the pneumatic sensor has a comparatively high sensitivity and a high output pressure. The design values used in the analysis give a 10 psi differential full scale pressure output.

SUPPORT EQUIPMENT

State-of-the-art support equipment for each of the detecting devices was investigated as to limitations and availability for this application.

FOIL THERMOCOUPLE

Two types of amplifiers were considered for amplifying the thermocouple signal: d.c. electronic amplifier and magnetic amplifier. The two most severe environmental conditions which would be encountered by conditioning equipment are high ambient temperature (up to 800°R) and high radiation levels and dosage (10^{13} nv, 10^{18} nvt). The d.c. electronic amplifier has the problem of excessive drift at temperatures above 760°R. Manufacturers that build this type equipment indicate that the basic problems in constructing temperature resistant equipment are component selection and circuit design. Some work has been done in this area by component suppliers; amplifiers of the type required for this application can be developed but it is beyond the present state-of-the-art. One solution to this problem is to cool the amplifier at the expense of complicating the measurement system. In any event cooling would probably be required for adequate rejection of gamma induced heat.

The magnetic amplifier has been used successfully in certain KIWI reactor experiments up to a total integrated dose of 2×10^{13} Nvt. Current work is presently being done by NASA to develop magnetic amplifiers which are designed to operate in a radiation environment where the integrated neutron flux is as high as 10^{17} Nvt. The

response of a typical thermocouple magnetic amplifier follows the response of a first order system up to approximately one tenth the AC power supply carrier frequency. Amplification of a signal as small as 2 μ volts is possible. It is believed that the use of a radiation resistant magnetic amplifier and some shadow shielding would probably be satisfactory for this application.

If the design approach suggested in the previous paragraph is practical then there is a good possibility of using the magnetic amplifier for conditioning the signal at the point of measurement and locating the associated power supply above the reactor shield. This approach would eliminate the transmission of the low level voltage output (0 - 6.6 MV) over the transmission distance which is about eight feet to the top of the reactor shield.

A silico-ceramic coated wire is designed for nuclear application and will withstand the environmental conditions specified for short term operation (2 or 3 hours). The conductors available are stainless steel, nickel clad copper or pure aluminum. Nickel conductors also look promising.

Connectors are also designed for nuclear application. The standard connectors are made of stainless steel and inconel. These connectors have a temperature limit of $1500^{O}F$ for short term operation.

EDDY CURRENT
The conditioning equipment recommended by a local supplier for use with the eddy current sensor is designed to withstand an integrated

neutron flux of 10^{17}Nvt. All of the support equipment can be located above the reactor shield; the signal cable is not critical for transmission of the signal levels involved. The probe coils are stock items but the standard signal modifiers would have to be altered for this application. Cable and connectors recommended are similar to those described for the foil thermocouple. It is believed that signal conditioning equipment can be provided for the eddy current sensor without extending the state-of-the-art providing judicious use is made of available shadow shielding.

PNEUMATIC PROBE

The output of the pneumatic sensor was designed to operate over a differential pressure range of 10 psi. This probe could be re-designed to operate over a differential pressure range of 0 to 4 psi and there-by use available fluid amplifiers which have a control pressure swing of $\pm$ 2 psi. Experimental data is available on this type of amplifier at ^{R}ocketdyne. These amplifiers have been used successfully in working applications but at this time there is a scarcity of experimental data available and a limited choice of equipment. It is apparent that the fluid device has a significantly lower signal to noise ratio than the electronic amplifier and there are also problems of impedance matching. At this time the fluid amplifier cannot be considered a state-of-the-art component in the same sense as the electronic or magnetic ampli-fier. This is a new technology based primarily on experimental work and progress will depend largely on development of analytical methods or empirical aids for design.

RECOMMENDED SENSOR CONCEPT

The foil thermocouple was selected for further experimental study in connection with the development of a radiation pyrometer. The selection from among the three sensors considered was based primarily on sensitivity, signal to noise ratio, well defined technology, fabrication and test experience at Rocketdyne. A conceptual design of a twin foil thermocouple configuration to discriminate against nuclear radiation is presented in figure 11. This configuration will also compensate for variations in heat sink temperature. A twin foil thermocouple arranged back to back as shown in figure 12 is an alternate method that can be employed for nuclear heating compensation. Table 4 presents the physical and operating characteristics of the respective transducers, comments on application and support equipment status are also included.

The dimensionless sensitivity of the foil thermocouple as previously mentioned is comparatively high; because of its small size and mass it has an advantage in a nuclear environment where gamma heating is a problem. The foil thermocouple is a conventional approach to temperature measurement which has been experimentally verified at Rocketdyne as a feasible approach for measuring radiant energy. Its disadvantages are attributable mainly to a low voltage output, it is not as rugged as the other two devices considered and some experimental work may be necessary in connection with fabrication.

It should be noted that the eddy current sensor has not been used previously for measuring temperature by means of movement of a conducting plate due to a temperature change in the sensing element.

INACTIVE TARGET

ACTIVE TARGET

0.100 DIA. TYP. 2
PL. FOR ALUMEL
TARGET DIAMETER

0.010

0.165

0.026 TAB
WIDTH TYP. 6
PL.

THERMAL RADIATION
SHIELD HELD AT
TEMP. T_r

OPTICAL FUNNEL

ELECTRICAL INSULATION UNDER
TARGET FOIL

0.001

0.115

0.075

0.330

COOLED HEAT SINK AT
TEMPERATURE T_r

0.001 DIA. CHROMEL WIRE,
TYP. 2 PL.

ELECTRICAL INSULATION
TYP. 2 PL.
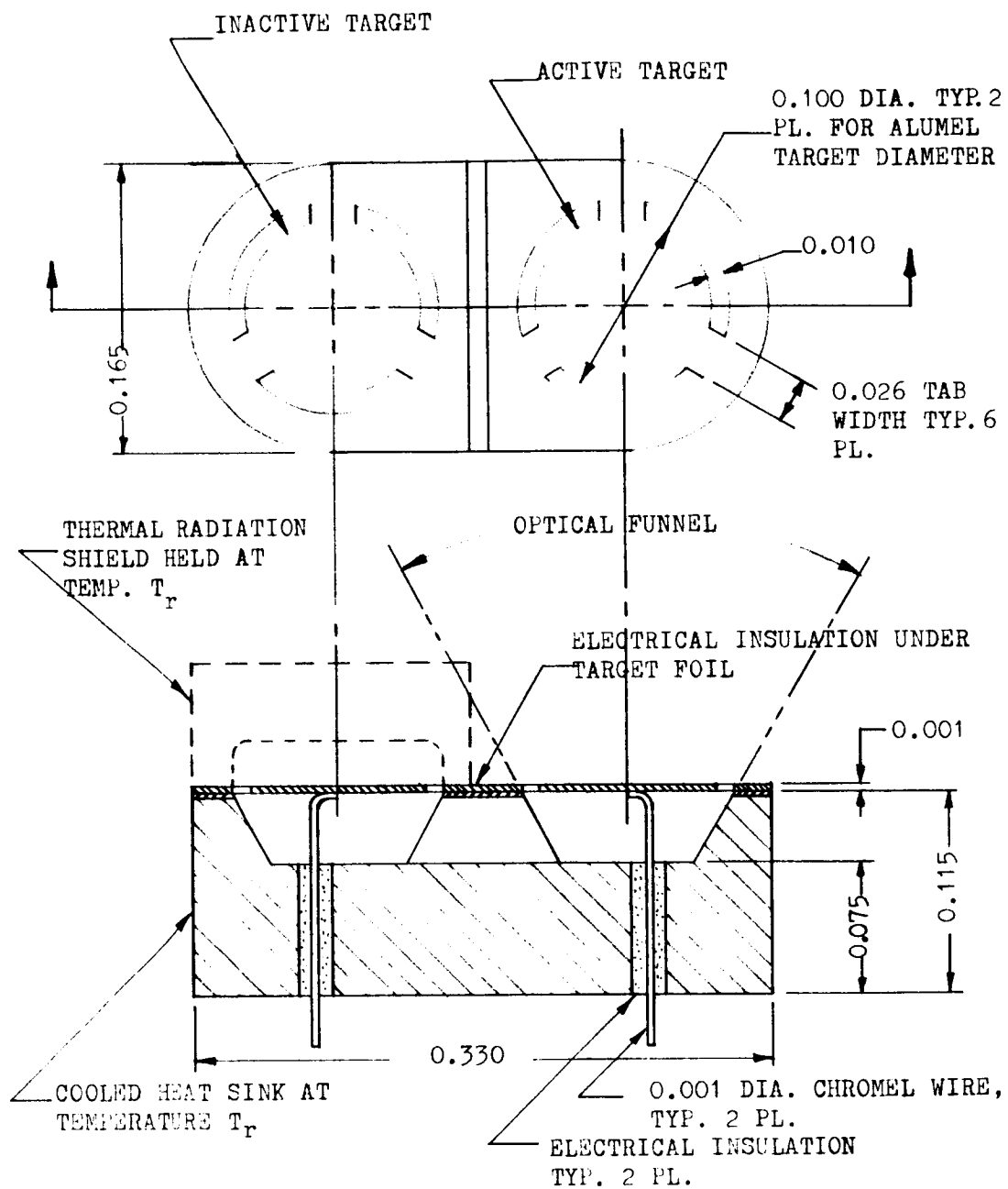
FIG. 11
TYPICAL TARGET INSTALLATION WITH COMPENSATION
FOR NUCLEAR HEATING

0.165 DIA.

0.100 DIA. ALUMEL TARGET

0.010

0.026 TAB WIDTH
TYP. 3 PL.

ACTIVE TARGET

0.001

0.500

0.001

INACTIVE TARGET

0.001 IN. CHROMEL WIRE AND ELECTRICAL
INSULATION, TYP. 2 PL.

COOLED HEAT SINK AT
TEMPERATURE T_r
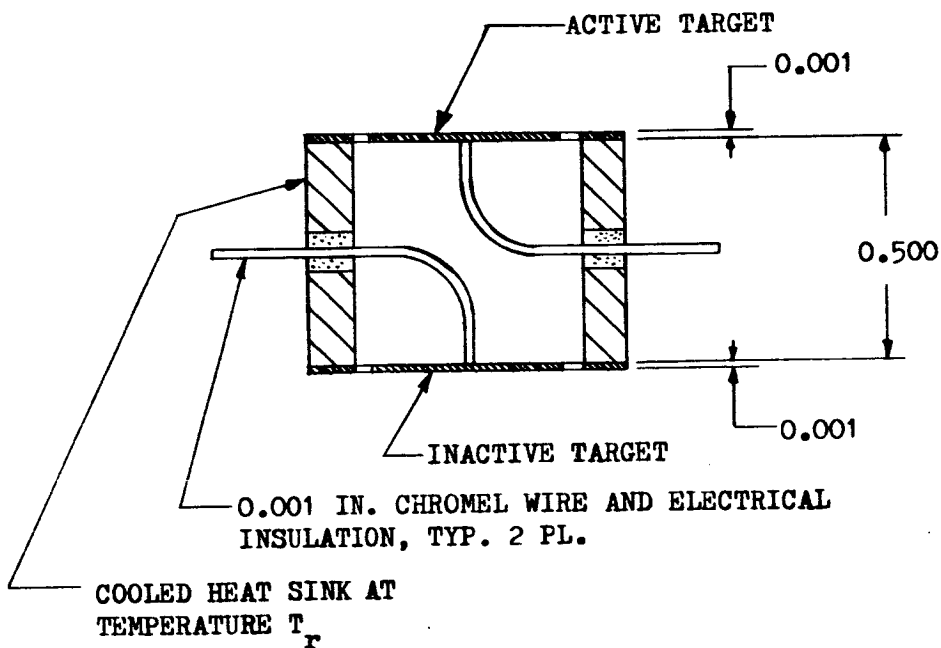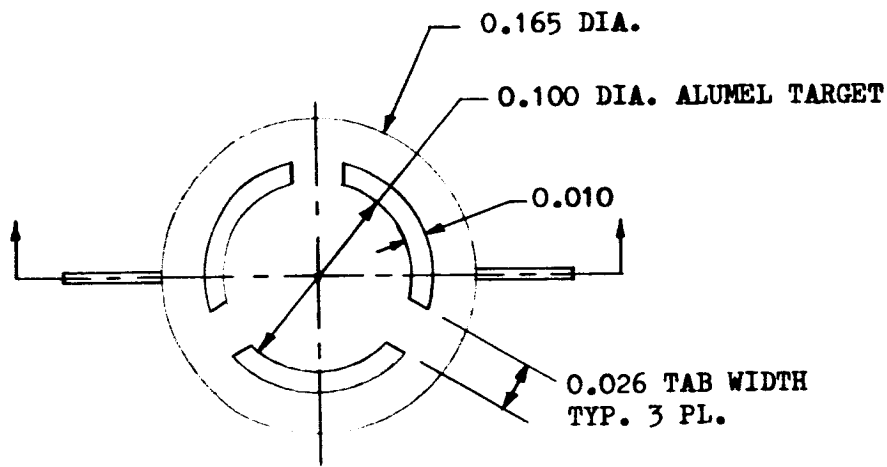
FIG. 12

TYPICAL TARGET ARRANGEMENT (BACK-TO-BACK)
WITH COMPENSATION FOR NUCLEAR HEATING

TABLE 4
SUMMARY OF PERTINENT SENSOR DATA

Item	Foil Thermocouple	Eddy Current	Pneumatic
Dimensionless Sensitivity			
1% of full power	0.0149	0.000523	0.033
100% of full power	0.603	0.498	0.439
Thermal/Gamma Heat^x Ratio @ 5000°R	218	34.5	39.1
Signal to Noise Ratio at Rated Output without Filtering	200:1*	200:1+	150:1+
Excitation	Self excited	Closely regulated power supply	Constant Pressure source
Size	Minimum of 0.1 in. foil diameter	Limited by cone dim.(1in.x1in.)	Limited to minimum area 0.25 sq.in.
Detector Availability	Has been built and tested	Has not been built, relatively complex to fabricate	Has not been built, appears simple to fab.
Support Equipment	Magnetic amplifier appears adequate to 10^{17} Nvt	Marginal in environment, can improve by shielding and design	Compatible with enviro.,limited choice of components not in present state-of-the-art
Practical Ref. Temp.Range	80°R to 500°R	Must operate at cryo. temp.(60°R) to meet response requirement	70°R to 500°R

*Based on experimental data
+Based on vendors estimates
xBased on no compensation for gamma heating. Gamma heating 1 BTU/lb (without attenuation.)

It has been used as a temperature measuring instrument by changing resistivity of a conducting plate but its main drawbacks in this form are slow time response and circuit complexity.

The pneumatic probe approaches the sensitivity of the foil thermo-couple and has the advantage of a high pressure output 0 to 10 psi differential. Its main advantages are inherent simplicity and the capability of enduring a high radiation environment. A bridge arrangement similar to that proposed for the foil thermocouple could be used to reduce gamma heating effects on the output. There remain the problems of pneumatic noise and interstage coupling which should be determined experimentally before pyrometer system development can be initiated.

Problem areas and design data associated with the recommended sensor concept are discussed in the section on the final Radiation Pyrometer system. The remainder of this section treats briefly a fixed foil thermocouple design, figure 11.

The thermocouple materials selected are chromel-alumel mainly because this combination has been found to be the most stable of the thermo-couples investigated in a high intensity nuclear radiation environ-ment (15, 16, 17) and it also has an adequate output voltage over the temperature range of interest. The data on thermocouple materials that were investigated for this application are presented in table 5. Although either chromel or alumel can be used for the foil, the latter was selected because its thermal properties are more compatible with the desired dimensions used in the thermocouple design.

TABLE 5

SUMMARY OF THERMOCOUPLE MATERIAL CHARACTERISTICS[a,b]

MATERIAL	SENSITIVITY OUTPUT $(\mu V/°C)$	USEFUL TEMPERATURE RANGE °C	THERMAL CONDUCTIVITY $(cal/sec-cm/°C @ \ldots)$	SPECIFIC HEAT $(cal/g°C @ 25°)$	DENSITY (lb/in^3)
Chromel P-Alumel	40 to 55	-200 to +1200			
Iron-Constantan	45 @ 0°C 57 @ 750°C	-200 to +800			
Copper-Constantan	15 @ -200°C 60 @ +350°C	-200 to 350			
Pt-Pt$_{90}$Rh$_{10}$	5 @ 0°C 12 @ 500°C	0-1450			
Chromel P			0.046	0.107	0.315
Alumel			0.071	0.125	0.311
Iron			.18	.11	.284
Constantan (45 Ni, 55 Cu)			.0546	.094	.32
Copper			.941 ± .005	.092	.324
Platinum			.165	.0314	.775
Rhodium			.21	.059	.447

[a]Lion, K.S., Instrumentation in Scientific Research, Electrical Input Transducers, Mc-Graw-Hill Book Co.,Inc. New York, 1959, p. 171.
[b]Metals Handbook, Vol. 1, Properties and Selection of Metals, 8th Edition, American Society of Metals.

The heat sink for the compensated sensor could be copper or some other highly conductive material; for a single sensor the heat sink would be one of the thermocouple materials.

Limitations exist on the types of insulation materials which may be used in the specified radiation environment. It appears that mica could be used as an electrical insulator; high thermal conductivity ceramic cement or refractory metal oxides could be used for insulating the lead wires (18).

The output of the chromel alumel sensor over the operating temperature range is plotted in figure 13 for a reference temperature of $500^{\circ}R$ ($40^{\circ}F$).

The sensitivity over the same source temperature range is presented in figure 14. Sensitivity is defined here as a ratio of a change of millivolt output for a corresponding change in source temperature. This value is plotted for a mean source temperature. A sample calculation can be found in Appendix C.

Both of the above curves are for a time constant of 0.1 seconds. If the time constant is relaxed to 0.5 seconds then the physical dimensions can be altered which will result in an increase in sensitivity. The expression for the time constant can be arranged as follows:
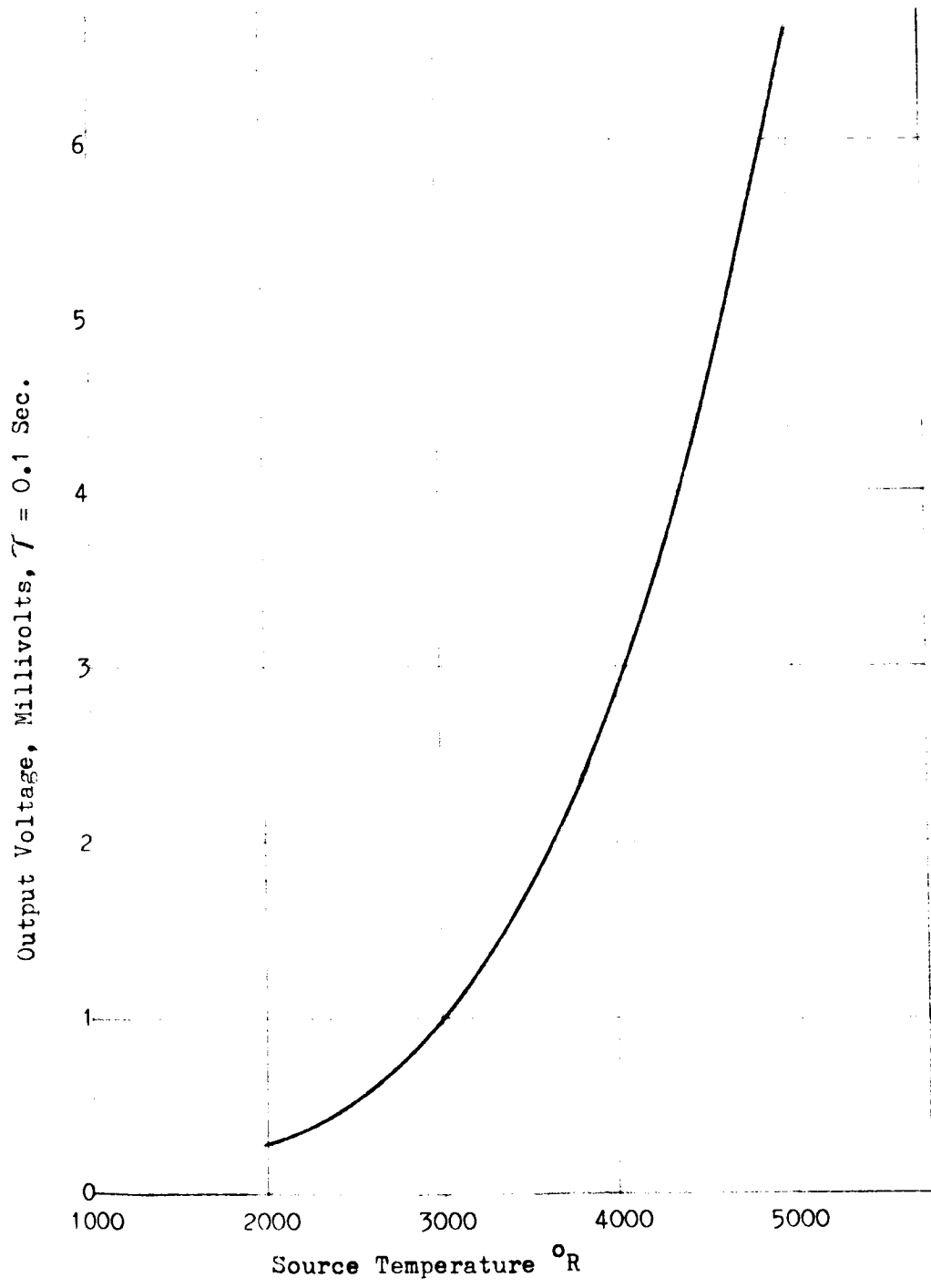
FIGURE 13. TEMPERATURE-MILLIVOLT CURVE FOR CHROMEL VS. ALUMEL FOIL THERMOCOUPLE
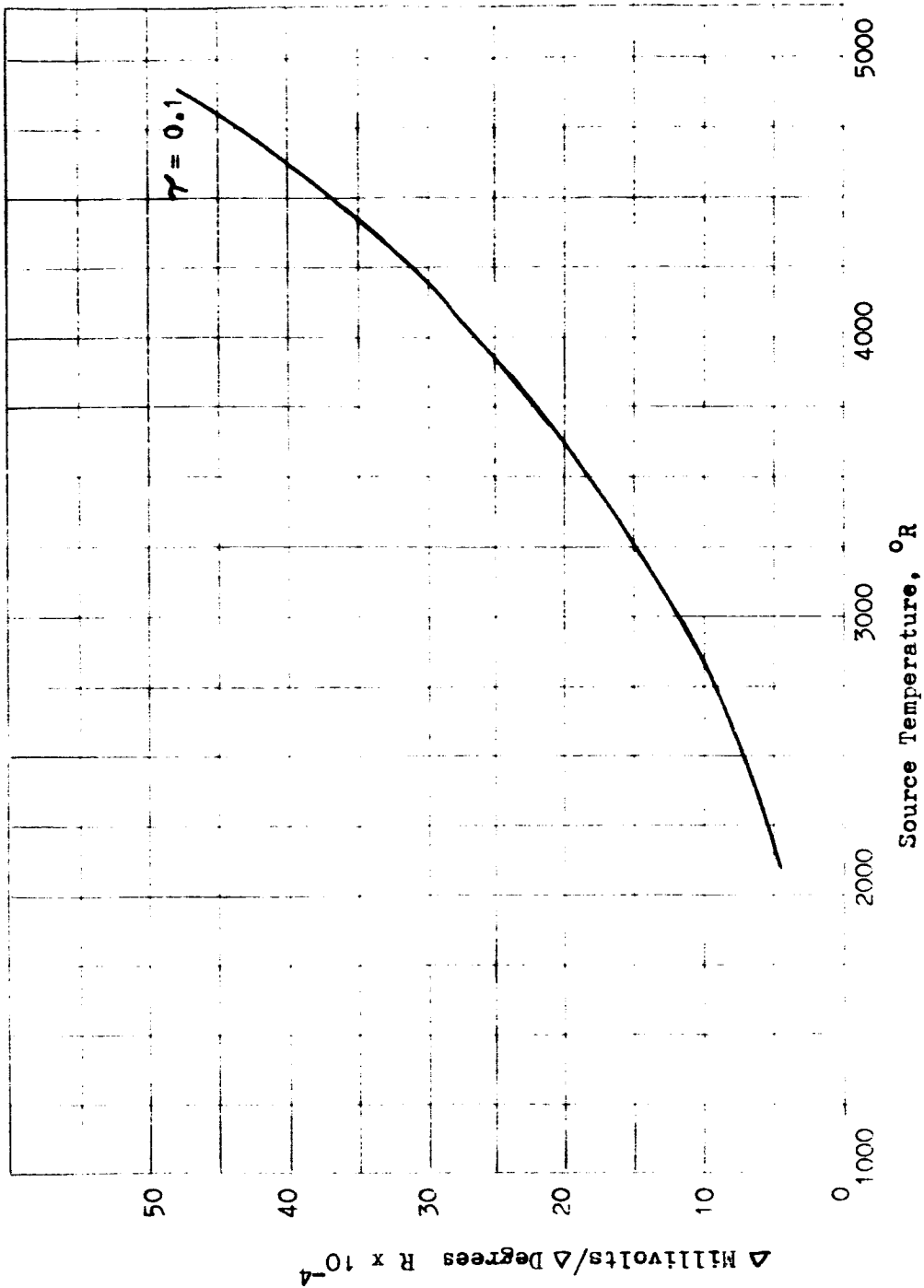
FIGURE 14. TEMPERATURE – SENSITIVITY CURVE FOR CHROMEL VS ALUMEL
FOIL THERMOCOUPLE

$$T = \frac{\delta\ell}{K}\left(\frac{A_t}{A}\right) C_p \rho \gamma$$

$$T = \frac{\delta\ell}{K}\left(\frac{A_t}{\gamma \Delta x}\right) C_p \rho \gamma$$

$$T = \left(\frac{\rho C_p}{K}\right)\left(\frac{\delta\ell \, A_t}{\Delta x}\right)$$

The expression ($\rho C_p / K$) is the reciprocal of thermal defusivity; this term is invariant for a given material but changes with temperature. For the heat sink temperature of 500°R and a temperature rise of 752°R $\rho C_p / K$ will change slightly but it can be considered constant. Therefore the above expression indicates that three terms can be varied to increase the time constant to 0.5. These are: $\delta\ell$ (conduction path length), A_t (foil area) and ΔX (conduction path width). If the path length $\delta\ell$ is increased from .010 to .046, the corresponding time constant will increase to 0.5 seconds. The longer $\delta\ell$ will result in a proportional increase in the tab resistance which will in turn increase the temperature rise of the foil for a given temperature, thus increasing the millivolt output (sensitivity). This increase in voltage output and sensitivity due to an increase in $\delta\ell$ is shown graphically in figures 15 and 16 respectively for a 0.2 second time constant and for a 0.5 second time constant.

Decreasing the tab width ΔX will also increase the time constant but in this case a limit is approached where the structural integrity of the conductive path material will be effected.
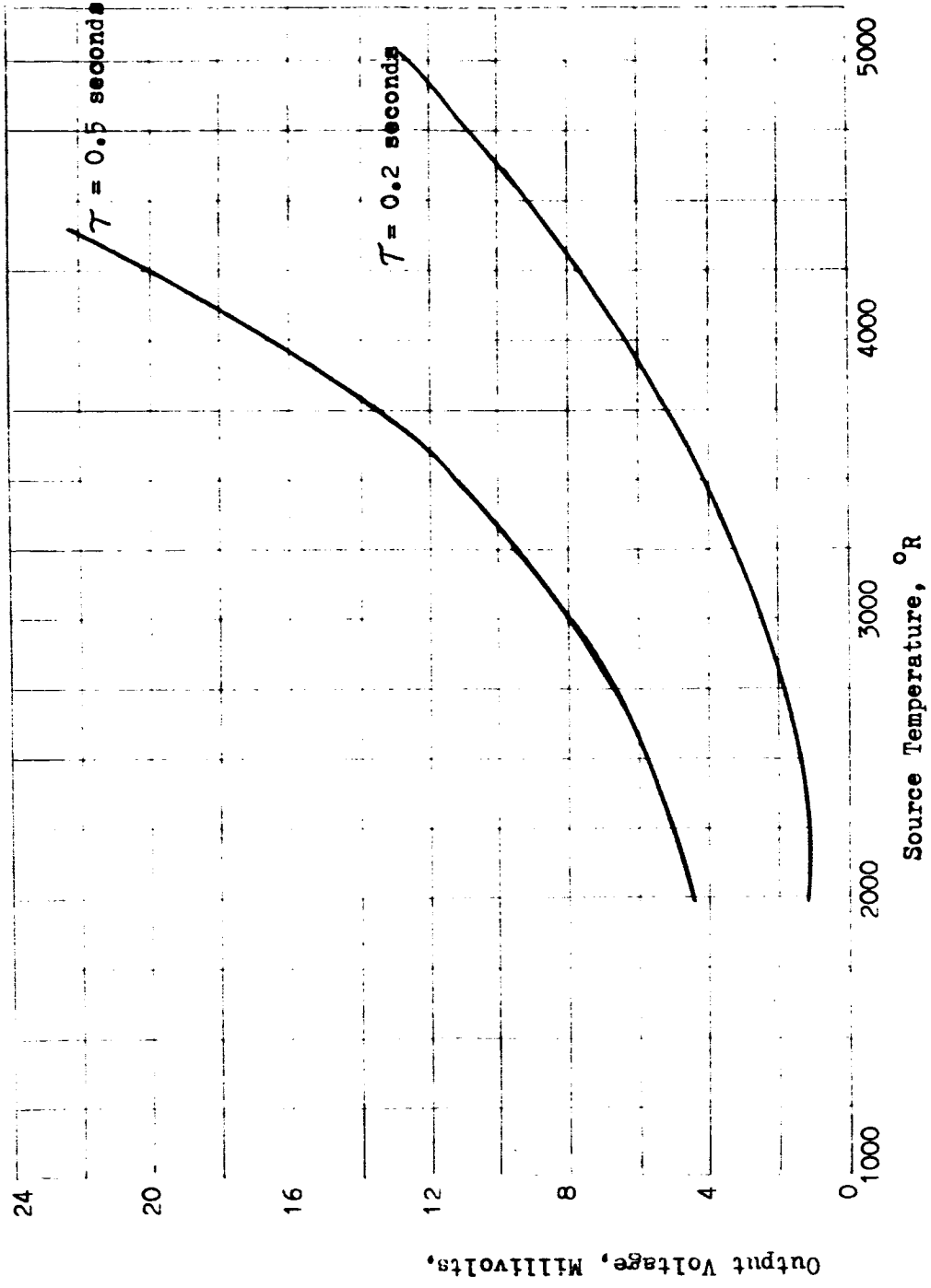
FIGURE 15. TEMPERATURE – MILLIVOLT CURVE FOR CHROMEL VS ALUMEL FOIL THERMOCOUPLE ($\tau = 0.2$, $\tau = 0.5$)
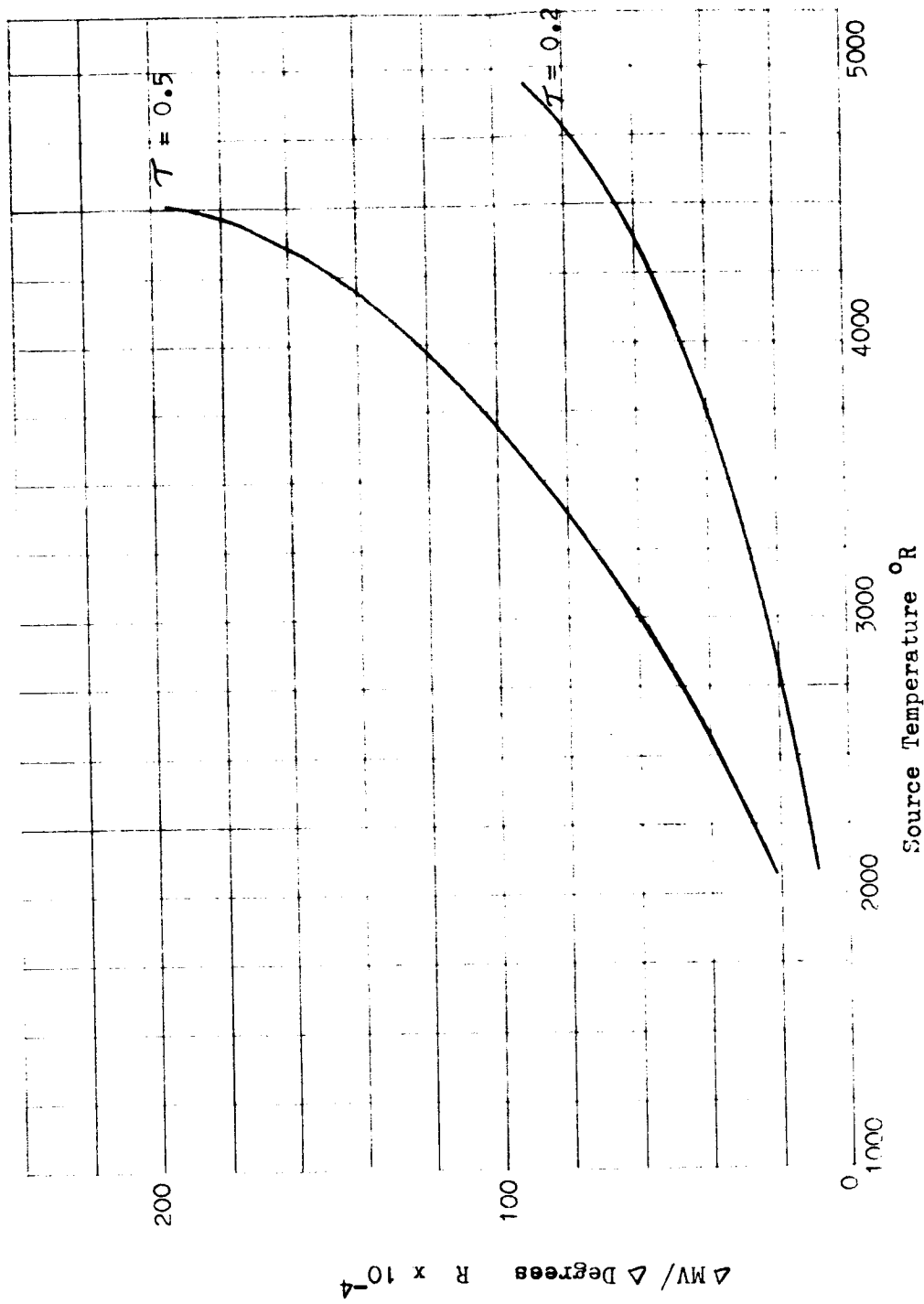
FIGURE 16. TEMPERATURE – SENSITIVITY CURVE FOR CHROMEL VS ALUMEL FOIL THERMOCOUPLE ($\tau = 0.2$, $\tau = 0.5$)

Increasing A_t will increase the time constant but in this case the foil resistance will be increased and the conduction path length tab $d\ell$ will decrease proportionately. The net effect of these two values will determine the temperature rise of the foil.

Optical system concepts are discussed in the next section.

BASIC CONSIDERATIONS FOR VIEWING SYSTEMS

The basic pyrometric system will be composed of a source whose temperature is to be measured, possibly a reference source, a viewing system, and a detector with associated components. This portion of the study relates to the viewing system and to the problems of developing a viewing system which is compatible with the requirements and limitations of the other components and with the nuclear environment to which it will be subjected. The viewing system must allow the detector to view a sufficient portion of a hot (1000°R to 5000°R) surface from which is emanating a high gamma and neutron flux.

Basically, there are three types of viewing systems: (1) direct viewing systems by which the detector is exposed to the source through a limited aperture, (2) transmission viewing by which the radiation from the source, after passing through a limiting aperture, is focussed onto the detector by lens assemblies, and (3) reflection viewing by which the radiation, after passing through an aperture, is reflected (and perhaps focussed) onto the detector by means of mirrored surfaces.

The major factors influencing the choice and design of the viewing system are: (1) operational stability of the viewing system under nuclear radiation environment, (2) ability to transmit sufficient energy to the detector, and (3) ability to allow the detector to be shielded or compensated from gamma heating. Each of these factors will be discussed separately in the paragraphs which follow.

RADIATION DAMAGE TO OPTICAL VIEWING SYSTEMS

Direct Viewing Systems

The use of a direct viewing system presently appears practical only for sensors which are radiation resistant or those which can be compensated for nuclear heating. At some temperatures, gamma heating produces nearly as much response from an uncompensated detector as does the thermal radiation to be measured. Any attempt to reduce the gamma heating through shielding so far has also reduced incident thermal radiation on the detector to an intolerably low level.

The compensated foil thermocouple sensor sketched in figure 12 merits consideration for use with the direct viewing system. It is shown in the error analysis section that a single foil thermocouple element on the other hand is not feasible for this application primarily because of the effect of heat sink variation on the sensor output voltage. (A 1% change in heat sink reference temperature results in a $\pm 56^{\circ}R$ change in the output signal at $5000^{\circ}R$; the heat sink design temperature is $500^{\circ}R$)

Transmission Systems

The use of conventional lens materials to collect and focus the radiation in a transmission optical viewing system is presently considered unfeasible due to the discoloration (i.e. increase in absorption coefficient) of quartz and conventional glasses during irradiation.

If the lens transmission were to change uniformly at all wavelengths through the spectral region of interest, it would be possible (though perhaps not practical) to devise an optical system which would perform

independently of such changes. However, if temperature dependent selective absorption occurs to a significant degree, the resulting system would be impractical for temperature measurement purposes even if the average transmission were fairly high.

In glass and ionic crystals, the change in characteristic absorption is due to the excitation of electrons within the solid by incident radiation; these electrons are subsequently trapped in nearby lattice defects in the crystal; such trapped electrons or combinations of them have characteristic absorption spectra. (19) Recovery or "bleaching" of the irradiated materials can be accomplished in certain cases by heating the material to a prescribed temperature; the thermal activation presumably permits movement and removal of the defect or of the trapped electron. The possibility of "simultaneous discoloration and bleaching" by maintaining the lens at an elevated temperature during irradiation is feasible for a pyrometric observing system only when the thermal radiation emitted by the lens by virtue of its temperature is an insignificant fraction of the total radiation received by the detector. At those wavelengths where the lens trans-mission is negligibly small, the lens itself will radiate as an opaque solid. A one inch diameter quartz lens at $800^{\circ}C$ (possible annealing temperature of quartz) located four inches from a detector of $1/2$ inch diameter will radiate of the order of 10^{-4} to 10^{-5} BTU/sec onto the detector. This is the energy emitted when quartz is at a temperature of $800^{\circ}C$. (Refer to Appendix B-Calculation of Thermal Signal Arriving at Detector from Quartz Lens).
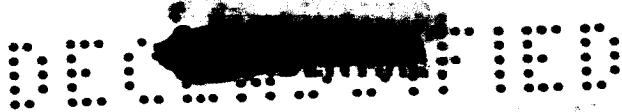
Reflection Systems

The total effect of neutron and gamma irradiation upon the reflectance of mirrored surfaces employed in a pyrometric viewing system is not certain. It is known that neutron irradiation can cause length variation and changes in electrical resistance of metals. Changes in the electrical resistivity (ϱ) of metals are related to changes in the spectral reflectivity by the Hagen-Rubens relation noted below. (20)

$$r = 1-0.365 \sqrt{\varrho/\lambda} + 0.0667 \, \varrho/\lambda +. \ldots$$

This relation is presumably valid for wavelengths longer than 4 μ but may not be valid for shorter wavelengths. Therefore, conclusions concerning the effect of irradiation upon the spectral reflectivity of mirrored surfaces cannot be drawn from resistivity data by the use of the Hagen-Rubens relation except for wavelengths greater than 4 μ. Irradiation and reflectance tests must be performed to determine the degradation in the ultraviolet, visible and near infrared portions of the spectrum. In pyrometric systems, the wavelength range of interest depends upon the spectral distribution of the energy emitted by the source, and hence on the source temperature. For example, a source at 1500°R emits 35% of its energy at wavelengths shorter than 4 μ while a source at 5000°R emit 93% of its energy at wavelengths shorter than 4 μ. However, until such irradiation tests are performed, change in resistance, and hence reflectance above 4 μ will be considered indicative of reflectance changes below 4 μ.

In general, the room temperature resistivity of metal samples exposed to nuclear irradiation at such temperatures changes very little, less than 1%, while at lower temperatures of exposure and measurement,

significant changes are observed. (21) Table 6 indicates changes in resistivity of aluminum for various conditions of exposure and resistivity measurement and indicates the corresponding change in reflectivity as computed from the Hagen-Rubens relation when assuming the reflectance of the unirradiated material as 97%.

The literature also indicates that annealing subsequent to irradiation at low temperatures can return the aluminum to its original, unirradiated, resistivity. Table 7 indicates the time and temperatures required to anneal aluminum samples irradiated at 80°K (145°R) and with a neutron flux of $1.1 \times 10^{19}/cm^2$ to within 5% of the resistivity of an unirradiated sample. If extrapolation of the annealing curve from which the table was obtained can be considered valid, then samples irradiated at 80°K for 3000 hours with a flux of $10^{12} n/cm^2$-sec would be annealed in 0.4 seconds to within 5% of their original resistivity by raising their temperature to 295°K (535°R). It therefore seems reasonable to assume that if an aluminum mirror were maintained at room temperature (535°R) during irradiation there would be no significant change in resistivity and hence no significant change in the reflectance of the surface insofar as its behavior in the proposed application is concerned.

If an aluminum mirror were employed in the system, it would be advisable to protect the surface from oxidation by the application of a thin layer (less than 1μ) of Si O_2. However, the effect of irradiation upon the overcoating is not known. Of course, if the mirror is maintained in an atmosphere of hydrogen or in an evacuated enclosure, oxidation will not occur and overcoating will not be required.
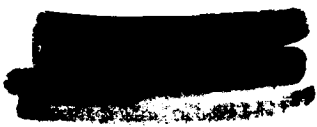
TABLE 6

Effect of Neutron Irradiation Upon Spectral Reflectance of Aluminum for Wavelengths Greater Than 4 μ

Material	Temperature of Specimen during Irradiation	Dose	Temperature of Specimen during Resistivity Measurement	Change in Resistance Measure- ment	Calculated Change in Spectral Reflectance Above 4 μ for aluminum
Al, 2S	50°C	4×10^{19}/cm^2 fast neutron	20°C	+0.7%[*]	0.015%
Al, 2S	50°C	"	-190°C	+10%[+]	0.15%
Al, 2S	80°K	1.1×10^{19}/cm^2 neutron	80°K	+33%[+]	0.5%

[*] Nuclear Engineering Handbook, ibid, Sec. 10, p. 106.

[+] "Neutron Effects in Cu and Al at 80°K", Physical Review, Vol. 98, No. 2, Apr. 1955, McReynolds et al, pp. 418-425.

TABLE 7

Annealing Conditions to Decrease Resistance of Irradiated Aluminum Samples

to Within 5% of their Resistance at 80°K.*

Annealing Temperature		Time of Annealing		
°R	°K	Seconds	Hours	
(535)	(295)	(0.4)		(extrapolation)
(450)	(250)	(10)		(extrapolation)
400	222	160		
365	200	4×10^3	1.1	
(300)	(165)	(7×10^5)	(195)	(extrapolation)

*Neutron effects in CU and AL, at 80°R, physical review, Vol. 98,
No. 2 April 1955, McReynolds et al, pp. 418-425
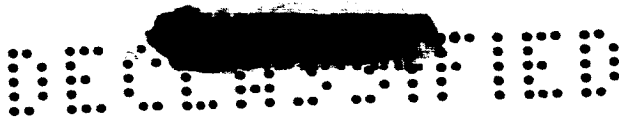
SOURCE EMISSIVITY & ENERGY REQUIREMENTS

Thermal Radiation Source

The reactor surface to be viewed will probably be coated with NbC.
Approximately 30% of the surface viewed will be coolant hole passages.
The energy emitted per unit area from a surface of niobium carbide
which has a 30% void fraction (holes) is not strictly according to
the 4th power radiation but varies between the 2.6 and the 5.5 power
depending upon temperature. This condition results from the combined
effect of the apparently odd emissivity characteristics of niobium
carbide, figure 17 and the effective emissivity of the holes or voids
in the reactor core. For holes with a very large length to diameter
ratio the emissivity is essentially that of a black body so that
$\epsilon \approx 1.0$. A plot of this combined effect is shown in figure 18.

It can be seen that the plot of the energy emitted with surface
temperature can be approximated in a log-log plot by three straight
lines. The emissivity first increases with temperature and then
decreases causing "q" to vary as the 5.5 power over the range of 1660°
to $2460^{o}R$, as the 2.64 power over the range of 2860° to $4260^{o}R$ and as
the 3.6 power over the range from 4860° to $5460^{o}R$. This non-linearity
can be compensated for in the detector signal conditioning equipment.
Signal conditioning equipment with a variable gain (function genera-
tor) would produce a linear output. Such an output is desirable for
the control system. Other factors that may change the emissivity
such as nuclear radiation have to be corrected by calibration.
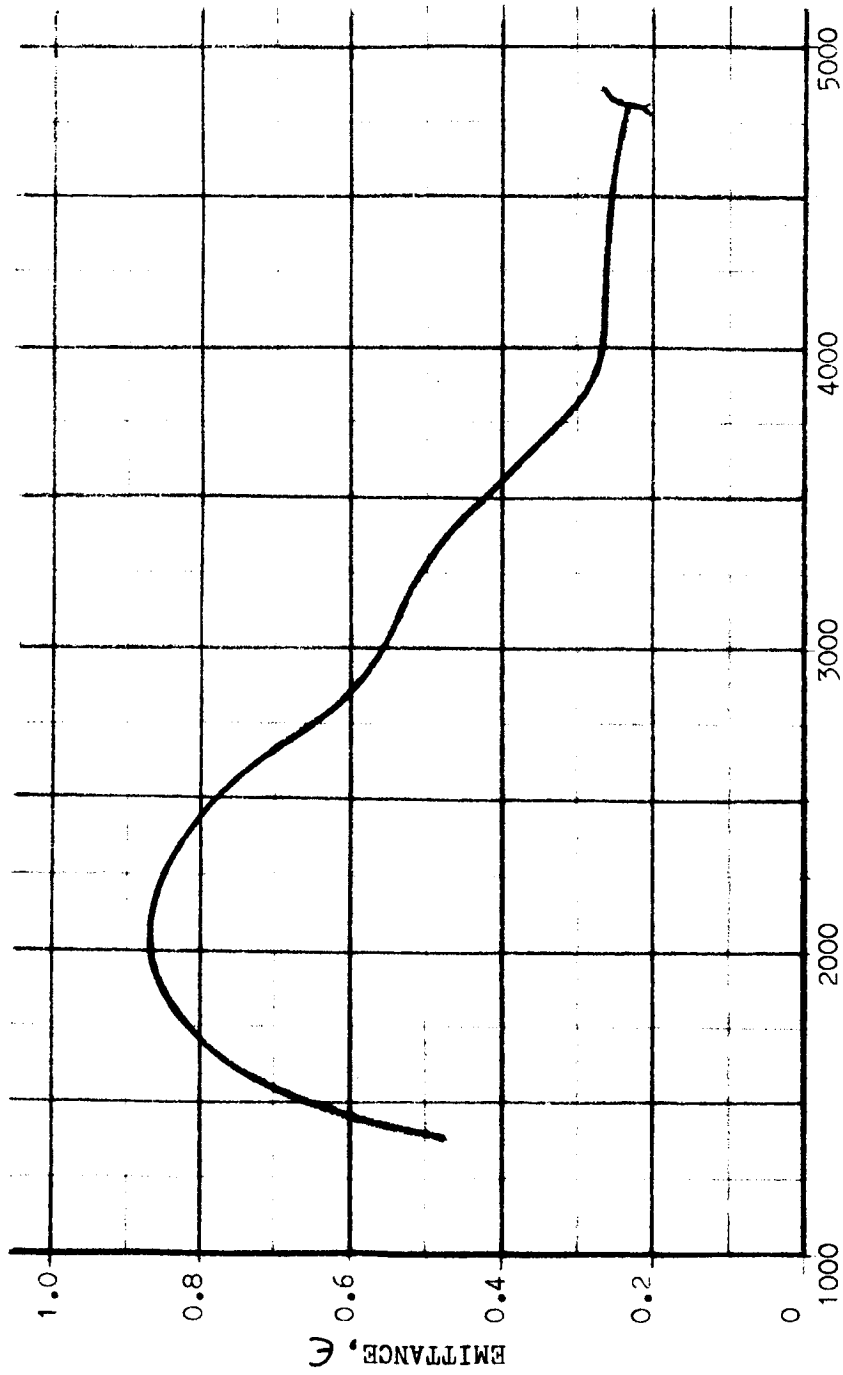
FIGURE 17, TOTAL NORMAL EMITTANCE OF COLUMBIUM CARBIDE
(SOUTHWEST RESEARCH INSTITUTE)

SOURCE TEMPERATURE, °R
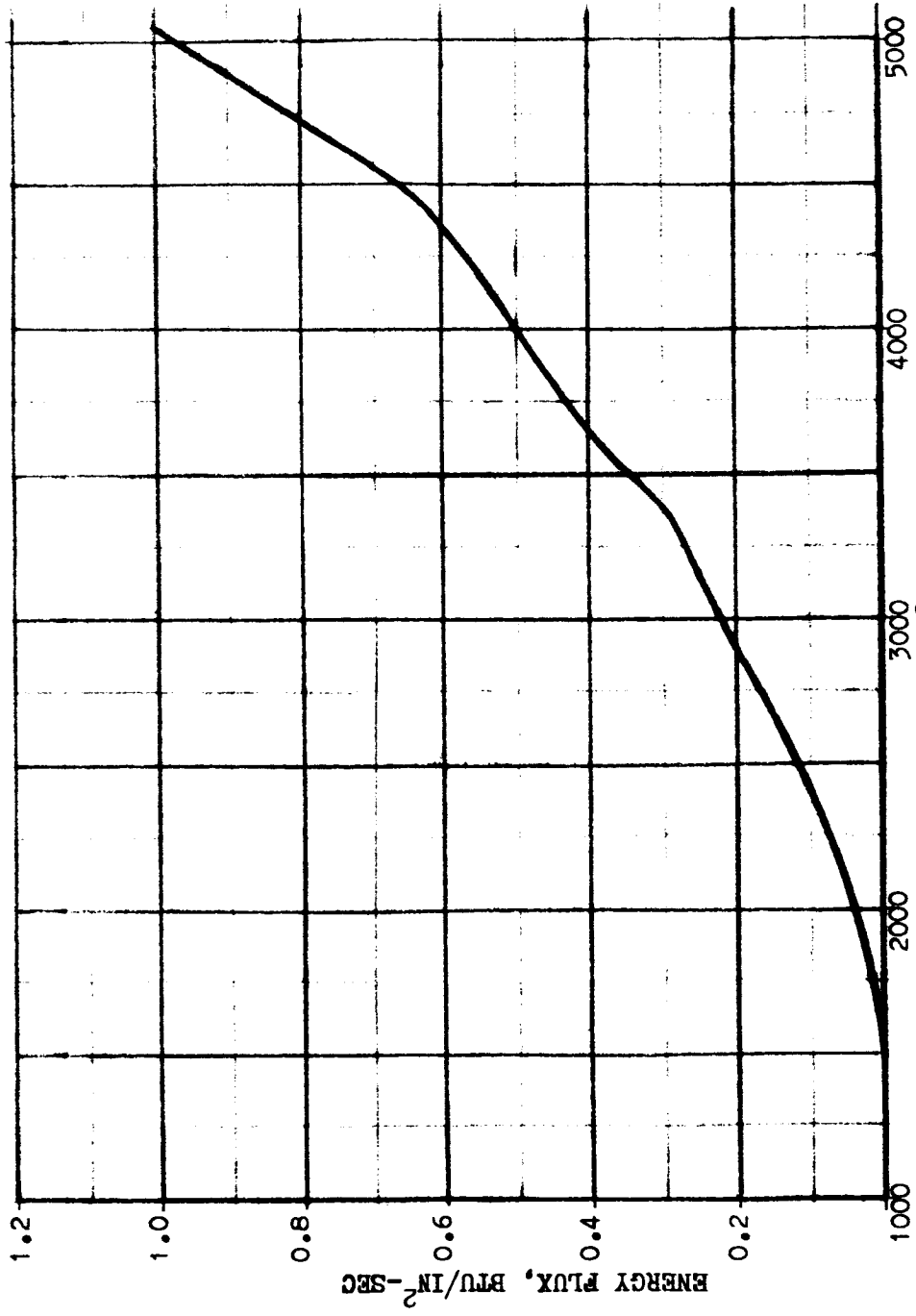
FIGURE 18, ENERGY EMITTED FROM SOURCE
WITH 30% VOID FRACTION $(q = \sigma \in T^4)$

ENERGY FLUX, BTU/IN^2-SEC

It should be noted that the emittance of graphite is a weak function of temperature. In the vicinity of 4000° to $5000^\circ R$ it is about 0.75; the emitted energy of graphite is close to the 4th power radiation law and at $5000^\circ R$ give about 70% more energy than niobium carbide.

It is recognized that graphite combines with hydrogen to form methane gas (CH_4) and other hydrocarbons at high temperatures and therefore is not likely to be exposed to hydrogen gas in high temperature regions of the core.

It is important to note at this point that because the available emissivity data on niobium carbide could not be verified and a complete literature search could not be made due to time limitations, it was suggested by NASA that a constant emissivity of 0.85 be used in this study over the operating temperature range $(1000^\circ R$ to $5000^\circ R)$. Therefore the constant emissivity of 0.85 was used for all design calculations in this study.

Energy Requirements

The present detector state-of-the-art information indicates that the thermal detectors under consideration require a signal in the range of 10^{-4} BTU/sec (~ 0.1 watt) to 10^{-1} BTU/sec (~ 100 watts) with reasonable operational characteristics at 10^{-2} BTU/sec (~ 10 watts). Therefore the energy transmitted by the optical system must be of the order of 10^{-2} BTU/sec. (Refer to Appendix C)

The amount of energy γ which can be transmitted by the optical system is given by the following equation

$$\mathcal{T} = t_{eff} \int_0^A F_{dA} \, \epsilon_{dA} \, \sigma \, T_{dA}^4 \, dA \quad \text{(refer to Appendix B)}$$

where dA represents a small area at temperature T and emittance ϵ_{dA} emitting a fraction F_{dA} of its total energy into the optical system and hence onto the detector. t_{eff} represents the overall transmission or reflectance of the optical system which transfers the radiation onto the detector.

Calculations of the above quantities are made difficult by the variation of F_{dA}, the view factor across the source. Estimates of this variation for viewing systems accommodating $10°$, $30°$ and $70°$ plane angles and for a limiting aperture placed 20" along the optical axis from the source were investigated; the optical axis was assumed to be at $45°$ to the plane of the source. Thus under these conditions, F_{dA}, the view factor across the source, varies by a factor of 1.5 over the area seen within a $10°$ plane angle, by a factor of 2.8 over the area seen by a $30°$ plane angle, and by a factor of 5.8 within a $70°$
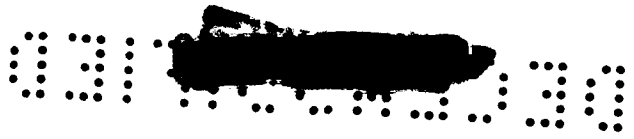
plane angle viewing a source of 40" diameter. (For a source of 60" diameter, the view factor would vary by a factor of 8.8 for the 70° plane angle.) From these approximations, it is then conceivable that for large angles (70°) and large source diameters (50") a view factor variation over the surface of a factor of 10 might be expected. The average view factor will have to be experimentally determined.

The magnitude of the view factor is approximated in the following manner: when R is larger compared to d.

$$F_{dA} = \frac{d^2}{8R^2} = \frac{\pi\, d^2/4}{2\pi R^2} = \frac{A\ \text{Pass thru}}{A_{\text{hemisphere}}}\ \text{(refer to Appendix B)}$$

where R is the distance of the area dA from the limiting aperture of diameter d. For the specific case R = 20", d = 3/16", the view factor is 1.1×10^{-5}.

If for purposes of estimation, it is permissible to assume an average view factor of 1.1×10^{-5} across the source, the detector would receive about 10^{-2} BTU/sec from a 60" diameter source of emittance 0.85 and at a temperature of 5000°R when viewed through an optical system accommodating a 70° plane angle. This estimation assumes a limiting aperture of 3/16" diameter located 20" from the source as measured along the optical axis of the viewing system. The energy received by the detector under the same conditions but with a 11° plane angle limit is about 4×10^{-5} BTU/sec. (An 11° plane angle indicates that an effective source area of about 8 sq. in. is in view by the detector.) Curves of thermal radiant energy for various angles of core viewing at given core temperatures are presented in figure 19.
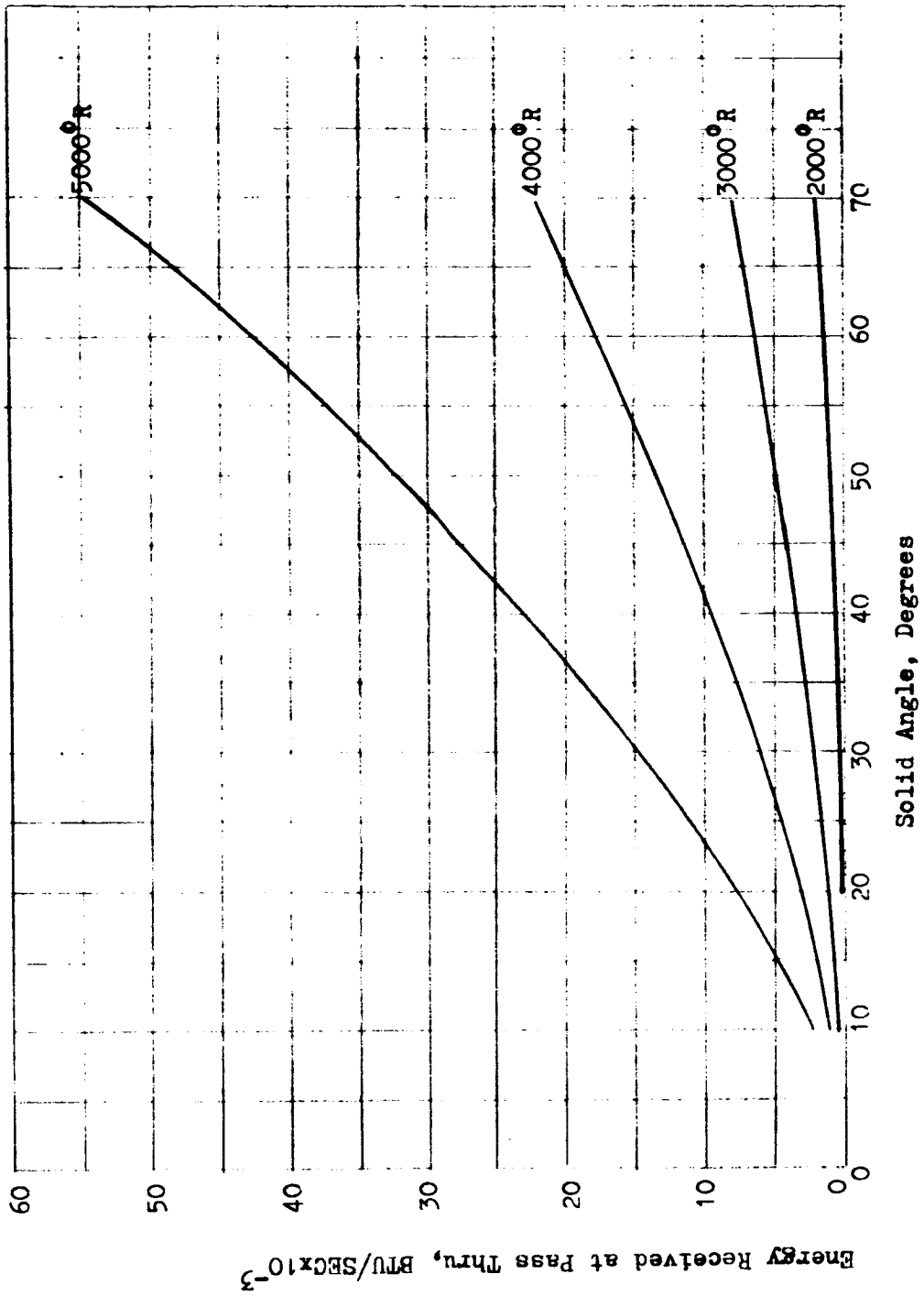
FIGURE 19. RADIANT ENERGY RECEIVED AT PASS THRU FOR VARIOUS ANGLES OF VIEWING

It should be noted that the maximum permissible aperture size of 3/16 inch diameter was established as a ground rule for this study. Therefore in order to deliver the necessary signal to the detector, an optical system capable of accommodating a plane angle of the order of 70° is considered necessary. Further investigation of the nozzle pass-thru indicated that a one inch diameter aperture is feasible in the Rocketdyne nozzle configuration. This increased area in the pass-thru would result in a more accurate viewing system because a smaller plane angle would be required (about 15°). A further reduction in the viewing angle would be possible if the minimum operating temperature were increased above $1000^\circ R$.

Reference Cavity

The extent of the calibration required for the optical system is not known at this time. It may be possible to obtain sufficient system stability so that an initial preflight calibration will be adequate. If not, periodic calibration during operation might possibly be accomplished by allowing the detector to periodically view a reference cavity of known temperature.

RECOMMENDED VIEWING SYSTEM

As previously stated, three types of optical viewing systems were considered for application in the pyrometric system. The types were: direct viewing, transmission viewing, and reflection viewing.

The direct viewing optical system is practical if the sensor can be adequately compensated for nuclear heating or if the sensor is compatible with the specified nuclear radiation.

Estimates made in the previous section indicate that a mirror system is not significantly effected by nuclear radiation at ambient temperature and is expected to be much less affected by radiation than transmission optics. Therefore reflection optics is also a feasible method to be employed in the viewing system.

The principal advantage of the direct viewing system is its simplicity. No intermediate component (mirror) is required to transmit the radiant energy onto the detector. The reflection optics, on the other hand permits simple nuclear shielding of the detector and if necessary a conventional calibration approach using a reference cavity. It is also adaptable to common shielding for the amplifier and the detector if a pre-amplifier is used to amplify the output signal at the point of measurement.

If the radiation effects data presented in the current literature on Chromel-Alumel thermocouples as noted in references 15, 16, 17 are valid for this application then the direct viewing system is a
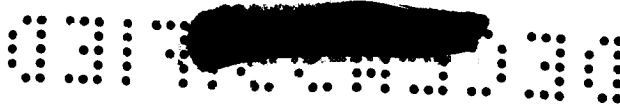
logical choice. Reflector optics is also feasible and represents a more conservative approach to the viewing problem. The reflection type optical system was chosen for detail study primarily because of the uncertainty of nuclear radiation in future nuclear rocket engines. The gamma heating rate for the present nuclear rocket engines was estimated to be 1 BTU/lb/sec. For this particular condition the direct viewing system appears to be adequate from the standpoint of nuclear heating. It should be noted, however that the viewing problems with the exception of mirror degradation in the reflection optics are essentially the same for both systems.

REFLECTION VIEWING

Many reflection type optical systems have been considered however, only one of these could accommodate a large (60°) plane angle, the requirement imposed by the specified limitation of the maximum feasible aperture diameter (3/16") and by the requirement of 10^{-2} BTU/sec energy deposition rate required for operation of the detector.

Because of the very large solid angles and off-axis radiation involved, the optical quality of such a system will be only moderate. The design is sketched in figure 20.

At the initiation of this study, the maximum feasible aperture was about 3/16"; the requirement of 10^{-2} BTU/sec energy deposition rate necessary for the operation of the detector required that the optical viewing system accommodate a plane angle of about 70°. As mentioned in the previous section, the minimum aperture diameter was set as a ground rule for this study and was found to be too restrictive.

Further investigation of this problem has shown that a pass thru diameter of one inch is feasible. Calculations now indicate that a reasonable amount of energy can be obtained through this opening without the use of a 70° plane angle. For example: a 70° plane angle and a 1" diameter opening would allow about 2×10^{-1} BTU/sec to be incident on the detector; an 11° plane angle with a 1" diameter aperture allows a maximum of about 10^{-3} BTU/sec to be incident upon the detector. It is therefore advised that the viewing system be sized to accommodate a smaller (perhaps 15°) plane angle, thus allowing conventional reflection optics to be utilized. It is thought that a more accurate system requiring less calibration and adjustment will result.

Discussion of Conceptual Design (Reflection Viewing)

The reflection viewing system, figure 20, consists of a section of an ellipsoidal mirror of semi-major axis of 3.51" and semi-minor axis of 2.89" mounted onto the outside of the nozzle wall. This system accommodates a plane angle of 60° and permits 2" of shielding between source and detector. The base of the ellipsoidal section is positioned at an angle of 50° with respect to the plane of the wall and with one focal point coinciding with the center of the pass thru of diameter 3/16". The radiation entering the optical system from the pass thru is focussed onto the detector of $1/2$" diameter located at the second focal point of the ellipse. It is possible to concentrate the energy on a smaller area by means of a high reflectance cone or funnel with the sensing element recessed in the convergent end (refer to figure 11). The ellipsoidal mirror is to be maintained at 535^OR (room temperature) to reduce degradation resulting from nuclear irradiation
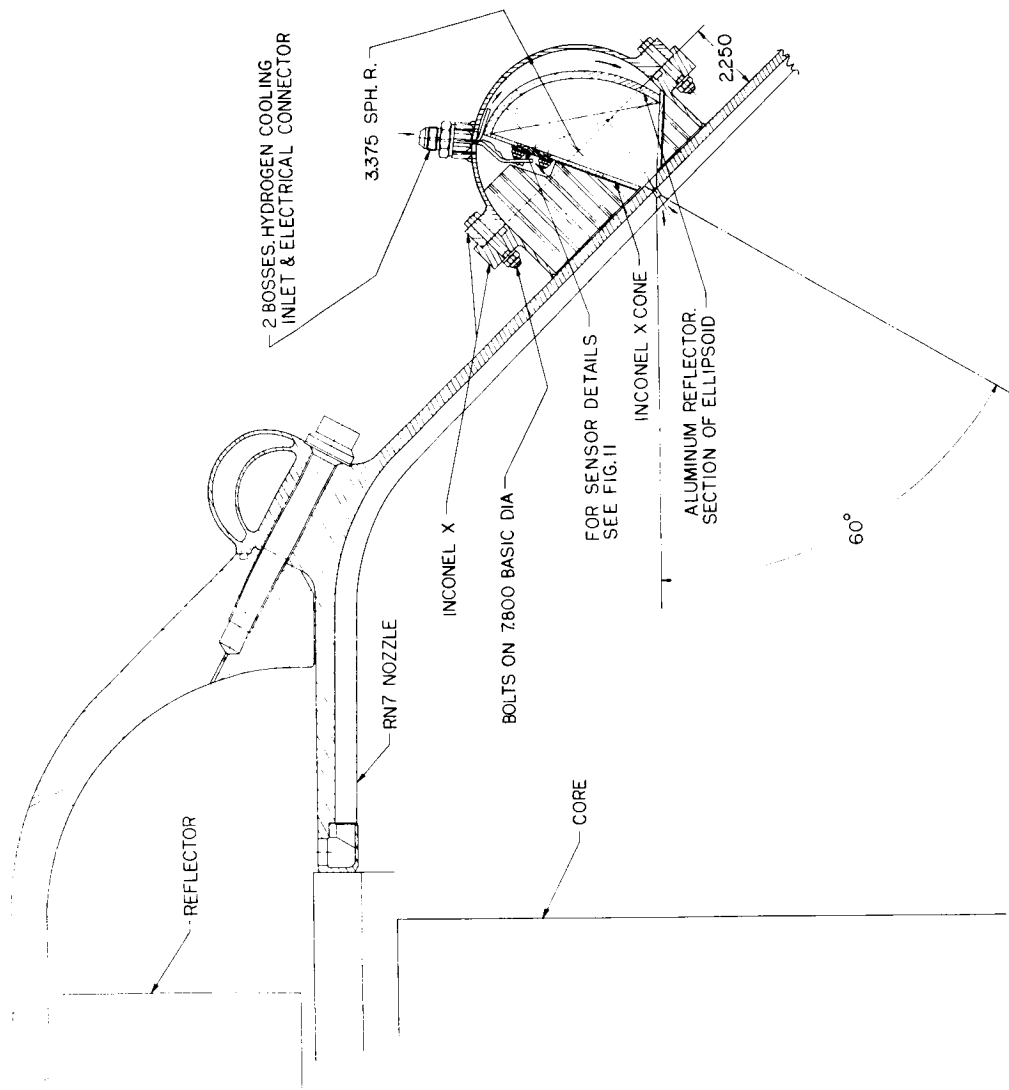
FIGURE 20. RADIATION PYROMETER, REFLECTION OPTICS

2 BOSSES, HYDROGEN COOLING
INLET & ELECTRICAL CONNECTOR

3.375 SPH. R.

2.250

REFLECTOR

RN7 NOZZLE

INCONEL X

BOLTS ON 7.800 BASIC DIA

FOR SENSOR DETAILS
SEE FIG. 11

INCONEL X CONE

ALUMINUM REFLECTOR.
SECTION OF ELLIPSOID

60°

CORE
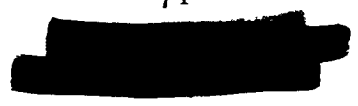
and to facilitate initial laboratory calibration of the system. The
side, base plate, and aperture should be maintained at temperature
less than 300°R in order to minimize dark current. An ellipsoidal
mirror machined from aluminum and of $\frac{1}{8}$" wall thickness, polished,
and with a vapor deposited aluminum overcoating should form a reflect-
ing surface of adequate quality. Unless the system will be maintained
in an inert atmosphere during laboratory testing and when in operation,
a thin (less than 1 μ) protective overcoating of SiO_2 is required to
prevent oxidizing of the aluminum and hence reflectance degradation of
the mirrored surface. If laboratory irradiation indicates that the
SiO_2 degrades under nuclear irradiation then a reflecting surface
other than aluminum must be chosen. (Specifications for the mirror
should include focussing requirements and spectral reflectance
requirements.)

The side plate, base plate and apertures of the viewing system chamber
should probably be blackened with a coating of high diffuse emittance
material in order to reduce stray reflections within the chamber and
should be cooled to reduce dark current. (The term dark current is
used to describe the radiation signal produced by the thermal emission
from the optical components themselves.)

Estimations of the radiation contributions of various optical compo-
nents for several operating conditions are listed in Table 8. How-
ever, these dark current contributions will exist and, hopefully,
remain constant during both source and reference viewing. A measure
of dark current can be obtained by closing both the source and
reference apertures and could therefore be eliminated by zero adjust-
ment of the detector system during calibration procedures.

TABLE 8

ESTIMATIONS OF SOURCES OF DARK CURRENT FOR OPTICAL SYSTEM

Source	Rate of Energy Deposition onto Detector having 1/2" Diameter
Emitted by detector at 200°R and reflected by ellipsoidal mirror back to detector	5×10^{-8} BTU/sec
Emitted by detector at 700°R and reflected by ellipsoidal mirror back to detector	7×10^{-6} BTU/sec
Emitted by ellipsoidal mirror at 300°R	2×10^{-6} BTU/sec
Emitted by ellipsoidal mirror at 535°R	2×10^{-5} BTU/sec
Emitted by base and side of reflection cavity at 300°R	6×10^{-6} BTU/sec
Emitted by pass thru at 300°R	8×10^{-7} BTU/sec

76

A second source of error is that related to multiple reflections within the chamber of radiation initially incident on the detector from the target and reference. The magnitude of the reflected portion varies (possibly by a factor of 5) for source and reference and may be of the order of 10^{-5} to 10^{-6} BTU/sec. The effect is minimized by increasing the absorptance of the detector until it is effectively black ($\epsilon \approx 1$). Initial calibration of the system with a reference black body simulating the source and with a pass-through aperture of the type expected to be in use in the final system will indicate the magnitude of this error and possibly allow for its correction.

DIRECT VIEWING

Except for the mirror reflector the direct viewing system (figure 21) requires the same design approach as mentioned for mirror optics in connection with multiple reflection, dark currents and cooling.

The sensor can be made adjustable along the optical axis of the instrument which will change the area viewed and thus make the pyrometer selective in this respect.

It appears possible to calibrate this type of instrument in a laboratory by means of a simulator utilizing a black body source.

The conceptual design of the direct viewing method is discussed further in the following section: Final Pyrometer System.

SHELL, AS IN FIG.20

ELECTRICAL
CONNECTOR

.880

FOR SENSOR DETAILS
SEE FIG.12

HYDROGEN COOLING INLET
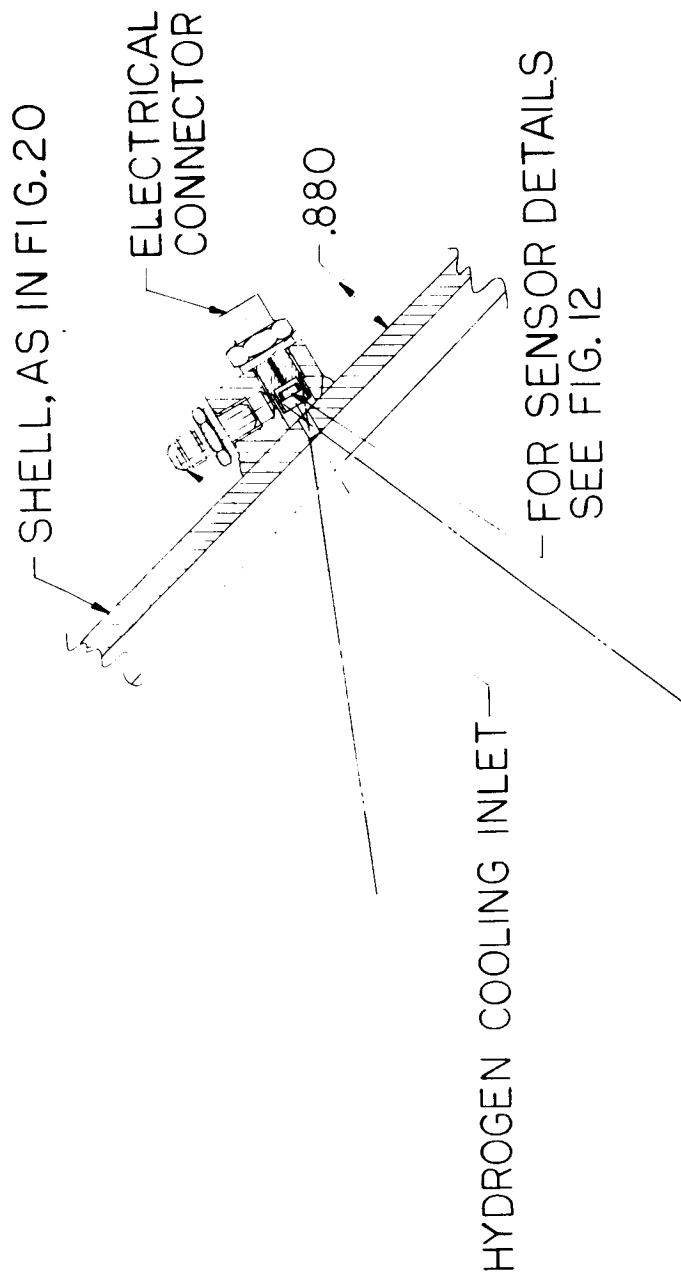
FIGURE 21. RADIATION PYROMETER, DIRECT VIEWING

78

FINAL PYROMETER SYSTEM

The study thus far has been concerned with evaluation and selection of components for the total radiation pyrometer. This section deals with the final electrical pyrometer system recommended to demonstrate "proof of principle" and to be used for experimental study in connection with resolving problem areas.

The specific items covered are error analysis, design and operating problem areas, suggestions and recommendations for resolving problem areas and testing a minimum radiation pyrometer system.

ERROR ANALYSIS

In general the output of the sensing device is a function of many parameters in addition to source temperature. The attainable precision of temperature measurement is limited by the non predictable variations of factors which affect the output of the sensing system. The purpose of this error analysis was to evaluate the relative effect of these factors on sensor output and, if possible, to estimate the probable precision of temperature measurement which can be obtained.

The output of the system may be represented by a function of the form

$$\Delta E = f(X_1, X_2, X_3, \ldots X_n)$$

where X_1, X_2, X_3, ... are independent variables
which affect system output

This general nonlinear relationship may be expressed in perturbation form for small independent variable changes by use of the following
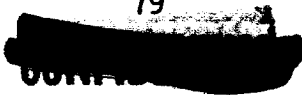
relations

$$d_{\Delta E} = \sum_{i=1}^{n} \left(\frac{\partial f}{\partial x_i}\right) dx_i$$

$$\frac{d_{\Delta E}}{\Delta E} = \sum_{i=1}^{n} \left(\frac{\partial f}{\partial x_i}\right)\left(\frac{x_i}{\Delta E}\right) \frac{dx_i}{x_i}$$

Thus a linearized perturbation equation may be obtained which relates the change of the dependent variable, E, to a change in any independent variable. The coefficients of the linearized equation,

$$\left[\left(\frac{\partial f}{\partial x_i}\right) \frac{x_i}{\Delta E}\right]$$

are often referred to as influence or error coefficients. These coefficients relate fractional change of output to corresponding fractional changes in any independent variable. Correspondingly the variance of any independent variable can be converted to a corresponding variance in the output. The resulting linearized perturbation equation for the final pyrometer system is

$$\frac{d_{\Delta E}}{\Delta E} = \frac{dK}{K} + 4\frac{dT_s}{T_s} - \frac{dk_u}{k_u}$$

$\qquad\qquad$ THERMOELECTRIC $\quad$ SOURCE $\qquad$ HEAT SINK
$\qquad\qquad$ CONSTANT $\qquad\qquad$ TEMP. $\qquad\quad$ RESISTANCE

*Refer to Appendix C for derivation

$$+ \frac{dA_u}{A_u} \qquad + \frac{dx_u}{x_u} \qquad + \frac{d(AF)}{AF}$$

CONDUCTION FLOW   CONDUCTION FLOW   VIEW
PATH AREA   PATH LENGTH   FACTOR

$$+ \left(\frac{q_r}{q_{en} + q_s} \right) \frac{dq_r}{q_r} + \frac{d(AF T_s^4)}{AF T_s^4} + \frac{d\epsilon}{\epsilon} - \left(\frac{q_{conv.}}{q_K + q_{conv.}} \right) \frac{dq_{conv.}}{q_{conv.}}$$

GAMMA   HOT SPOT   SOURCE   CONVECTION
HEATING   TEMP.   EMISSIVITY   HEATING

The first three factors in the above equation (thermoelectric constant, source temperature and heat sink resistance) are expected to vary during normal operation. The variation of thermoelectric constant with target temperature can be expressed as

$$K = a_{TC} + b_{TC} \, T_t$$

then
$$\frac{dK}{K} = \frac{b_{TC}}{a_{TC} + b_{Tt}} \, dT_t$$

Over the range of $460°R$ to $760°R$ the thermoelectric constant in millivolts per degree rankine is

$$K_1 = .0220 + 3.5 \times 10^{-6} \, T \text{ millivolts/}°R \quad \text{(refer to Appendix}$$
$$\text{C)}$$

The variation of the thermoelectric coefficient with target temperature caused by source temperature variations is predictable by calibration. However, sink temperature variations which are not predictable also affect target temperature proportionally.

The effect of a change in reference heat sink temperature on a single foil thermocouple can be expressed as

$$\frac{d \Delta E}{\Delta E} = -\frac{dT_r}{(T_t - T_r)} - \frac{T_r}{(T_t - T_r)} \cdot \frac{dT_r}{T_r} \qquad \text{(refer to Appendix C)}$$

Thus for design values of $T_r = 500^{\circ}R$ and $T_t = 792^{\circ}R$ the influence factor or error coefficient can be expressed as

$$\frac{d \Delta E}{\Delta E} = -1.716 \frac{dT_r}{T_r}$$

so for a 1% change in dT_r ($\pm 5^{\circ}R$)

$$\frac{d \Delta E}{\Delta E} = .01716$$

Therefore a 1% change in T_r yields a 1.72% variation in ΔE at $5000^{\circ}R$.

This source of error can be reduced to a limit determined by the precision of heat sink temperature control.

The effect of a change in reference heat sink temperature on a double foil thermocouple (refer to figures 11 and 12) is essentially eliminated because the two foil thermocouple elements are connected in opposition and therefore changes in the heat sink temperature are

82
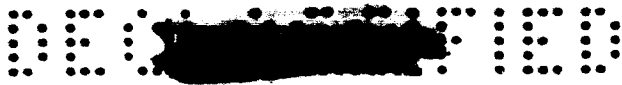
nulled out. However if there is a slight variation between the target heat sink temperature and the reference heat sink temperature then the error due to this small change in heat sink temperature will have the same effect as that noted above for the single foil thermocouple. Equations applicable to the dual foil thermocouple for reference temperature variation are presented in Appendix C.

The error due to gamma heating for the single element (foil is in electrical contact with the heat sink) is given by the expression

$$\frac{d \, \Delta E}{\Delta E} = 100 \, d q_\gamma$$

(refer to Appendix C)

The gamma heating error will have a proportional effect on the single foil thermocouple similar to that noted for the reference temperature variation but this error can also be reduced by the use of a dual foil thermocouple with both foils exposed to identical nuclear radiation conditions. The estimated magnitudes and effects of gamma heating are discussed in the section on Sensor Analysis; calculations pertaining to gamma heating are presented in Appendix C. The gamma heating values used in the error analysis were ratioed over the operating range by an approximate equation which describes the engine temperature – flow relationship for constant pump specific speed. (Refer to Appendix C).

Estimates of convection error were made for both natural and forced convection. It should be noted that the convection error was calculated for convection heat flow across the sensor which is loacted in a cavity away from the chamber gas stream. The heat transfer value calculated for natural convection was 0.445×10^{-3} BTU/sec. This value

can be reduced to .311 x 10^{-4} BTU/sec. if the effective length of gas flow can be reduced by recessing the sensor. Forced convection heating was calculated for gas velocities of 10 in/sec and 100 in/sec across the face of the foil thermocouple. The respective heat flow values calculated for these conditions were 0.82 x 10^{-3} BTU/sec and 2.3 x 10^{-3} BTU/sec.

The influence or error coefficient for convection heating is

$$\frac{d \Delta E}{\Delta E} = -.311 \times 10^{-2} \frac{dq_{conv.}}{q_{conv.}} \qquad \text{(refer to Appendix C)}$$

The conduction flow path length and conduction flow path area are factors that can be controlled in fabrication. For a .001 inch foil and a tab width of 0.026 inch the error coefficient $1/A_\mu = 1/2.6 \times 10^{-5}$ or 2.85 x 10^4 and for the path length the error coefficient $1/X_\mu = 1/.010$ or 100. The combined error factor due to the conduction heat flow can be expressed as

$$\frac{d \Delta E}{\Delta E} = 2.85 \times 10^4 \, d A_\mu + 100 \, d X_\mu$$

The significance of this expression is that the output voltage is extremely sensitive to the heat sink conduction path area as evidenced by the large value of 2.85 x 10^4. This means that close tolerances must be held on this item if the desired voltage output range is to be obtained. For example, a 0.1 mil tolerance on a 1.0 mil thick thermocouple foil the output voltage change for 5000°R would be

$$d(\Delta E) = \Delta E \frac{d A_\mu}{A_\mu} = 6.6 \, mv \left(\frac{0.1}{1.0} \right) = 0.66 \, MV$$

84

where the full voltage output is only 6.6 millivolts giving a 10% variation in desired full range ΔE. It should be noted however that tolerance of the order of $\pm 30 \times 10^{-5}$ inch can be attained for the foil dimensions required. These factors (conduction flow path length and area) do not affect measurement precision directly because their effect can be accounted for during system calibration.

The view factor errors can arise from area change in the pass thru, mirror degradation, misalignment of focus area and sensor. This factor is calculated later in this section using assumed values.

The effect of a hot spot in the core can be determined from the incremental change in $(AFT_S)^4$. Consider a hot spot core temperature of $5500^\circ R$ over 10% of the area viewed with the rest of the core at $5000^\circ R$ then the incremental increase in AFT_S^4 is

$$d\left(AFT_S^4\right) = AF\left[0.9 \times (5000)^4 + 0.1(5500)^4\right]$$

so that $d\left(AFT_S\right)^4 / AFT_S$ = .0464 which is the incremental change of output voltage. If the total surface temperature had increased uniformly to give a 4.64% increase in E, the new surface temperature would have been $5062^\circ R$, starting from $5000^\circ R$. Thus the system will be relatively insensitive to hot spots.

Emissivity will vary with temperature and possibly time and nuclear radiation. Its temperature dependence for a particular core material and core configuration is shown in figures 17 and 18.
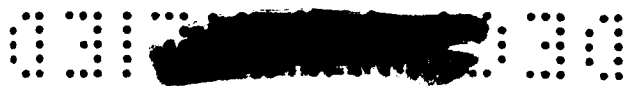
A change in emissivity which may occur during operation and which is not a repeatable function of temperature will reduce system precision. No attempt was made to estimate possible random emissivity change magnitudes. This will have to be determined experimentally.

Because it is difficult to make any reasonable estimates of the system error without experimental data, a one percent change was assumed in each of the operating parameters with the exception of emissivity. The estimated precision with which emissivity can be measured over the temperature range of interest was assumed to be the emissivity error. The percent change assumed for four temperature points is as follows:

Source Temperature	% Change in Emissivity
5000°R	$\pm 4.5\%$
4000°R	$\pm 3\%$
3000°R	$\pm 3\%$
2000°R	$\pm 2\%$

Calculations were made in order to show the relative magnitude of the error factors. (refer to Appendix C)

The influence coefficients for the operating variables discussed are presented in Table 9. The operating variables are also grouped into non predictable errors which are assumed random and potential errors which may be eliminated by the process of calibration. These are summarized in Tables 10 and 11 respectively for 5000°R operating conditions. The data indicate that the largest relative errors result from changes in surface emissivity, reference temperature, conduction flow path length and conduction path area. The view factor physical dimensional effects may be calibrated out during an initial calibra-
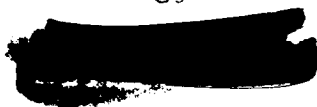
TABLE 9

INFLUENCE COEFFICIENTS FOR OPERATING VARIABLES AT NOMINAL POWER AND 5000°R

Ractional Change in Output Voltage

$$\frac{d(\Delta E)}{\Delta E}$$

Effect of Emissivity

$$1\,\frac{d\epsilon}{\epsilon}$$

Effect of View Area

$$1\,\frac{d(AF)}{AF}$$

Effect of Gamma Heating

$$.04 \times 10^{-2}\,\frac{d(q_r)}{q_r}$$

Effect of Hotspot Temperature

$$1\,\frac{d(AF\,T_s^4)}{AF\,T_s^4}$$

Thermoelectric Constant

$$1\,\frac{dT_e}{T_e}$$

Heat Sink Temperature

$$1.716\,\frac{dT_r}{T_r}$$

Convection Heating

$$.311 \times 10^{-2}\,\frac{dq_{conv}}{q_{conv}}$$

TABLE 10

NON PREDICTABLE ERROR, CHANGE IN INDICATED TEMPERATURE ASSUMED FOR

A GIVEN PERCENT CHANGE IN VARIABLE AT 5000°R

Variable	Incremental Change of Variable (%)	Error Coefficient	Dimensionless Incremental Change in EMF $(d\Delta E_i/\Delta E)$	Indicated Temperature Change $\frac{T_S}{4}\cdot\frac{d\Delta E_i}{\Delta E}$ $(dT_S =)$
Surface Emissivity	.045	1	.045	± 56.2°R
*Heat Sink Temperature	.01	-1.716	.0176	± 21.5°R
*Gamma Heating	.01	$.22 \times 10^{-4}$	$.04 \times 10^{-4}$	± 0.005°R
Convection Heating	.01	$-.311 \times 10^{-2}$	$-.311 \times 10^{-4}$	$\pm .0390$°R

*These values apply to single foil thermocouple only, for the dual foil thermocouple heat sink temperature and gamma heating would be nulled out or essentially zero.

TABLE 11

FACTORS AFFECTING OUTPUT WHICH MAY BE COMPENSATED BY CALIBRATION
INDICATED TEMPERATURE CHANGE FOR ONE PERCENT CHANGE IN VARIABLE AT 5000°R

Variable	Incremental Change of Variable (%)	Error Coefficient	Dimensionless Incremental Change in EMF $\left(\dfrac{d\Delta E}{\Delta E}\right)$	Indicated Temp. Change $\left(dT_S - \dfrac{T_S}{4} \, \dfrac{d\,\Delta E_\lambda}{\Delta E}\right)$
Thermoelectric Constant	.01	1	.01	$\pm 13°R$
Conduction Flow Path Length, X_μ	.01	1	.01	$\pm 13°R$
Conduction Flow Path Area, A_μ	.01	1	.01	$\pm 13°R$
View Factor	.01	1	.01	$\pm 13°R$

These values apply to both single element and dual foil thermocouples

tion; however, dimensional and reflectivity changes may occur during operation. These would appear to be relatively non predictable. Gamma heating effects are insignificant at upper temperature operating levels; below 2000°R the gamma effect can be significant. (Refer to Table 1)

The assumptions made are purely arbitrary but the results are adequate for showing relative effects for both foil thermocouple configurations (single element and twin element), and for estimating the probable precision of temperature measurements which can be obtained.

The significant estimated errors and the corresponding measurement precision (rms value) are plotted as a function of temperature in figure 22 for the single element sensor. From these data it is evident that the single foil thermocouple design will not meet the specified measurement precision unless the heat sink temperature can be controlled to a tolerance of better than $\pm 5^{\circ}$R. For a 1.0% variation in the heat sink temperature ($\pm 5^{\circ}$R) the output voltage will vary from 0.44% at 5000°R to 10% at 2000°R. Because this sensor requires such a precisely controlled reference temperature (complex control device) it would not be practical for this application. The estimated gamma heating and heat convection error do not have a significant effect on the performance of the single foil thermocouple, refer to figure 23.

For the dual foil thermocouple configuration the voltage output due to the surface emissivity variation is essentially the root mean square value, figure 24. The gamma heating and heat sink temperature errors are less than the values noted in figure 22 for the single foil thermocouple because the twin foil thermocouples as already mentioned are connected in opposition, thus reducing these factors to a minimum

90
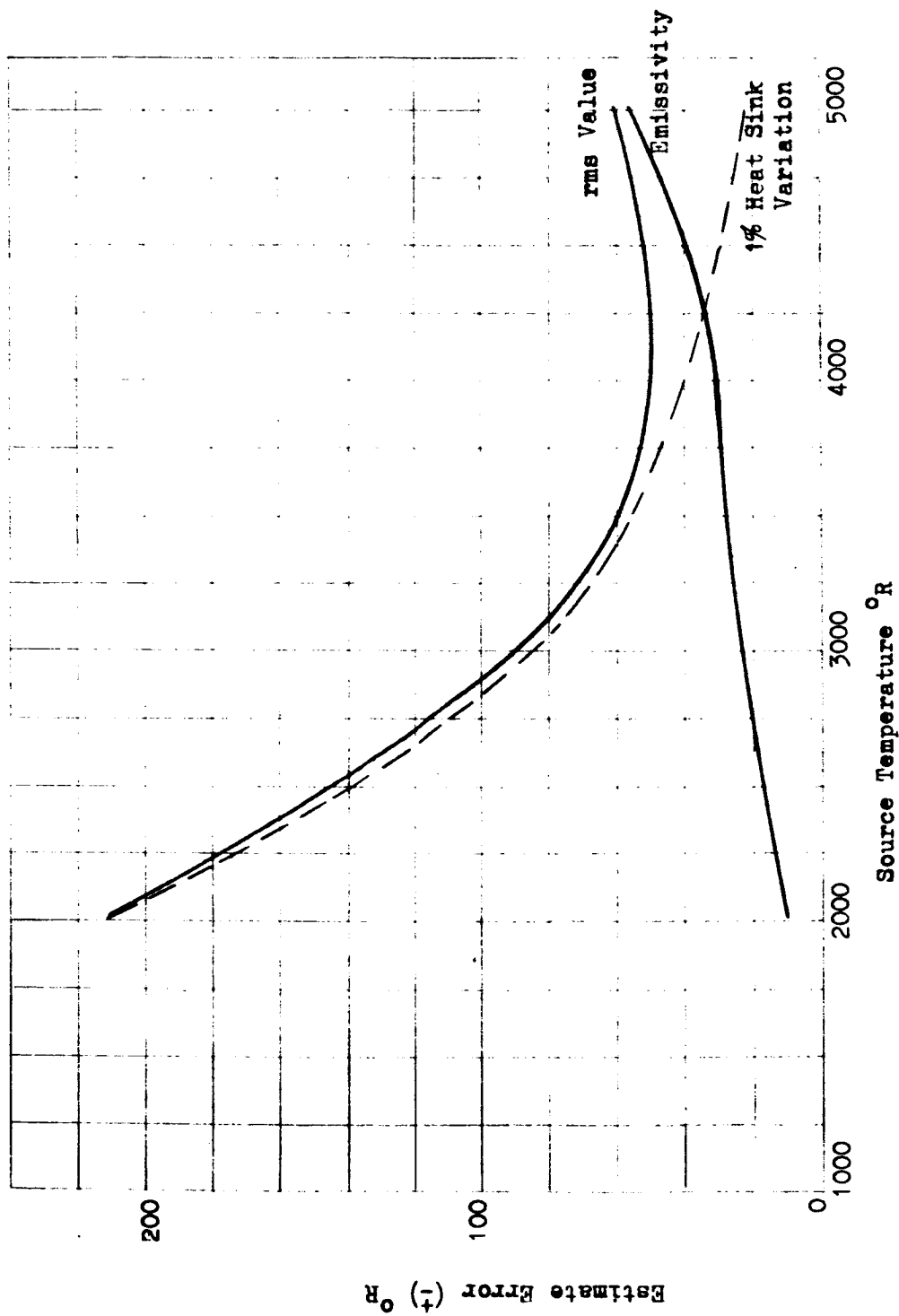
FIGURE 22. SIGNIFICANT ESTIMATED ERROR FOR SINGLE FOIL
THERMOCOUPLE
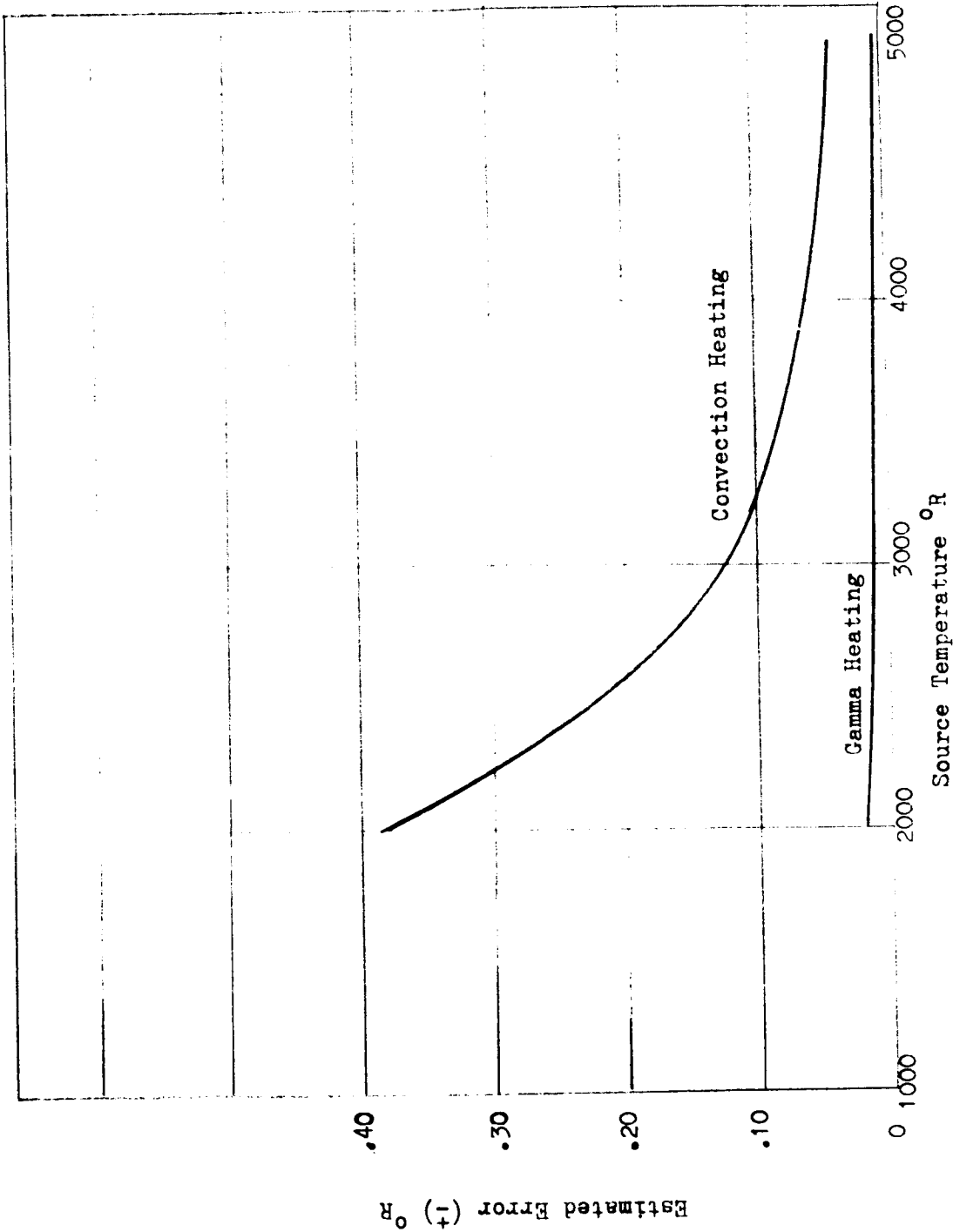
FIGURE 23. ESTIMATED ERROR OF GAMMA AND CONVECTION HEATING
(FOR SINGLE ELEMENT SENSOR)
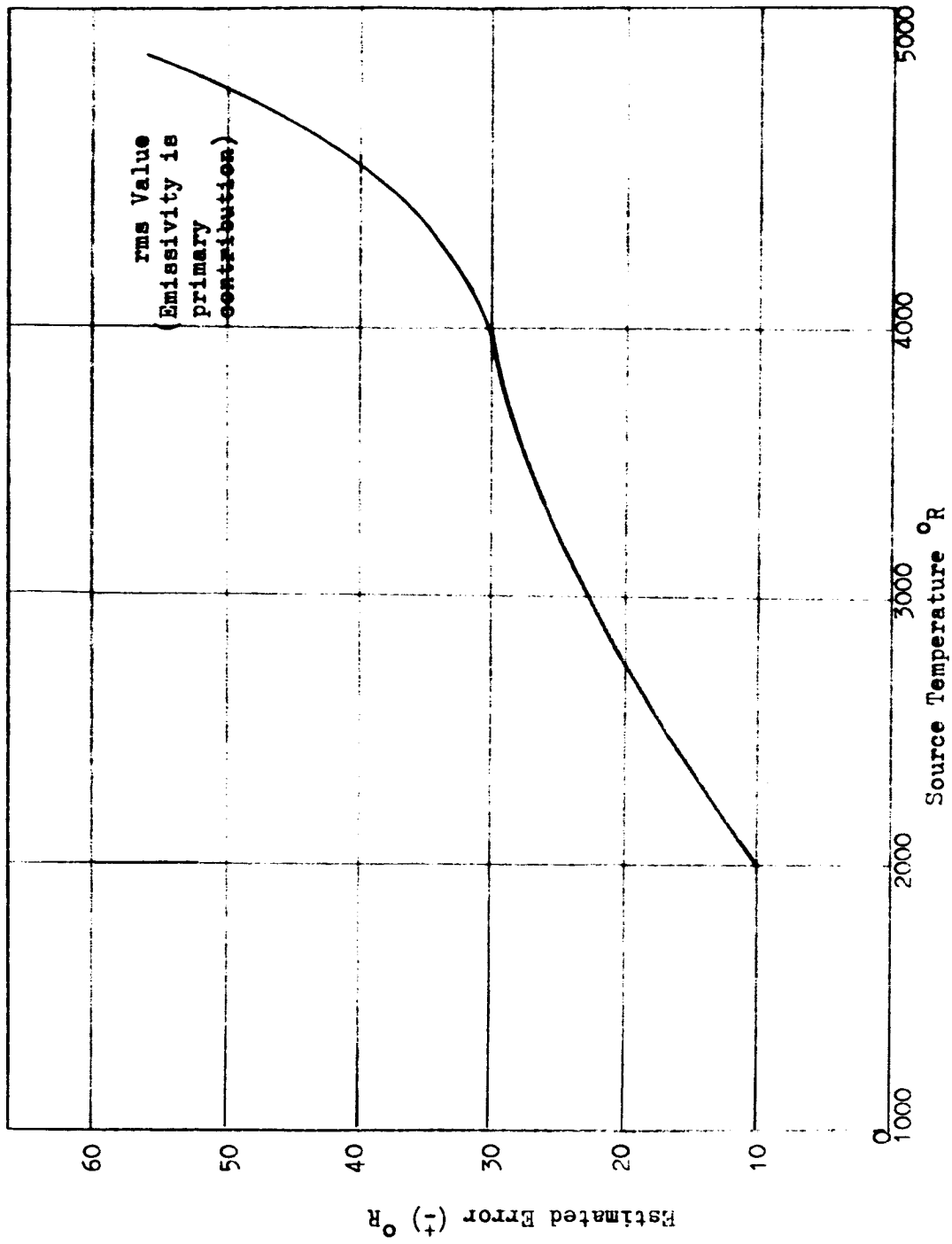
FIGURE 24. SIGNIFICANT ESTIMATED ERROR FOR DUAL FOIL THERMOCOUPLE

(essentially zero).

It is recognized that perfect compensation will not be attained but will be a function of the thermoelectric power at the operating temperatures of the foil thermocouple. For example, given the temperature-millivolt data for the Chromel vs Alumel thermocouple (22), the average thermoelectric output dE/dT for the temperature range of 460° to 560^oR is .0220 MV/^oR and over the temperature range of 660° to 760^oR it is .0227. The difference of these two values divided by the average Δ T or 200^oR is 3.5×10^{-6} MV/^oR. This is an approximate value which represents the difference in thermoelectric power for a heat sink temperature of 510^oR and a target temperature of 710^oR. However, since the thermoelectric constant is predictable this is an error that could be removed or compensated by calibration.

The one error factor which could influence the final output voltage is the forced convection heating which will be proportional to the gas velocity across the sensor foil.

Based on the assumptions made and the error factors considered, a precision of $^+_-50^oR$ variation appears reasonable for the dual foil T.C. over the temperature range of 2000^oR to 5000^oR. It should be recognized further that this precision does not include conditioning equipment. At the lower temperature limit of 1000^oR the signal to noise ratio is below the operating range of the foil thermocouple but some improvement may be possible by restricting the bandwidth of the signal and by filtering out the high frequencies (refer to section on Sensor Analysis). The estimated measurement precision and influence factors that were considered in this section are applicable to both

the direct viewing system and the reflection optics.

RECOGNIZED PROBLEM AREAS

The problems associated with the development of a radiation pyrometer are essentially materials problems arising from exposure to a high intensity nuclear radiation environment. The specific areas which require investigation prior to hardware development are as follows:

1. Behavior of the foil thermocouple in a nuclear environment.
2. Nature and extent of degradation of mirrors in the nuclear environment if reflection optics is employed in the viewing system.
3. Significant influence factors in the measuring system: emissivity of the source and view factor.
4. Limitations and possible modification of signal conditioning equipment.
5. Purge system to eliminate chamber gas effect.

It is important to determine the radiation effects on the transducer since it does introduce an error into the measurement when the thermal radiation (gamma) incident on the detector is a significant fraction of the energy received from the source. Heating of the detector by gamma irradiation can be reduced by shielding the detector or by using a compensating element.

Because of the possibility that some (probably slight) degradation may occur in the reflectance of the mirrors in the reflection type optical system, further study should be made of the nature and extent of such degradation. (A funnel type reflector can be used in the direct viewing system to direct the incident energy onto the detector surface, refer to figure 11).

It was found from the error analysis that the most significant influence factors in the measuring system are surface emissivity, view factor and possibly convection gas effects. As the velocity of forced convection across the foil thermocouple is increased from the calculated value (100 in/sec), the error due to convection heating will increase proportionally. (Refer to equations in Appendix C). These factors are difficult to predict and therefore should be checked experimentally. Vibration could be troublesome in the optical system but it appears that the necessary optical components and their mountings can be made sufficiently rugged to withstand the physical environment. Pressure equalization will be used in the measurement system to minimize the effect of pressure transients on the sensing element (foil). Pressure tests of the copper foils at Rocketdyne indicate that a copper disc of 0.3 inch diameter and .001 inch thick will withstand a differential pressure of 65 psi.

Amplification of the foil thermocouple output will be required preferrably at the point of measurement. State-of-the-art electrical conditioning equipment is marginal for the nuclear environment specified without some modification or redesign. The magnetic amplifier appears to hold more promise for this application if the semi conductor diodes in the output circuit can be replaced with vacuum tubes. Cable and connectors are available for short term operation in the specified nuclear environment.

One method for limiting the gamma heating and radiation damage effects on the conditioning equipment is to take advantage of available shadow shielding on the engine system in the area near the point of measurement and above the reactor shield. Another approach which is

within the present state-of-the-art is to actually design for degradation of amplifier characteristics for a given operating time.

RECOMMENDATIONS

It is evident from this study that there are two areas which require attention before a full scale hardware development program can be initiated.

1. The problem areas noted in the previous section should be resolved experimentally by nuclear irradiation testing of components.

2. The final pyrometer system should be designed and fabricated to demonstrate "proof of principle".

It is felt that the problem areas and the "proof of principle" tests could be handled concurrently. A minimum pyrometer system would be fabricated to demonstrate proof of principle. The "minimum system approach" means building a basic pyrometer (detector and viewing system), testing it and adding operating features and modifications as required based on test results. Following this approach the direct viewing instrument figure 21 is recommended for the proof of principle tests because it is the less complex of the two viewing methods. Reflection optics would be considered for the viewing system if the nuclear irradiation tests showed that nuclear shielding is required for satisfactory operation of the sensing element. Such a system in this particular case would include the essential components: detector, viewing optics, pass thru and facilities type support equipment. A reference black body and associated equipment would not be included since the purpose of the test is to demonstrate initially the operation of the sensor-viewer combination only with the

hope that cyclic calibration during operation would not be required. The proof of principle or feasibility testing would be done in a non-nuclear environment. Concurrent with this testing it is recommended that the problem areas be investigated experimentally.

It is suggested that the problem areas with the exception of changes in emissivity and view factor be studied by irradiating selected components of the pyrometer in the specified nuclear radiation environment. This will provide radiation effects data relative to the problem areas.

The influence of emissivity and view factor under operating conditions would of course have to be determined by testing the pyrometer instrument on a nuclear rocket engine or under simulated conditions. The proposed experimental model is presented in figure 21. The radiation pyrometer is contained in an envelope of approximately 2 in. by 2 in. by 1.5 in. This envelope or case is welded to the converging section of the nozzle. The sensing element can be designed integrally with a threaded connector to mate with the case receptacle. For test purposes the nozzle section shown would be replaced with a suitable base and pass thru which would approximate the nozzle configuration.

The sensor is a "back-to-back" foil design, figure 12. It is shown as an integral part of the direct viewing pyrometer in figure 21. The radiant energy (thermal plus gamma radiation) will be incident on the first sensor or the foil exposed directly to the source temperature causing a heat rise in the first foil. The gamma radiation will pass through the first foil essentially unattenuated and cause a temperature rise in the second foil. The heat rise due to the gamma energy
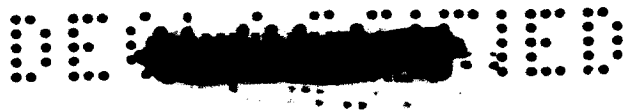
in each foil will be cancelled out or reduced to an insignificant value because the two sensors are connected in opposition. The separation between the two sensing elements must be such that there is no heat exchange between the two foils. A separation distance of 0.5 inches is probably adequate to prevent this interaction. An alternate approach that can probably be used to minimize this effect is to interpose a metal shield (aluminum) between the two foils. This arrangement would permit gamma radiation to pass through to the second sensing element but the aluminum would stop the thermal energy from reaching the second sensor or the compensating element.

The thermocouple materials that would be used initially are chromel alumel (refer to Section on Sensor Analysis for design data). Other materials can of course be selected for the final design; materials which have a high thermoelectric power and are highly resistant to nuclear radiation are needed. Copper constantan was used by Gardon because the change in thermoelectric power with temperature cancelled the change in thermal conductivity. The change in the latter is not a significant factor for chromel because the conductivity of chromel over the temperature rise ($290^{O}R$) is not a strong function of temperature. The output voltage – source temperature relationship for chromel alumel is given in figure 13.

The cooling requirements for the viewing system are discussed in the section on viewing system design.

The initial sensor design has a 0.1 in. foil diameter and a reference temperature of $500^{O}R$. For a 3/16 inch pass thru the energy incident on the dual sensor configuration as well as the viewing area can be varied by making the sensor adjustable along the optical axis. One

method of collection this energy is to increase the diameter of the foil and to reduce the heat sink to cryogenic temperature, about $80^{\circ}R$ in order to preserve the 0.1 time constant. An alternate approach which appears to be operationally more desirable is to recess a 0.1" diameter foil in an "optical funnel" (figure 11)which would direct the available energy onto the highly reflecting surfaces to the foil located at the apex of the funnel or cone (0.1 inch disc surface). In this configuration it would be possible to maintain a heat sink temperature of $500^{\circ}R$ without any degradation in time constant. The total temperature rise of the transducer in each case would be $292^{\circ}R$.

The latter approach has the advantage of a less critical heat sink temperature control problem. Room temperature operation would also simplify development testing and application operation. The coolant system for this transducer must be designed to minimize dark currents, to maintain a constant heat sink temperature and finally to serve as a purge for the pass thru. This particular problem has not been studied in detail but it appears that adequate cooling can be realized if the hydrogen coolant flow is directed initially around the sensor annulus and then exhausted into the nozzle gas stream. It has been estimated that the walls surrounding the sensor and the pass thru should be at a temperature of $300^{\circ}R$ to minimize dark currents. Cooling of the pass thru should not be a problem because the coolant flow in the nozzle tubes will maintain the surface of the pass thru at a temperature of less than $300^{\circ}R$.

A factor in the design of the coolant system is to minimize convective heat transfer to the sensor. A further reduction of convection heat can be accomplished by recessing the sensor in its container, provi-

ding an optical funnel as already described or installing a highly reflective "egg crate" configuration in front of the sensor.

The experimental radiation pyrometer model, figure 21 would be tested initially in a non-nuclear environment to demonstrate "proof of principle". For the purpose of this test the pass thru would have to be cooled, therefore the cooling system would have to be modified or a separate cooling system designed to keep the pass thru at the proper temperature.

It is suggested that an adaptor be fabricated that would house a black body or an actual reactor core specimen to simulate the source temperature. These simulators could be installed alternately over the pass thru and thus provide a variable source temperature for determining the pyrometer characteristics. The model would be cali- brated with a standard black body source and a laboratory optical pyrometer. Upon successful completion of this experiment the same source temperature adaptors could probably be used for testing in an irradiation facility.

It is anticipated that for the non-nuclear tests the conditioning equipment would be of the facilities type. Support equipment required for the radiation experiment would be based on specifications and safety requirements of the irradiation facility selected for this experiment. In testing the instrument in a nuclear environment all problem areas noted in this section would be considered and evaluated except the view factor which would require operating the device in an actual engine system or a simulated reactor-nozzle combination.

It should be noted that the viewing system will also accommodate with minor modification the heat exchanger sensor which was one of the sensors analyzed in this study. This sensor can be designed to intercept the radiant energy with the recommended viewing system.

The alternate view system proposed (reflection optics) is described in the section on viewing system design.

REFERENCES

1. Levy, P. W., "Reactor and Gamma Ray Induced Coloring of Corning Fused Silica," J. Phys. Chem. Solids, Pergamon Press 1960, Vol. 13, pp. 287-295.

2. Conn, G. K. T., D. G. Avery, <u>Infra Red Methods, Principles and Applications</u>, Academic Press, New York and London 1960, pp. 28-49.

3. <u>Space Materials Handbook</u>, ML-TDR-64-40, Air Force Materials Laboratory, Research and Technology, Division Air Force Systems Command, Wright-Patterson Air Force Base Ohio, DDC 440-234, March 1964, pp. 187-205.

4. Crawford, J. H., M. C. Wittels,"A Review of Investigations of Radiation Effects in Covalent and Ionic Centers," <u>Proceedings Internal Conference on Peaceful Uses of Atomic Energy</u>, Vol. 7, pp. 654-665.

5. Levy, P. W., "Reactor and Gamma-Ray Induced Coloring in Crystalline Quartz and Corning Fused Silica, <u>Journal of Chemical Pysics</u>, Vol. 23A, 1955, pp. 764-5.

6. Gardon, R., "An Instrument for the Direct Measurement of Intense Thermal Radiation," Review of Scientific Instruments, Vol. 24, May 1953, pp. 366-377.

7. Harrison, Thomas R., <u>Radiation Pyrometry and its Underlying Principles of Radiant Heat Transfer</u>, John Wiley & Sons, Inc. New York, 1960, p. 23.

8. Mouly, P. G., "An Impedance Bridge for Surface Temperature Measurement," American Institute of Electrical Engineers, <u>Communication and Electronics</u>, No. 44, September 1959, pp-388-393.

9. Hollander, L. E., "Pyroelectricity for Fast Response, Black Body Thermal Power Measurement," Instrument Society of America Proceedings, <u>9th Annual ISA Aerospace Instrumentation Symposium</u>, San Francisco, California, May 6-8, 1963, Vol. 9, 1963.

10. McAdams, W. H., <u>Heat Transmission</u>, McGraw-Hill Book Company, New York, 1954, pp. 2-30.

11. Baumeister, T., Editor: <u>Mechanical Engineers Handbook</u>, McGraw-Hill Company, New York, 1958, pp. 4-110, 4-99, 4-7.

12. Jakob, M., <u>Heat Transfer</u>, Volume I, John Wiley and Sons, Inc., New York, 1944, pp. 6-9, 23-52, 443-480.

13. Rockwell, J., (Editor), <u>Reactor Shielding Design Manual</u>, United States Atomic Energy Commission, Naval Reactors Branch, Division of Reactor Development, Washington D.C., T1D-7004, March 1956, pp. 37, 353 and 346.

14. Blizard, E. P., L. S. Abbot, <u>Reactor Handbook</u> Volume III
    Part B Shielding, Interscience Publishers, New York 1962,
    pp. 105-115.

15. Kelly, M. J., W. W. Johnston, C. D. Bauman, "The Effects of
    Nuclear Radiation on Thermocouples," <u>Temperature-Its Measurement</u>
    <u>and Control in Science and Industry</u>, Vol. 3, Part 2, Reinhold
    Publishing Corporation, New York, 1962, pp. 265-269.

16. Browning, Jr. W. E., C. E. Miller, Jr., "Calculated Radiation
    Induced Changes in Thermocouple Composition," <u>Temperature - Its</u>
    <u>Measurement and Control in Science and Industry</u>, Vol. 3, Part 2,
    Reinhold Publishing Corp., New York, 1962, pp. 271-276.

17. Levy, G. F., R. R. Fouse and R. Sherwin, "Operation of Thermo-
    couples under Conditions of High Temperature and Nuclear Radia-
    tion", <u>Temperature - Its Measurement and Control in Science and</u>
    <u>Industry</u>, Vol. 3, Part 2, Reinhold Publishing Corp., New York,
    1962, pp. 277-282.

18. William, K. C., "Status Report of the Investigation of Thermo-
    couple Materials for Use at Temperatures Above $4500^{\circ}F$", <u>SAE</u>
    <u>National Aeronautics and Space Engineering and Manufacturing</u>
    <u>Meeting</u>, Los Angeles, California, September 23-27, 1963.

19. Etherington, H., "Radiation Damage to Solids," <u>Nuclear Engineer-</u>
    <u>ing Handbook</u>, McGraw-Hill Book Company, Inc., New York 1958,
    Sec. 10, p. 123.

20. Blan and Fisher, <u>Radiative Transfer from Solid Materials</u>, The McMillan Company Inc., New York 1962, pp. 3-7.

21. Etherington, H., "Radiation Damage to Solids," <u>Nuclear Engineering Handbook</u>, McGraw Hill Book Company, Inc., New York 1958, Sec. 10 p. 105.

22. Hodgman, C. D. Editor, <u>Handbook of Chemistry and Physics</u>, Chemical Rubber Publishing Co., Cleveland, Ohio, 1953-54, p. 2369.

23. Shapiro, A. H., <u>The Dynamics and Thermodynamics of Compressible Fluid Flow</u>, Volume 1, The Ronald Press Company, New York, 1953, p. 85.

APPENDIX A[*]
SYMBOLS USED IN TEXT AND APPENDICES

SYMBOL	MEANING	UNITS
A	Area	in^2
C	Specific Heat	$BTU/lbm-^oR$
D	Diameter	in.
E	Voltage	volts
F	View Factor	
f	Fraction of Energy	
g	Gravitational Factor	in/sec^2
h	Heat Transfer Coefficient	$BTU/sec-in^2-^oF$
k	Thermal Conductivity	$BTU/sec-in^2-^oF-in^{-1}$
K	Gain Factor	
ℓ	Length	in.
L	Length	in.
m	Mass	lb
$\dot{m}$	Mass Flow Rate	lbm/sec.
P	Pressure	psi
q	Heat Flow	BTU/sec.
r	Radius	in.
S	Sensitivity	(sss Appendix C)
S	Laplace Transform Variable	
T	Temperature	^oR
t	Time	sec.
U	Overall Heat Transfer Coefficient	$BTU/sec-in^2-^oF$
V	Volume	in^3
X	Thickness	in.

APPENDIX A (CONTINUED)

SYMBOL	MEANING	UNITS
y	Target Thickness (Foil Thermocouple)	in.
Nu	Nusselt Number	
Pr	Prandtl Number	
Re	Reynolds Number	
$\propto$	Thermal Coefficient of expansion	$^{\circ}R^{-1}$
γ	Gamma Heating	BTU/sec.
$\int$	Incremental Value	
Δ	Differential Value	
ϵ	Emissivity	
η	Effectiveness	
μ	Viscosity	lbm/in-sec
ρ	Density	lbm/in^3
σ	Boltzman Constant	$.334 \times 10^{-14} BTU/^{\circ}R^4\text{-sec-in}^2$
τ	Time Constant	sec
e	Electrical Resistivity	ohm-cm
λ	Wave Length	micron
R	Resistance	

* Certain calculations on the foil thermocouple were made using the metric system (c.g.s. units) but the final results were converted into English system.

SYMBOL (SUBSCRIPT)	MEANING
*	Reference Value
a	Distance
b	Distance
e	Equivalent
H	Gas
i	Insulator
m	Maximum
n	Exponent
o	Initial Value
r	Reference Heat Sink
S	Source
t	Target
W	Wall
TC	Thermoelectric Constant
th	Thermal
c	Choked Orifice
D	Transport Delay
conv.	Convection
tS	Between T_t and T_S
rS	Between T_r and T_S
St	Target Heat Sink Temperature
Sr	Reference Heat Sink Temperature
g	Gas
T	Total

APPENDIX B

CALCULATIONS PERTAINING TO OPTICAL VIEWING SYSTEMS

The sample calculations presented here represent the basic methods
employed in the estimations necessary to indicate the feasibility
(or unfeasibility) of optical viewing systems for the total radiation
pyrometer.

CALCULATION OF VIEW FACTOR

The view factor represents that fraction ($F_{A-A'}$) of the total (hemi-
spherical) radiation emitted by a small area A (at temperature T) into
the small solid angle ω subtended at A by area A' located at a
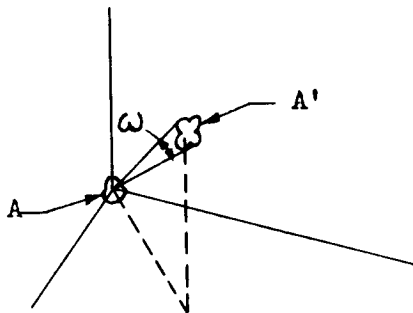distance R from the small emitting area A. (Refer to Figure B-1).

FIGURE B-1, MODEL FOR HEMISPHERICAL RADIATION EMITTANCE

Assume that the area A' is the area of a disc of diameter d; then,
$A' = \pi d^2/4$. For the case where R is large compared to d, the
fraction of the radiation impinging on A' is approximately equal to
the ratio of the area A' to the surface area of the hemisphere of

radius R; or,

$$F_{A-A'} = \frac{\pi d^2/4}{2\pi R^2} = \frac{d^2}{8R^2}$$

(B-1)

For the specific case where A represents a minute core area, where A' represents the area of the pass-thru of diameter 3/16 inch, and R represents the distance (20 inch) from the area A to the pass-thru, the view factor is approximated as:

$$F_{A-A'} = \frac{d^2}{8R^2} = \frac{(3/16)^2}{8(20)^2} = 1.1 \times 10^{-5}$$

CALCULATION OF THERMAL SIGNAL FROM CORE

The thermal signal, E_A, emitted by the core and emerging from the pass-thru and seen by the detector is approximated by use of the following equation

$$E_A = \int_0^A F_{dA} \, \mathcal{E}_{dA} \, \sigma \, T_{dA}^4 \, dA$$

(B-2)

where dA represents a small area of the core which has associated with it a temperature T_{dA}, an emittance $\mathcal{E}_{dA}$, and a view factor F_{dA} with respect to the pass-thru. The symbol σ represents the Stefan-Boltzmann constant. For purposes of estimation, it is assumed that the core is of uniform temperature and emittance and that the view factor does not vary across the core. Then:

$$E_A = AF(\mathcal{E} \, \sigma \, T^4)$$

(B-3)

The area A represents that portion of the area of the core which is in view by the detector.

The sample calculation for Equation B-3 assumes the following values

B-2

for the various parameters:

D = 60"; diameter of area of core in view

F = 1.1×10^{-5} (See Calculation of view factor)

ε = 0.85

T = 5000°R

A = $\pi D^2/4$ = $\pi (60)^2/4$ = 2.8×10^3 sq.in.

The quantity $(\varepsilon \sigma T^4)$ = 9.3×10^5 BTU/sq. ft.-hr.

For convenience, this value is converted to BTU/sq. in.-sec.

$$\frac{9.3 \times 10^5 \text{ BTU}}{\text{Sq. ft-hr}} = \frac{9.3 \times 10^5 \text{ BTU}}{\text{Sq.ft-hr}} \times \frac{1 \text{ hr}}{3600 \text{ sec}} \times \frac{1 \text{ sq.ft.}}{144 \text{ sq.in.}} = \frac{1.79 \text{ BTU}}{\text{sq.in.-sec}}$$

Then:

$$
\begin{aligned}
E_A &= AF (\varepsilon \sigma T^4) \\
&= (2.8 \times 10^3 \text{ sq.in.}) \times (1.1 \times 10^{-5}) \times (1.79) \frac{\text{BTU}}{\text{sq. in.-sec.}} \\
&= 5.5 \times 10^{-2} \frac{\text{BTU}}{\text{sec}}
\end{aligned}
$$

CALCULATION OF PARAMETERS FOR ELLIPSOIDAL MIRROR

Consider Figure B-2, an ellipse of semi-major axis a, of semi-minor axis b, and whose focal points, F' and F'' are separated by a distance 2K. The equation for the ellipse is given by the following equation:

$$\frac{x^2}{a^2} + \frac{y^2}{b^2} = 1 \qquad\qquad (B\text{-}4)$$

The distance, M, between focal points is given by

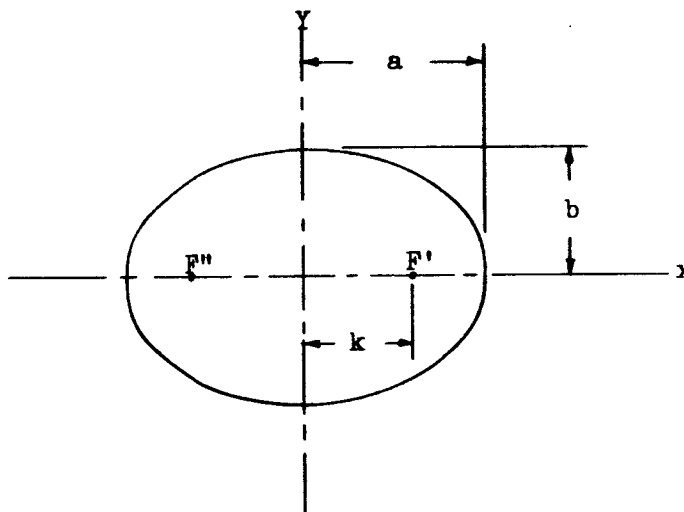$$M \;=\; 2K \;=\; \sqrt{a^2 - b^2} \qquad\qquad (B - 5)$$

FIGURE B-2, ELLIPSOIDAL MIRROR DIMENSIONS

The characteristic parameters, a and b, of the ellipse are determined by the system requirements. Consider Figure B-3.
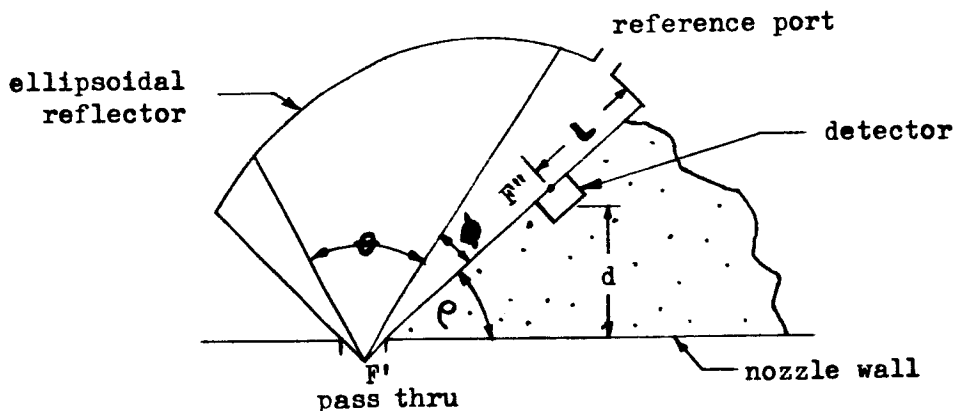
FIGURE B-3, CONCEPTUAL DESIGN-REFLECTION OPTICS

The focal point F' of the ellipsoidal reflector is located at the
nozzle pass-thru; the detector is located at the focal point F'';
the detector base is at a minimum distance d from the nozzle wall.
The angle θ is determined by the energy requirements of the detector
system. The distance d is fixed by the shielding requirements and
detector size. If a reference port is required for calibration then
angle ϕ must be of that size which allows sufficient room at the end
of the ellipsoidal reflector for illumination of the detector by the
reference during calibration.

A mirror assembly with dimensions convenient for shielding and
manufacturing is represented by a 4 inch separation between focal
points (i.e., K=2), by setting d=2 in., and letting L =1.5 in. (i.e.,
a=K+L = 3.5 in.), and ρ = 50°. Since

$$K = \sqrt{a^2 - b^2}$$
$$b = \sqrt{a^2 - K^2}$$
$$b = \sqrt{(3.5)^2 - 2^2} = 2.9"$$

CALCULATION OF THERMAL SIGNAL ARRIVING AT DETECTOR FROM
QUARTZ LENS

Page 58 of the report states:

"A one inch diameter quartz lens at 800°C,
located four inches from a detector of $\frac{1}{2}$ inch
diameter will radiate of the order of 10^{-4} to
10^{-5} BTU/sec onto the detector."

Exact calculation of the energy $E_{dA'}$ received by a small area dA' of the detector should be performed by the following integration.

$$E_{dA'} = \int_{\lambda = -\infty}^{\lambda = \infty} \int_{A=0}^{A=A} F_{dA-dA'} \, \varepsilon_{\lambda \, dA} \, c_1 \lambda^{-5} \left(e^{\frac{c_2}{\lambda T}} - 1 \right)^{-1} d\lambda \, dA$$

$$(B-6)$$

where $F_{dA-dA'}$ represents the view factor from area dA to dA' $\varepsilon_{\lambda \, dA}$ is the spectral emittance of area dA at temperature T $c_1 = 2\pi c^2 h$, (c = speed of light in vacuum, h = Planck's Constant), $c_2 = hc/k$ (k = Boltzmann's Constant).

The total energy received by the detector of area A' is given by the integral of $E_{dA'}$ over the area A'.

$$E_T = \int_0^{A'} E_{dA'} \, dA' \qquad\qquad (B-7)$$

Exact calculations from Eq. B-6 are considered unnecessary at this point in the study; therefore certain simplifying assumptions have been made. These assumptions are noted below.

A) At any specific wavelength and temperature the following equation is valid

$$1 = \alpha_\lambda + r_\lambda + \mathcal{T}_\lambda$$

where α_λ is the spectral absorption, r_λ is the spectral reflectance, and $\mathcal{T}_\lambda$ is the spectral transmission.

It is assumed that the following equation also holds.

$$\alpha_\lambda = \varepsilon_\lambda$$

B-6

For quartz, the spectral transmission of a lens may be expected to be about 90% from the visible region to 3.5μ; the emittance of the lens is then less than 0.1 (i.e., $\varepsilon_1 = 0.1$) in this region. (The lens can probably be considered opaque to radiation emitted by the interior of the lens, since a great portion will undergo internal reflections and not emerge from the surface of the lens.) A black body at $800^\circ C$ emits 44% of its energy at wavelengths below 3.5μ. (For subsequent calculations let f_1 represent this fraction; i.e. $f_1 = 0.44$).

Within the region 3.5 to 5μ the transmission of quartz decreases to nearly zero at 5μ. For this region, the average spectral emittance is taken to be 0.5 ($\varepsilon_2 = 0.5$). A black body at $800^\circ C$. emits 24% of its energy within this spectral region ($f_2 = 0.24$).

From 5μ into the infrared, quartz is opaque, $\mathcal{T}_\lambda = 0$. The maximum emittance for this region is 1 ($\varepsilon_3 = 1$); the remaining 32% of the energy emitted by a black body at $800^\circ C$ is emitted within this region. ($f_3 = 0.32$).

B) For simplification, it is again assumed that the view factor $F_{A-A'}$ is constant over A and A' and is given by

$$F_{A-A'} = \frac{\pi\, d^2/4}{2\pi R^2} = \frac{d^2}{8R^2} = \frac{(1/2)^2}{8(4)^2} = 2\times10^{-3}$$

where d represents the diameter of the lens (d = $\frac{1}{2}$") and R is the separation distance between lens and detector (R = 4").
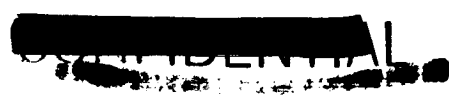
Under these assumptions the total energy impinging on the detector is given by utilization of Equation B-8 and substitution of the appropriate values of the parameters.

$$E_T = (\varepsilon_1 f_1 + \varepsilon_2 f_2 + \varepsilon_3 f_3)(F_{A-A}A)(\sigma T^4)$$

$$E_T = [(0.1)(.44) + (0.5)(.24) + (1)(.32)][2 \times 10^{-3}][\tfrac{\pi}{4}][\tfrac{2.4 \times 10^{-1}}{3600 \times 144}] \, BTU/SEC$$

$$\approx 3 \times 10^{-5} \; BTU/SEC$$

EFFECT OF VARIATION OF SOLID ANGLE OF VIEWING SYSTEM UPON ENERGY ARRIVING AT DETECTOR

The energy received by the detector through the solid angle ω from the source of area A is given by the following equation.

$$E \quad \int_0^A F_{dA} \, \varepsilon_{dA_T} \sigma T^4 dA$$

where F_{dA} represents the view factor from dA to the pass thru at O, T_{dA} is the temperature of the small emitting area da, ε_{dA} is the emittance of the area dA, and σ represents the Stefan-Boltzmann constant. The problem considered here is the estimation of the variation in energy received by the detector caused by a variation in the solid angle ω. For convenience, consider that the solid angle viewed by the detector is formed by rotation of the plane angle θ about the optical axis of the viewing system. Consider Figure B-4.
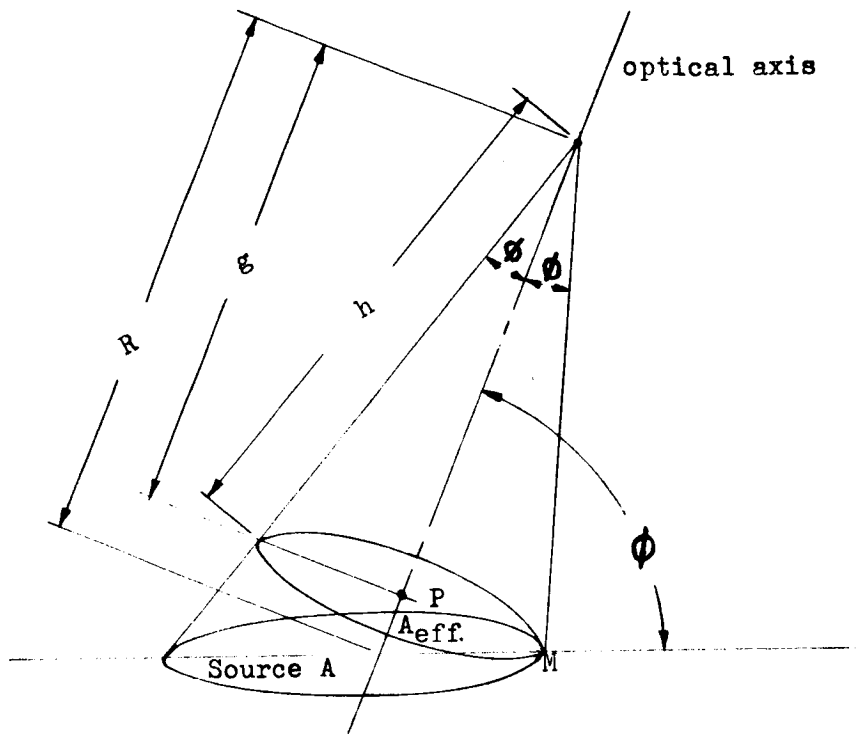
FIGURE B-4 MODEL FOR VIEW FACTOR VARIATION

The area A_{eff} lies in a plane normal to the optical axis and intercepts the plane of the source at point M. A_{eff} subtends the same solid angle as does the area A; or area A can be considered the projection from O of A_{eff} on the source area. A_{eff} is located at a distance h from O when measured along the optical axis; A is at a distance R from the point O when measured along the axis. It is hereby assumed that

$$\int_0^A F_{dA}\, dA = \int_0^{A_{eff}} F_{dA_{eff}}\, dA_{eff}$$

and that ε_{dA_T} is constant across the source which is at a uniform temperature. Therefore:

$$E = \int_0^A F_{dA}\, \varepsilon_{dA_T}\, \sigma\, T_{dA}^{\,4}\, dA$$

$$= \varepsilon_T\, \sigma\, T^4 \int_0^{A_{eff}} F_{dA_{eff}}\, dA_{eff}$$

Variation, V, in the view factor across A_{eff} is indicated by the ratio of the view factor from the point M to that at the point P; or,

$$V = \frac{h^2}{g^2} = \frac{h^2}{h^2/cos^2\theta} = cos^2\theta$$

The variation will be greatest for large angles; for $\theta = 35°$, cos θ = 0.8; $cos^2\theta$ = 0.67; that is, if point P has a relative view factor of 1, point M will have a view factor of 0.67. For purposes of estimation, it will be assumed that the view factor is constant.

Therefore,
$$E = \varepsilon_T\, \sigma\, T^4\, F A_{eff}$$

Figure B-5 shows variation of A_{eff} with 2θ for R = 20 in. and ϕ = 45°. It is seen that for R = 20 in. and ϕ = 45°, and an included plane angle of 70°(2θ = 70°), the effective area is about 4 times that seen through an included plane angle of 30°, about 7 times that seen through an included plane angle of 20°, and about 25 times that seen through an included plane angle of 10°. Under the above assumptions, the energy received by the detector is proportional to the effective area.
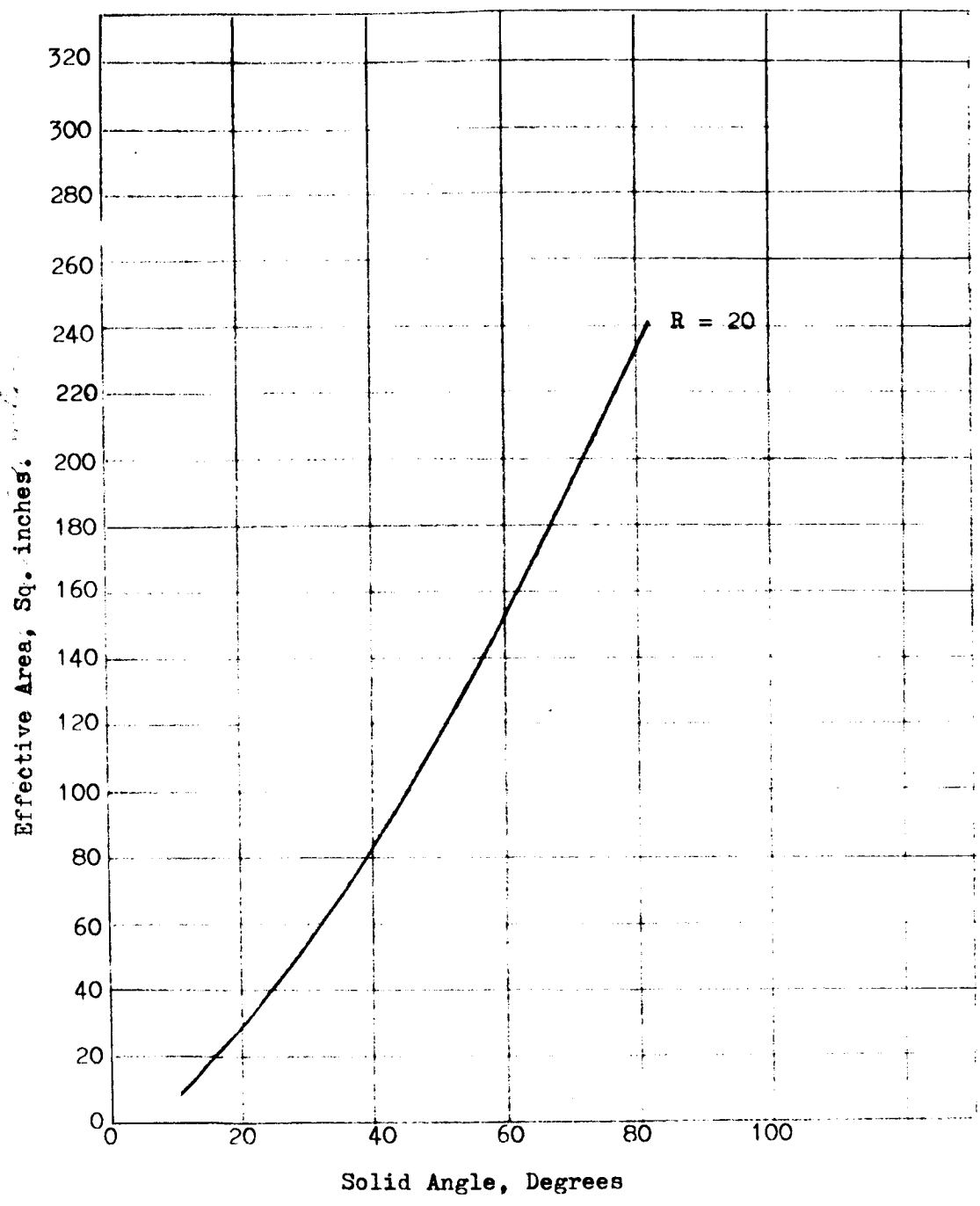
FIGURE B-5. VARIATION OF EFFECTIVE AREA WITH SOLID
ANGLE 2θ (Reference Fig. B-4)

APPENDIX C

DERIVATIONS AND SAMPLE CALCULATIONS FOR FOIL THERMOCOUPLE

OUTPUT VOLTAGE

The output voltage of a thermocouple follows the expression

$$E = K_1 T + K_2 \frac{T^2}{2} + K_3 \frac{T^3}{3} \qquad (\text{C-1})$$

for a narrow range of temperatures the output voltage of the thermo element is proportional to the difference of temperature between the two junctions, or

$$E - E_c \approx K_1 \left(T_t - T_r \right)^* \qquad (\text{C-2})$$

TIME CONSTANT

A time dependent energy balance can be expressed as

$$\dot{q}_{in} - \dot{q}_{out} = c_p \rho V \frac{d T_c}{d t} \qquad (\text{C-3})$$

It is assumed here that all or nearly all heat dissipation from the target is via the conductive path.

Then

$$\dot{q}_{out} = k A \frac{dT}{d\ell}$$

and

$$\dot{q}_{in} - k A \frac{dT}{d\ell} = c_p \rho V \frac{d T_c}{d t} \qquad (\text{C-4})$$

*Lion, K.S.: <u>Instrumentation in Scientific Research</u>, McGraw-Hill Book Company, New York 1959, p. 169.

Solving for dT_t,

$$dT_t = \left(\frac{1}{c_p \rho V}\right)\left(\dot{q}_m - \frac{kA}{\delta\ell}\delta T\right)dt = \frac{1}{c_p \rho V}\left[\dot{q}_m - \frac{kA}{\delta\ell}(T_t - T_r)\right]dt$$

$$= \frac{1}{c_p \rho V}\left[\dot{q}_m + \frac{kAT_r}{\delta\ell} - \frac{kA}{\delta\ell}T_t\right]dt \tag{C-5}$$

Let

$$u \equiv \dot{q}_m + \frac{kAT_r}{\delta\ell} - \frac{kA}{\delta\ell}T_t \tag{C-6}$$

$$du = -\frac{kA}{\delta\ell}dT_t$$

or

$$dT_t = -\frac{\delta\ell}{kA}du \tag{C-7}$$

Substituting equations (C-5) and (C-6) in (C-7) and rearranging,

$$\frac{du}{u} = -\left(\frac{k}{\delta\ell}\right)\left(\frac{A}{c_p \rho V}\right)dt \tag{C-8}$$

From this it can be seen that the system time constant is

$$\tau^{-1} = \left(\frac{k}{\delta\ell}\right)\left(\frac{A}{c_p \rho V}\right)$$

or

$$\tau = \left(\frac{\delta\ell}{k}\right)\left(\frac{c_p \rho V}{A}\right) \tag{C-9}$$

For a target thickness y and area A_t,

$$V = A_t y$$

so that

$$\tau = \left(\frac{\delta\ell}{k}\right)\left(\frac{A_t}{A}\right)(c_p \rho y) \tag{C-10}$$

SENSITIVITY

Sensitivity has been defined in a dimensionless form in order to compare the three transducers studied. However, for the foil thermo-couple sensitivity was also defined as the ratio of a small change in source temperature T_S to the change in target-to-reference temperature difference $\int T$ which it produces. The latter definition was used to determine performance characteristics of the foil thermocouple. Both sensitivity terms are defined mathematically in this section.

Dimensionless Sensitivity

The dimensionless sensitivity is defined in terms of output voltage and power to the detector.

$$S = \frac{\Delta E / E}{\Delta q / q} \tag{C-11}$$

For the foil thermocouple the voltage output is

$$E = AT + B\frac{T^2}{2} + C\frac{T^3}{3}$$

where A, B & C are constants depending on material used. However, over the limited range ($500°R$ to $790°R$) the slope is essentially linear therefore

$$E = AT + B\frac{T^2}{2} \tag{C-12}$$

But

$$T = T_r + q / \left(\frac{kA}{x_i}\right)_i = T_r + \Delta T_m q / q_m \tag{C-13}$$

$$\frac{dE}{dT} = A + BT$$

$$\frac{1}{E} \cdot \frac{dE}{dT} = \left(\frac{1}{AT + BT^2/2}\right)(A + BT) = \frac{1}{T}\left(\frac{A + BT}{A + \frac{B}{2}T}\right) \tag{C-14}$$

C-3

$$\frac{T}{E} \cdot \frac{dE}{dT} = \frac{dE/E}{dT/T} = \left(\frac{A + BT}{A + B/2\, T} \right) \tag{C-15}$$

$$\frac{dT}{T} = \frac{\Delta T_m \; {}^{\Delta q}/_{q_m}}{T_r + \Delta T_m \; {}^{q}/_{q_m}} = \left(\frac{\Delta T_m \; {}^{q}/_{q_m}}{T_r + \Delta T_m \; {}^{q}/_{q_m}} \right) \frac{dq}{q} \tag{C-16}$$

$$\frac{\Delta E/E}{\Delta q/q} = \left(\frac{\Delta T_m \; {}^{q}/_{q_m}}{T_r + \Delta T_m \; {}^{q}/_{q_m}} \right) \left[\frac{A + B\left(T_r + \Delta T_m \; {}^{q}/_{q_m} \right)}{A + \frac{B}{2}\left(T_r + \Delta T_m \; {}^{q}/_{q_m} \right)} \right] \tag{C-17}$$

If this is simplified further by considering ΔE as a perturbation about E then

$$E = AT$$

$$\frac{dE}{dT} = A$$

$$\frac{1}{E} \cdot \frac{dE}{dT} = \frac{A}{AT} = \frac{1}{T}$$

$$\frac{\Delta E/E}{\Delta T/T} = 1 \tag{C-18}$$

$$\frac{\Delta E/E}{\Delta q/q} = \frac{\Delta T_m \; {}^{q}/_{q_m}}{T_r + \Delta T_m \; {}^{q}/_{q_m}}$$

$$\frac{\Delta E/E}{\Delta q/q} = \frac{{}^{q}/_{q_m}}{{}^{T_r}/_{\Delta T_m} + {}^{q}/_{q_m}} \tag{C-19}$$

For the sensitivity at a particular temperature

$$\frac{\Delta E/E}{\Delta \phi/\phi} = \frac{\phi/q_m}{T_r/\Delta T_m + \phi/q_m}$$

where output voltage has been taken as $E = AT$ and detector tempera-
ture $T = T_r + \Delta T_m \phi/q_m$. (T_r = heat sink reference temperature,
ϕ = energy into detector, q_m = full power energy input, ΔT_m = detector
maximum temperature rise at full power).

Target Sensitivity

Target sensitivity is defined as $\dfrac{1}{S_t} \equiv \left[\dfrac{\partial T_s}{\partial (\delta T)}\right]_{T_r}$
and as already mentioned it was used in this study to investigate
performance characteristics.

The partial derivative notation is used here because the basic
equilibrium equations are of the form $f(T_r, T_s, T_t) = 0$
so that any two of the three variables may be varied while the third
is held constant.

The basic equations used in this derivation are:

$$T_s^4 = T_t^4/\delta \epsilon_s + T_o^3 (T_t - T_r) = T_t^4/\delta \epsilon_s + T_o^3 \delta T \qquad (C-20)$$

where
$$T_o = \left[\left(\frac{k}{\partial \ell}\right)\left(\frac{A}{A_t}\right)\left(\frac{1}{\epsilon_{eff} \text{ or } F_{eff}}\right)\right]^{1/3} \qquad (C-21)$$

By differentiating the basic equation

$$4 T_s^3 \left[\frac{\partial T_s}{\partial(\delta T)}\right]_{T_r} = \frac{4 T_t^3}{\delta \epsilon_s}\left[\frac{\partial T_t}{\partial (\delta T)}\right]_{T_r} + T_o^3$$

But
$$\left[\frac{\partial T_t}{\partial(\delta T)}\right]_{T_r} = \frac{\partial}{\partial(\delta T)}\left[T_r + \delta T\right] = 1$$

Substituting and re-arranging gives

$$\frac{1}{S_t} = \left[\frac{\partial T_s}{\partial (\delta T)}\right]_{T_r} = \frac{1}{f \epsilon_s}\left(\frac{T_t}{T_s}\right)^3 + \frac{1}{4}\left(\frac{T_o}{T_s}\right)^3 \qquad (C-22)$$

When the target temperature T_t is small enough compared with the characteristic temperature T_o so that the first term above is negligible.

$$\frac{1}{S_t} \approx \frac{1}{4}\left(\frac{T_o}{T_s}\right)^3, \qquad T_t << T_o \qquad (C-23)$$

In this situation it is interesting to note that sensitivity becomes independent of reference temperature. Therefore, in design work, changing the reference temperature does nothing to improve the sensitivity whenever $T_t << T_o$.

ERROR ANALYSIS

The influence coefficients of the final radiation pyrometer using the foil thermocouple as the sensing element is derived from the basic expression for output voltage of a thermoelectric element

$$E = K T + K_2 \frac{T^2}{2} + K_3 \frac{T^3}{3}$$

or

$$E - E_0 \approx K_1 \left(T_t - T_r\right)$$

(refer to data on output voltage in this Appendix)

Then the dimensionless output voltage change is

$$dE = \left(\frac{\partial E}{\partial K_1}\right) dK_1 + \frac{\partial E}{\partial (\Delta T)} d(\Delta T) \qquad (C-24)$$

or for

$$q = \left(KA/x\right)_u \left(T_t - T_r\right) \; ; \quad \Delta T = \left(q/KA/x\right)_u$$

and for

$$\frac{d(\Delta E)}{\Delta E} = \frac{dK_1}{K_1} + \frac{d(\Delta T)}{\Delta T} \tag{C-25}$$

$$K_1 = a_{TC} + b_{TC} T \tag{C-26}$$

$$\frac{dA_u}{A_u} = \left(\frac{b_{TC}}{a_{TC} + b_{TC} T_t}\right) dT_t \tag{C-27}$$

$$\frac{d(\Delta T)}{\Delta T} = \frac{d(T_t - T_r)}{\Delta T} = \frac{1}{\Delta T} d\left(\frac{q_{th} - q_r}{KA/x_u}\right) = \frac{1}{\Delta T} d\left(\frac{\sigma A F \epsilon T_s^4 + q_\sigma}{KA/x_u}\right)$$

$$\frac{d(\Delta T)}{\Delta T} = \frac{d\epsilon}{\epsilon} + \frac{d(AF)}{AF} + \frac{4 dT_s}{T_s} + \frac{d(q_{\sigma i})}{q_{th} + q_\sigma} + \frac{dx_u}{x_u} - \frac{dK_u}{K_u} + \frac{d(AF T_s^4)}{AF T_s^4}$$
$$\tag{C-28}$$

Heat Sink and Gamma Heating Error

Errors in foil thermocouple output voltage with respect to sink temperature and gamma heating are presented for two cases.

    I. Single foil thermocouple exposed to thermal and gamma heating (foil in electrical contact with heat sink).

    II. Double foil thermocouple (bucking arrangement) with both junctions exposed to thermal and gamma heating. (foil electrically insulated from heat sink.)

Case I

Let E_t = voltage out of center foil thermocouple junction

exposed to q_{th} & q_r

$$E_t = K T_t$$

E_r = voltage out of ref. foil thermocouple junction

$$E_r = K T_r$$

Then voltage to amplifier is

$$\Delta E = E_t - E_r = K T_t - K T_r = K(T_t - T_r) \qquad (C-29)$$

For error in reference temperature (heat sink temperature)

$$d(\Delta E) = d\left[K(T_t - T_r)\right] = -K\, dT_r \qquad (C-30)$$

Divide by ΔE

$$d\frac{(\Delta E)}{\Delta E} = -\frac{K\, dT_r}{K(T_t - T_r)} = -\frac{dT_r}{(T_t - T_r)} \qquad (C-31)$$

$$d\frac{\Delta E}{\Delta E} = -\frac{T_r}{(T_t - T_r)} \cdot \frac{dT_r}{T_r} \qquad (C-32)$$

Note that $\quad -dT_r = d(T_t - T_r) \quad$ where only T_r
is considered a variable so that the foregoing could be expressed as

$$\frac{d(\Delta E)}{\Delta E} = \frac{d(T_t - T_r)}{(T_t - T_r)}$$

For design values of $T_r = 500^\circ R$ and $T_t = 792^\circ R$ the foregoing is

$$\frac{d(\Delta E)}{\Delta E} = -\frac{1}{292} \cdot dT_r = -.00342\ dT_r$$

For error due to gamma heating, the foil thermocouple temperature due to thermal and gamma heating is

$$T_t = T_r + \frac{q_{total}}{R_{th}} \tag{C-33}$$

where $q_{total} = q_{th} + q_\gamma = q_T$ (C-34)

R_{th} = thermal resistance

then

$$\Delta E = K(T_t - T_r) = K\left(T_r + \frac{q_T}{R} - T_r\right) \tag{C-35}$$

$$d(\Delta E) = K d\frac{q_T}{R} = \frac{K}{R} d(q_{th} + q_\gamma) = \frac{K}{R} dq_\gamma \tag{C-36}$$

$$\frac{d(\Delta E)}{\Delta E} = \frac{K/R \cdot dq_\gamma}{K q_T/R} = \frac{dq_\gamma}{q_{th} + q_\gamma} \tag{C-37}$$

Case II

For the double foil thermocouple the voltages at reference junction and target junction are

$$E_r = K T_r$$
$$E_t = K T_t$$
$$\Delta E = K(T_t - T_r)$$

and the two temperatures are

$$T_t = T_{st} + \frac{q_T}{R_{ts}} \tag{C-38}$$

$$T_r = T_{sR} + \frac{q_\gamma}{R_{rs}} \tag{C-39}$$

$$\Delta E = K \left(T_{sr} + \frac{q_T}{R_{ts}} - T_{sr} - \frac{q_r}{R_{rs}} \right)$$

$$= K \left(T_{st} + \frac{q_{th}}{R_{ts}} + \frac{q_r}{R_{ts}} - T_{sr} - \frac{q_r}{R_{rs}} \right) \quad \text{(C-40)}$$

where

R_{ts} = thermal resistance between T_t and T_S

R_{rs} = thermal resistance between T_r and T_S

T_{st} = target heat sink temperature

T_{sr} = reference heat sink temperature

Note that if $T_{St} \equiv T_{Sr}$ and $R_{tS} \equiv R_{rS}$ there is no error introduced from gamma heating and heat sink temperature so output voltage is

$$\Delta E = \frac{K\, q_{th}}{R_{ts}}$$

However, assume that there is a slight variation between T_{Sr} and T_{St} — assume T_{Sr} deviates slightly then

$$d(\Delta E) = -K\, d\, T_{sr} \quad \text{(C-41)}$$

$$\Delta E = K \left(T_t - T_r \right) \quad \text{(C-42)}$$
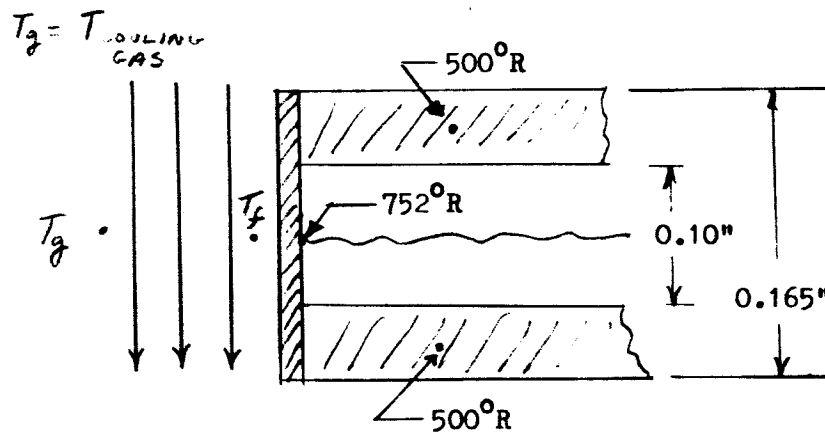
or

$$\frac{d(\Delta E)}{\Delta E} = -\left(\frac{T_{sr}}{T_t - T_r} \right) \frac{d\, T_{sr}}{T_{sr}} \quad \text{(C-43)}$$

Thus if there is a variation between T_{Sr} and T_{St} then the dual configuration behaves like a single sensing element with respect to heat sink temperature.

Convection Error

For natural convection across detector (foil face) and temperatures

Minimum cooling gas temperature is assumed to be 300°R. Film temperature is estimated as

$$T_f = \frac{(500 + 752)/2 + 300}{2} = 463^{\circ}R \tag{C-44}$$

For chamber pressure of 600 psia use physical properties of hydrogen at 450°R and 600 psia.

$$\rho = .000141 \text{ lbm/in}^3$$
$$C_p = 3.714 \text{ Btu/lbm-}^{\circ}R$$
$$\mu = 4.522 \times 10^{-7} \text{ lbm/in-sec}$$
$$k = 2.4189 \times 10^{-6} \text{ Btu/in-sec-}^{\circ}R$$

From which Prandtl No. is

$$P_r = \frac{c_p \mu}{K} = \frac{(3.714\ BTU/lbm\text{-}°R)(4.522 \times 10^{-7}\ lbm/in.\text{-}sec)}{2.4189 \times 10^{-6}\ Btu/in.sec.\text{-}°R} \quad (C\text{-}45)$$

$$P_r = 0.694$$

For Grashoff No. calculation*

$$L = 6.10\ in.$$
$$\rho_f = 0.00141\ lbm/in^3$$
$$g = 386\ lbm/in^3$$
$$\beta_f = 0.00216\ °R^{-1} \quad (\beta = 1/T_f)$$
$$\Delta T = 163°R \quad (T_g = 300°R,\ T_f = 463°R)$$
$$\mu_f = 4.522 \times 10^{-7}\ lbm/in.\,sec.$$

Grashoff No. is

$$G_r = \frac{L^3 \rho_f^2 g \beta \Delta T}{\mu_f^2} \qquad (C\text{-}46)$$

$$= \frac{(.10\ in.)^3 (.00141\ lbm/in^3)^2 \left(386 \frac{lbm\text{-}in}{lbf\text{-}sec^2}\right)(.00216/°R)(163°R)}{4.522 \times 10^{-7}\ lbm/in\text{-}sec^2}$$

$$= \frac{(10^{-3})(1.99 \times 10^{-6})(3.86 \times 10^2)(2.16 \times 10^{-3})(1.63 \times 10^2)}{20.4 \times 10^{-14}}$$

$$G_r = 1.33 \times 10^6$$

*See reference 10, p. 172

The Gr No. is $< 10^9$ so laminar natural convection flow exists and the correlation which should be applicable is*

$$Nu = 0.59 \left(Gr \cdot P_r \right)^{0.25} \qquad (C\text{-}47)$$

$$= 0.59 \left(1.33 \times 10^6 \times 0.694 \right)^{1/4}$$

$$= 0.59 \left(.923 \times 10^6 \right)^{1/4} = 0.59 \, (.995)(31.6)$$

$$Nu = 18.52$$

For heat transfer coefficient (average value across a 0.10 in. diameter for a vertical position with respect to gravity for $T_f = 463°R$ and $T_g = 300°R$)

$$h = Nu \times \frac{k}{L} = \frac{(18.52)(2.4187 \times 10^{-6} \, Btu/in\text{-}sec\text{-}°K}{(0.10 \, in)} \qquad (C\text{-}48)$$

$$h = 4.49 \times 10^{-4} \, Btu/in^2\text{-}sec\text{-}°R$$

*See reference 10, 3rd Ed., p. 172

For natural convection heat transfer from face of 0.10 in foil thermocouple

$$q = hA(T - T_g) \tag{C-49}$$

$$A = \pi D^2/4 = .785 \times 10^{-2}$$

$$q = (4.49 \times 10^{-4} \text{ BTu/in}^2 \text{ sec } ^\circ\text{K})(.785 \times 10^{-2} \text{ in}^2)$$

$$\times \left(\frac{752 + 502}{2} - 300^\circ R\right)$$

$$= (4.49 \times 10^{-4})(.785 \times 10^{-2})(3.26 \times 10^2)$$

$$q = 1.15 \times 10^{-3} \text{ BTu/sec}$$

If a gas temperature of 500°R is used

$$q = 1.15 \times 10^{-3}\left(\frac{200}{326}\right) = 0.445 \times 10^{-3} \text{ BTu/sec.}$$

For laminar forced convection across foil thermocouple face assume a low velocity of $10 \rightarrow 100$ m/sec.

$$Re_L = \rho U/\mu = \frac{(0.10 \text{ in})(.000141 \text{ lbm/in}^3)(10 \text{ m/sec})}{4.522 \times 10^{-7} \text{ lbm/in sec}} \tag{C-50}$$

$$= (10^{-1})(1.41 \times 10^{-4})(10)/(4.522 \times 10^{-7})$$

$$Re_L = 3.12 \times 10^2 \sim 312$$

From p. 249, reference 10, figure 9-29,

$$N_u = 0.0479 \, R_e \cdot P_r^{1/3} \qquad (C-51)$$

$$N_u = 13.24$$

$$h = 13.24 \times 2.4189 \times 10^{-6} / 0.10$$

$$h = 3.2 \times 10^{-4} \, BTU/in^2 \, sec \cdot {}^\circ R$$

For a velocity of 100 in/sec Re = 3120, and

$$N_u = .0134 \, (3120)(.885) = 37.1$$

$$h = 37.1 \times 2.419 \times 10^{-6} / 0.10 = 8.96 \times 10^{-4} \frac{BTU}{sec \cdot in^2 \cdot {}^\circ R}$$

So values of h for U = 10 and 100 in/sec bracket that for natural convection.

For comparison to natural convection,
at $U = 10 \, in/sec$, gas velocity across face of thermocouple

$$q = \left(3.2 \times 10^{-4} \frac{BTU}{in^2 \cdot sec \, {}^\circ R}\right)\left(.785 \times 10^{-2} in^2\right)\left(3.26 \times 10^2 \, {}^\circ R\right)$$
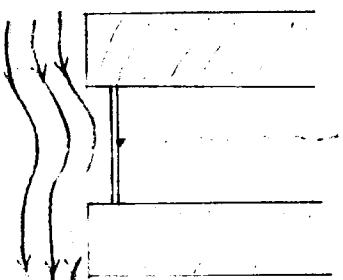
$$q = 0.82 \times 10^{-3} \, BTU/sec$$

at $u = 100 \text{ in/sec}$, gas velocity across face of thermocouple
is

$$q = \left(8.96 \times 10^{-4} \frac{Btu}{in^2 \ sec \ {}^\circ R}\right)\left(.785 \times 10^{-2} in^2\right)\left(3.26 \times 10^2 \ {}^\circ R\right)$$

$$q = 2.3 \times 10^{-3} \ Btu/sec.$$

Assume that recessing reduces effective length of flow buildup by $\frac{1}{2}$

then correct h by
$$\left[\left(\frac{L_{eff}}{L}\right)^3\right]^{1/4} = \left(\frac{L_{eff}}{L}\right)^{3/4}$$

$$h_{eff} = h\left(\frac{L_{eff}}{L}\right)^{3/4} = 4.49 \times 10^{-4} (0.5)^{3/4}$$

$$= 2.67 \times 10^{-4} \ Btu/in^2 \ sec$$

effective area $= A\left(\frac{D_{eff}}{D}\right)^2 = A\,(0.5)^2 = A/4$

so effective heat loss is

$$q = h_{eff} \ A_{eff} \ (T - T_g) \tag{C-52}$$

$$= (2.67 \times 10^{-4})(.785 \times 10^{-2})(.25)(326)$$

$$q = 1.71 \times 10^{-4} \ Btu/sec, \quad \text{or the heat loss by}$$
natural convection for recessed foil thermocouple.

Convection Error Coefficient

$$\Delta E = K\, q_{tn}/R_{TS} = K/R_{TS}\left(q_{tn} - q_{conv}\right) \tag{C-53}$$

(refer to page ___ in this appendix)

where R_{TS} = thermal resistance between T_t and T_S

$$d\Delta E = K/R_{TS}\, dq_{conv} \tag{C-54}$$

$$\frac{d(\Delta E)}{\Delta E} = -\frac{K/R_{TS}\, dq_{conv}}{K/R_{TS}\left(q_{tn} - q_{conv}\right)} = -\frac{dq_{conv}}{q_{tn} - q_{conv}} \tag{C-55}$$

$$\frac{d(\Delta E)}{\Delta E} = -\left(\frac{q_{conv}}{q_{tn} - q_{conv}}\right)\frac{dq_{conv}}{q_{conv}} \tag{C-56}$$

Error Coefficients for Operating Variables

The change in output voltage with respect to the operating variables which influence performance can be expressed as

$$\frac{d(\Delta E)}{\Delta E} = 1\frac{d\epsilon}{\epsilon} + 1\frac{d(A_F)}{A_F} + .04 \times 10^{-2}\frac{dq_r}{q_r}$$

$$+ \frac{d\left(A_F\, T_s^4\right)}{A_F\, T_s^4} + 1\frac{dT_t}{T_t} - 1.716\frac{dT_r}{T_r}$$

$$- .311 \times 10^{-2}\frac{dq_{conv}}{q_{conv}}$$

The numeral values have been substituted for the error coefficients in the above equation.
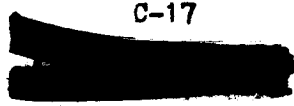
SAMPLE CALCULATIONS FOR FOIL THERMOCOUPLE

Time Constant

$$\tau = \left(\frac{\delta\ell}{k}\right)\left(\frac{A_t}{A}\right) c_p \rho y$$

$\delta\ell = 0.010$ m.

$k = 0.064$ cal/sec.-cm^2.$°C$-cm^{-1} for Alumel @ $500°k$

$c_p = 0.125$ cal/gram-$°C$

$\rho = 8.60$ gram/cm^3

$y = 0.001$ in

$A_t = \frac{\pi}{4} d_t^2$

$d_t = 0.1$ in

$A = 3wy$, $w = 0.026$ m.

$$\tau = \left(\frac{\delta\ell}{k}\right)\left(\frac{\frac{\pi}{4} d_t^2}{3wy}\right) c_p \rho y = \left(\frac{\delta\ell}{k}\right)\left(\frac{\pi d_t^2}{12w}\right)\left(c_p \rho\right)$$

$$= \left(\frac{\delta\ell}{w}\right)\left(\frac{\pi d_t^2 c_p \rho}{12k}\right)$$

$$\tau = \left(\frac{0.010}{0.026}\right)\left(\frac{\pi \cdot 6.45 \times 10^{-2} \cdot 0.125 \cdot 8.60}{12 \cdot 0.064}\right)$$

$$\tau = 0.169 \text{ sec.}$$

Target Temperature Rise at 500°R

$$\dot{q} = kA \frac{dT}{dl}$$

$$dT = \left(\frac{\dot{q}}{A}\right) \frac{dl}{k}$$

$A = 3wy$ (for 3 tubes of thickness y and width w)

$A_t = \frac{\pi}{4} d_t^2$ (for target of diameter d_t)

$$dT = \left(\frac{\dot{q}}{A_t}\right)\left(\frac{A_t}{A}\right)\left(\frac{dl}{k}\right) = \left(\frac{dl}{k}\right)\left(\frac{\pi d_t^2}{3wy}\right)\left(\frac{\dot{q}}{A_t}\right) = \left(\frac{dl}{k}\right)\left(\frac{\pi d_t^2}{12wy}\right)\left(\frac{\dot{q}}{A_t}\right)$$

$dl = 0.010$ m. $= 2.54 \times 10^{-2}$ cm.

$d_t = 0.100$ m

$w = 0.026$ m.

$y = 0.001$ m

$K = 0.071$ cal/sec. cm^2 - °C - cm^{-1}

$$dT = \left(\frac{2.54 \times 10^{-2}}{0.071}\right)\left(\frac{\pi \cdot 0.1^2}{12 \cdot 0.026 \cdot 0.001}\right)\left(\frac{\dot{q}}{A_t}\right) = \frac{2.54 \pi}{(0.71)(1.2)(2.6)} 10 \left(\frac{\dot{q}}{A_t}\right)$$

$$dT = 36.0 \frac{\dot{q}}{A_t}$$

$$\left[\frac{\dot{q}}{A_t}\right] \text{cal/sec cm}^2 = 39.1 \left[\frac{\dot{q}}{A_t}\right]_B \text{Btu/sec-in}^2$$

$$\left[dT\right]_{°C} = 1.8 \left[dT\right]_{°F}$$

$$dT = (39.1)(1.8)(36) = 2.53 \times 10^3 \left(\frac{\dot{q}}{A_t}\right)_B \text{°F}$$

Dimensionless Sensitivity

$$\frac{\Delta E/E}{\Delta q/q} = \frac{q/q_m}{T_r/\Delta T_m + q/q_m}$$

where $T_r = 500°R$

$$\Delta T_m = 752°R$$

$$q/q_m = 0.01$$

$$\frac{\Delta E/E}{\Delta q/q} = \frac{0.01}{0.66 + .01} = .0149$$

Sensitivity

$$\text{Sensitivity} = \frac{\Delta \text{ Millivolts}}{\Delta \text{ Degrees R}}$$

Millivolt output @ $2000°R$ and $500°R$ reference $= 0.26$ mV

Millivolt output @ $2200°R$ and $500°R$ reference $= 0.35$ mV

(refer to figure 13)

$$\frac{\Delta \text{ millivolts}}{\Delta \text{ degrees R}} = \frac{.35 \text{ mV} - .26 \text{ mV}}{200°R}$$

$$\frac{\Delta \text{ millivolts}}{\Delta \text{ degrees R}} = 4.5 \times 10^{-4}$$

C-20

Gamma Heating

The following conditions were assumed for these calculations:

1. Foil thermocouple diameter of 0.3 in. and .001 in. thick (gamma heating was not a limiting factor for the 0.3 in. diameter therefore these values were also used for the fixed design calculations.)

2. Gamma heating is 1.0 BTU/lbm-sec with no attenuation

3. For two decades of attenuation gamma heating is 10^{-2} BTU/lbm-sec.

Gamma heating of the thermocouple foil without shielding

$$m \times \frac{q}{t}_\gamma = \left(.1978 \times 10^{-4} \, lbm\right)\left(1.0 \; Btu/lbm-sec\right)$$

$$= .1978 \times 10^{-4} \; Btu/sec$$

Gamma heating of the thermocouple foil with shielding (two decades attenuation)

$$\left(.1978 \times 10^{-4} \, lb-m\right)\left(10^{-2} \; Btu/lb-m \, sec\right) = .1978 \times 10^{-6} \; Btu/sec$$

At full power (5000°R)

$$\frac{\text{Thermal heating}}{\text{Gamma heating}} = \frac{(0.3/1)^2 \times 3.62 \times 10^{-4}}{.1978 \times 10^{-6}} = 16,450$$

At low power (1000°), gamma heating is linear in power so that

$$\frac{q}{t}_\gamma = \frac{1.978 \times 10^{-7}}{12} = .1648 \times 10^{-7} \; Btu/sec$$

where power reduction factor is based on 50% flow rate at 1000°R

$$f = \frac{m C_p (5000 - 200)}{0.50 \; m C_p (1000 - 200)} = \frac{4800}{0.5 \times 800} = 12$$

but q radiation is down by $\sim (5000/1000)^4 = 625$

$$\frac{\text{Thermal heat}}{\text{Gamma heat}} \;\simeq\; \frac{9 \times 3.62 \times 10^{-4}/625}{0.1648 \times 10^{-7}} \;=\; 316$$

If flow rate at 1000°R is the same as for 5000°R then

$$f = \frac{m c_p (5000 - 200)}{m c_p (1000 - 200)} = \frac{4800}{800} \simeq 6$$

$$q_\gamma = \frac{1.978 \times 10^{-7}}{6} = .33 \times 10^{-7}$$

Then
$$\frac{\text{Thermal heat}}{\text{Gamma heat}} = \frac{9 \times 3.62 \times 10^{-4}/625}{.33 \times 10^{-7}} = 158$$

ERROR ANALYSIS CALCULATIONS

Thermoelectric Constant (Reference Fig. C-1)

K_1 (thermoelectric constant) was determined over a limited range of temperatures where dE/dT for the temperature ranges indicated below is as follows:

TEMPERATURE (TARGET)	dE/dT
360°R – 460°R	.0197
460°R – 560°R	.0220
560°R – 660°R	.0230
660°R – 760°R	.0227
760°R – 860°R	.0222
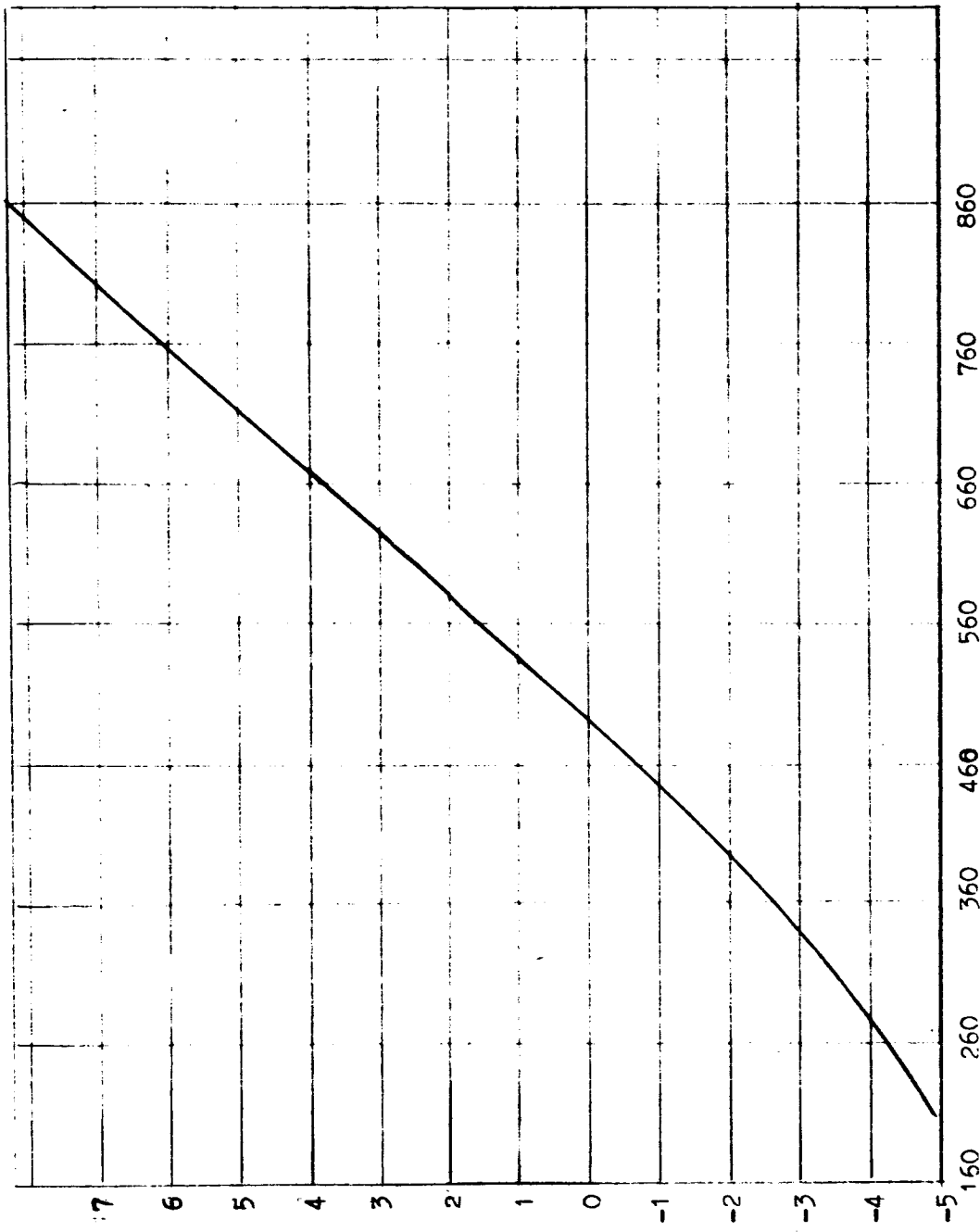
FIGURE C-1, TEMPERATURE-MILLIVOLT FOR CHROMEL VS ALUMEL (REFERENCE 22)

At the 742°R point

$$\frac{d}{dT}\left(\frac{\Delta E}{\Delta T}\right) \cong \frac{.0227 - .0220}{200}$$

$$\frac{d}{dT}\left(\frac{\Delta E}{\Delta T}\right) \cong 3.5 \times 10^{-6} \, mv/°R$$

$$K_1 = .0220 + 3.5 \times 10^{-6} \, T \quad \text{MILLIVOLTS}/°R$$

Heat Sink Temperature Error

$$\frac{d(\Delta E)}{\Delta E} = -\frac{dT_r}{(T_t - T_r)} = -\frac{T_r}{(T_t - T_r)} \cdot \frac{dT_r}{T_r}$$

$$= -\left(\frac{500°R}{292°R}\right)\frac{dT_r}{T_r} = -1.716 \frac{dT_r}{T_r}$$

so that for 1% change in T_r $(5°R)$

$$\frac{d(\Delta E)}{\Delta E} = -1.716(.01) = -.01716$$

A 1% change in T_r results in a 1.72% change in ΔE at a source temperature of 5000°R

$$dT_s = \frac{T_s}{4} \frac{d(\Delta E)}{\Delta E} = \frac{5000}{4} \times .0172 = \pm 21.5°R$$

Gamma Heating Error

$$\frac{d(\Delta E)}{\Delta E} = \frac{dq_r}{q_{tn} + q_r} = \frac{q_r}{q_{tn} + q_r} \frac{dq_r}{q_r}$$

For 5000°R

$$q_{en} = 2.5 \times 10^{-2} \; Btu/sec$$

$$q_r = 0.2 \times 10^{-4} \; Btu/sec$$

$$\frac{d(\Delta E)}{\Delta E} = \frac{0.2 \times 10^{-4}}{5.5 \times 10^{-2} + 0.2 \times 10^{-4}} \cdot \frac{dq_r}{q_r} = .0364 \times 10^{-2} \frac{dq_r}{q_r}$$

For a 1% change in q_r

$$\frac{d(\Delta E)}{\Delta E} = .0364 \times 10^{-2} (.01) = .0364 \times 10^{-4}$$

$$dT_s = \frac{T_s}{4} \frac{d(\Delta E)}{\Delta E}$$

$$dT_s = \frac{5000}{4} \times .0364 \times 10^{-4} = .00455 = \pm .005 °R$$

Gamma heating was ratioed for temperatures below 5000°R by using an approximate equation for the Engine Temperature – Flow Relationship for constant pump specific speed.

$$P = K_a T$$, to maintain constant specific speed

$$\gamma = K_b \dot{m} T$$, γ is proportional to thermal power

$$\dot{m} = \frac{K_c P}{\gamma T}$$, flow for sonic nozzle

$$\frac{\gamma_T}{\gamma_{5000}} = \frac{T^{1.5}}{(5000)^{1.5}}$$

$$\gamma = \frac{\gamma_{5000} \, T^{1.5}}{(5000)^{1.5}}$$

Convection Heating Error

$$\frac{d(\Delta E)}{\Delta E} = -\left(\frac{q_{conv}}{q_{th} + q_{conv}}\right) \frac{dq_{conv}}{q_{conv}}$$

$$= -\frac{1.71 \times 10^{-4}}{5.5 \times 10^{-2} + 1.71 \times 10^{-4}} \frac{dq_{conv.}}{q_{conv.}}$$

where $q_{conv} = 1.71 \times 10^{-4}$ is heat loss by natural convection for a recessed foil.

For a 1% change in $q_{conv.}$ at $5000^{\circ}R$

$$\frac{d(\Delta E)}{\Delta E} = -.311 \times 10^{-2}(.01) = -.311 \times 10^{-4}$$

$$dT_S = \frac{T_S}{4} \frac{d(\Delta E)}{\Delta E} = \frac{5000}{4} \times .311 \times 10^{-4} = \pm .0390^{\circ}R$$

As T_S decreases, q_{th} decreases, and $q_{conv.}$ decreases,

Then

$$q_{conv.}\Big|_{T_S < 5000^{\circ}R} = q_{conv.}\Big|_{5000} \times \frac{T_{avg.} - T_{gas}}{T_{t\,5000} - T_{gas}}$$

$$q_{conv.}\Big|_{T_S < 5000^{\circ}R} = 1.71 \times 10^{-2} \frac{T_t/2 - 50}{326}$$

APPENDIX D

DERIVATION OF PERFORMANCE CRITERIA
FOR EDDY CURRENT SENSOR

OUTPUT VOLTAGE

The output voltage for the eddy current sensor can be derived by starting with the detector movement due to thermal expansion of the cone

$$\ell = \ell_o \left[1 + \alpha \left(T_s - T_r \right) \right] \qquad (D\text{-}1)$$

$$\Delta \ell = \ell - \ell_o, \quad x = x_o + \Delta \ell$$

Voltage output of the eddy current probe is

$$E = E_o \left(\frac{x}{x_o} \right)^n \qquad (D\text{-}2)$$

Assume that x increases as q increases

$$\frac{E}{E_o} = \left(\frac{x_o + \Delta \ell}{x_o} \right)^n \qquad (D\text{-}3)$$

● $$\Delta \ell = \ell - \ell_o = \ell_o \alpha \Delta T$$

$$E = E_o \left(1 + \frac{\ell_o \alpha \Delta T}{x_o} \right)^n \qquad (D\text{-}4)$$

TIME RESPONSE

An energy balance on the detector for conduction controlled heat rejection is

$$m c_p \frac{dT_t}{dt} = \sigma A \epsilon F \left(T_s^4 - T_t^4 \right) - \left(\frac{kA}{x} \right)_M \left(T_t - T_r \right) \qquad (D\text{-}5)$$

Linearize and take Laplace transform to give

$$\delta T_t (s) = \left(\frac{K}{\tau s + 1} \right) \delta T_s (s) \qquad (D\text{-}6)$$

D-1

APPENDIX D (CONTINUED)

where
$$K = \frac{\sigma A \epsilon F T_s^3}{\sigma A \epsilon F T_t^3 + (kA/x)_u}$$

$$T = \frac{mC_\rho}{\sigma A \epsilon F T_t^3 + (kA/x)_u}$$

But for conduction heat rejection much greater than radiation

$$T \simeq \frac{mC_\rho}{(kA/x)_u} \tag{D-7}$$

The term (kA/x_i) is determined by the full power design point

$$q_m = (kA/x)_u (T_t - T_r) = (kA/x_u)\, \Delta T_m$$

or

$$(kA/x_u) = q_m/\Delta T_m \tag{D-8}$$

The detector mass is

$$m = \rho A X \qquad \text{(A is cone area fig. 5)} \tag{D-9}$$

Substituting gives

$$T = \frac{\rho A X C_\rho}{q_m/\Delta T_m} = \frac{\rho C_\rho A X \Delta T_m}{q_m} \tag{D-10}$$

Define a dimensionless time constant as

$$T' = T \frac{k}{\rho C_\rho A} \tag{D-11}$$

and a dimensionless detector thickness as

$$X' = X \frac{k \Delta T}{q_m}$$

Then

$$T \frac{k}{\rho C_\rho A} = X \frac{k \Delta T}{q_m}$$

or $\quad T' = x'$

or for fixed T, thickness is

$$\chi = \frac{T}{\rho\, C_\rho\, \Delta T_m} \cdot \frac{q_m}{A} \qquad\qquad (D\text{-}12)$$

SENSITIVITY

Define sensitivity as

$$S = \frac{\Delta E / E}{\Delta q / q} \qquad\qquad (D\text{-}13)$$

Energy balance on detector is

$$q = \sigma\, \overline{A\, \epsilon\, F} \left(T_s^4 - T_t^4 \right) = \frac{k_u A_u}{x_u}\left(T_t - T_r \right) \qquad\qquad (D\text{-}14)$$

Movement of detector is according to thermal expansion

$$\ell = \ell_0 \left[1 + \alpha \left(T_t - T_r \right) \right] \qquad\qquad (D\text{-}15)$$

$$\Delta\ell = \ell - \ell_0 \,, \qquad \chi = \chi_0 + \Delta\ell$$

Voltage output of eddy current probe is

$$E = E_0 \left(\frac{\chi}{\chi_0} \right)^n \qquad\qquad (D\text{-}16)$$

(Assume that χ increases as q increases)

$$\frac{E}{E_0} = \left(\frac{\chi_0 + \Delta\ell}{\chi_0} \right)^n$$

$$= \left[1 + \frac{\alpha\, \ell_0}{\chi_0} \left(T_t - T_r \right) \right]^n \qquad\qquad (D\text{-}17)$$

But at full power design point

$$k_u A_u / x_u = q_m / T_t - T_r = q_m / \Delta T_m \qquad\qquad (D\text{-}18)$$

$$T_t = T_r + \Delta T_m\, q / q_m \qquad\qquad (D\text{-}19)$$

APPENDIX D (CONTINUED)

or

$$\frac{E}{E_o} = \left[1 + \frac{l_o \alpha}{x_o}\left(\frac{\Delta T_m q}{qm}\right)\right]^n \tag{D-20}$$

For incremental change in q and E at a given q

$$\frac{\Delta E}{E_o} = n\left(1 + \frac{l_o \alpha \Delta T_m q}{x_o qm}\right)\left(\frac{l_o \alpha \Delta T_m}{x_o qm}\right)\Delta q$$

$$\Delta E = n E_o\left(1 + \frac{l_o \alpha \Delta T_m q}{x_o qm}\right)^{n-1}\left(\frac{l_o \alpha \Delta T_m}{x_o qm}\right)\Delta q \tag{D-21}$$

But at given q

$$E = E_o\left[1 + \frac{l_o \alpha \Delta T_m q}{x_o qm}\right]^n \tag{D-22}$$

so that

$$\frac{\Delta E}{E} = \frac{m E_o\left(1 + \frac{l_o \alpha \Delta T_m q}{x_o qm}\right)^{n-1}\left(\frac{l_o \alpha \Delta T_m}{x_o qm}\right)\Delta q}{E_o\left[1 + \frac{l_o \alpha \Delta T_m q}{x_o qm}\right]^n} \tag{D-23}$$

or

$$\frac{\Delta E/E}{\Delta q/q} = \frac{n\left(\frac{l_o \alpha \Delta T_m q}{x_o qm}\right)}{1 + \left(\frac{l_o \alpha \Delta T_m q}{x_o qm}\right)}$$

$$\frac{\Delta E/E}{\Delta q/q} = \frac{\left(\frac{l_o \alpha \Delta T_m}{x_o}\right)q/qm}{1 + \left(\frac{l_o \alpha \Delta T_m}{x_o}\right)q/qm} \tag{D-24}$$

D-4

ERROR ANALYSIS

The eddy current error coefficients can be found from the expression for the voltage output

$$E - E_0 = E_0 \frac{\alpha \ell}{x_0}\left(T_t - T_r\right) \tag{D-25}$$

$$dE = \left(\frac{\partial E}{\partial \alpha}\right)d\alpha + \left(\frac{\partial E}{\partial \ell}\right)d\ell + \left(\frac{\partial E}{\partial \Delta T}\right)d\Delta T - \left(\frac{\partial E}{\partial x}\right)dx$$

$$= \frac{\Delta E}{\alpha}d\alpha + \frac{\Delta E}{\ell}d\ell + \frac{\Delta E}{\Delta T}d(\Delta T) - \frac{\Delta E}{x_0}dx_0$$

or

$$\frac{d(\Delta E)}{\Delta E} = \frac{d\alpha}{\alpha} + \frac{d\ell_0}{\ell_0} + \frac{d(\Delta T)}{\Delta T} - \frac{d(x_0)}{x_0} \tag{D-26}$$

but

$$\frac{d\alpha}{\alpha} = \frac{d(a_\alpha + b_\alpha T_t)}{a_\alpha + b_\alpha T_t} = \left(\frac{b_\alpha}{a_\alpha + b_\alpha T_t}\right)dT_t \tag{D-27}$$

$$\frac{d(\Delta T)}{\Delta T} = \frac{d(T_t - T_r)}{\Delta T} = \frac{1}{\Delta T}d\left(\frac{g_{th} - g_\sigma}{kA/x_\mu}\right) = \frac{1}{\Delta T}d\left(\frac{\sigma A F \epsilon T_s^4 + g_\sigma}{kA/x_\mu}\right)$$

$$\approx \frac{d\epsilon}{\epsilon} + \frac{d(AF)}{AF} + \frac{4dT_s}{T_s} + \frac{d(g_\sigma)}{g_{th} + g_\sigma} + \frac{dx_\mu}{x_\mu} - \frac{dk_\mu}{k_\mu} \tag{D-28}$$

also

$$\frac{dk_\mu}{k_\mu} = \frac{d(a_\mu + b_\mu T_t)}{a_\mu + b_\mu T_t} = \left(\frac{b_\mu}{a_\mu + b_\mu T_t}\right)dT_t$$

APPENDIX D (CONTINUED)

Thus the total sum of factors estimated to influence detector output voltage is

$$\frac{d(\Delta E)}{\Delta E} = \left(\frac{b_\alpha}{a_\alpha + b_\alpha T_t}\right) dT_t + \frac{d\ell_0}{\ell_0} + \frac{d\epsilon}{\epsilon} + \frac{d(AF)}{AF} + 4\frac{dT_s}{T_s}$$

$$+ \frac{d(q_r)}{g_{th} + q_r} + \frac{d\lambda_u}{\lambda_u} - \left(\frac{b_u}{a_u + b_u T_t}\right) dT_t$$

$$+ \frac{d(AFT_s^4)}{AFT_s^4} \qquad\qquad (D-29)$$

GAMMA HEATING

The method of calculating gamma heating for the eddy current sensor is identical to the method used for the foil thermocouple. The same assumptions were also made in each case. The material used in these calculations was aluminum.

APPENDIX E

DERIVATIONS OF PERFORMANCE CRITERIA
FOR THE PNEUMATIC SENSOR

OUTPUT PRESSURE

The output pressure signal is related to the temperature out of the
radiation heat exchanger as

$$P_2 = \left(\dot{m}/k_c \right) \sqrt{T_3} \qquad \text{(refer to reference 23)} \qquad \text{(E-1)}$$

A schematic diagram of the sensor is given in Figure E-1 in order
to show the relative locations of the design parameters
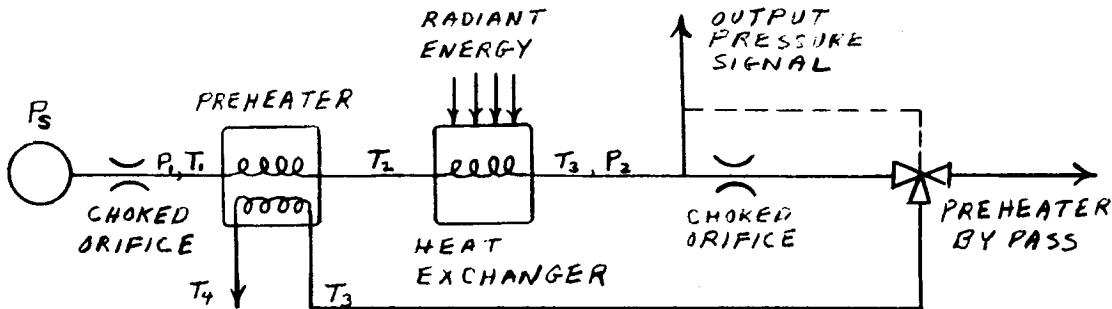
FIGURE E-1

PNEUMATIC HEAT EXCHANGER SENSOR

The temperature out of the radiation heat exchanger is related to
thermal radiation energy input as $\quad \dot{q} = \dot{m} \, C_p \left(T_3 - T_2 \right) \quad$ (E-2)

and the thermal energy input is related to the surface temperature as

$$\dot{q} = \sigma \, \overline{EAF} \left(T_s^4 - T_w^4 \right) \qquad \text{(E-3)}$$

The preheater performance can be characterized by its effectiveness
which is defined as

$$\eta = \frac{T_2 - T_1}{T_3 - T_1} \qquad \text{(E-4)}$$
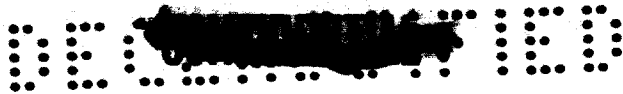
where T_1 = preheater primary inlet temperature

T_2 = preheater primary outlet temperature

T_3 = radiation ht. exch. outlet temperature

Equation (E-4) is for no bypass of the flow to the preheater. For flow being bypassed where f is the fraction of the flow going through the preheater, an energy balance on the preheater gives

$$\dot{m} C_p (T_2 - T_1) = f \dot{m} C_p (T_3 - T_4) = U A \left(\frac{T_3 + T_2}{2} - \frac{T_2 - T_1}{2} \right) \quad \text{(E-5)}$$

and for the radiation heat exchanger call the temperature rise across it ΔT so that

$$T_3 = T_2 + \Delta T \quad \text{(E-6)}$$

where f = fraction of flow going through preheater

U = overall heat transfer coefficient

Then with the energy balances of Eq. (E-5) and (E-6) the heat exchanger effectiveness can be expressed in terms of fraction of flow going through the preheater as

$$\eta = \frac{1}{1 + \sigma + \frac{1-f}{2f}} \quad \text{(E-7)}$$

where

$$\sigma = \dot{m} C_p / U A$$

The last expression relates bypass flow fraction (fraction to preheater) to effectiveness and effectiveness in turn determines the temperature of the gas passing through the second orifice. From Equations (E-4) through (E-6)

$$T_3 = T_1 + \frac{\Delta T}{1 - \eta} \quad \text{(E-8)}$$

And thus bypass flow fraction is related to output signal pressure as in Equation (E-1)

$$P_2 = \left(\dot{m} / k_c \right) \sqrt{T_3}$$

The calculational procedure to obtain pressure as a function of source temperature is to find: q from Eq. (E-3), T from Eq. (E-2), T_3 from Eq. (E-8), and P_2 from Eq. (E-1). This procedure can be followed for each source temperature point which will give a relationship between P_2 and f.

TIME RESPONSE

The time response of the transducer can be estimated from an energy balance on the wall of the radiation heat exchanger and the gas therein. For the wall

$$m_w C_{pw} \frac{dT_w}{dt} = \sigma \overline{\epsilon A F} \left(T_s^4 - T_w^4 \right) - h_w A_w \left(T_w - T_H \right) \quad (E-9)$$

Linearizing and taking the Laplace transform gives

$$\delta T_w(s) = \left(\frac{1}{m_w C_{pw} S + 4\sigma \overline{\epsilon F} T_w^3 + h_w A_w} \right) 4\sigma \overline{\epsilon A F} T_s^3 \delta T_s(s) + h_w A_w \delta T_H(s) \quad (E-10)$$

The time constant is then

$$T_w \simeq \frac{m_w C_{pw}}{h_w A_w} = \left(\frac{\rho C_p x}{h} \right)_w \quad (E-11)$$

where T_w = time constant of wall

Similarly for the gas inside the tube

$$m_H C_{pH} \frac{dT_H}{dt} = h_w A_w \left(T_w - T_H \right) - 2\dot{m} C_p \left(T_H - T_2 \right) \quad (E-12)$$

or

$$\delta T_H(s) = \left(\frac{1}{m_H C_{pH} S + h_w A_w + 2\dot{m} C_{pH}} \right) h_w A_w \delta T_w(s) + 2\dot{m} C_p \delta T_s(s) \quad (E-13)$$

and the gas time constant is

$$T_H = \frac{m_H C_{pH}}{h_w A_w + 2\dot{m}_H C_{pH}} \quad (E-14)$$

Another consideration is the transport time through the heat exchanger and it is

$$T_D = \frac{m_H}{\dot{m}_H}$$

where m_H = mass of gas in exchanger. It is important for the residence time of the gas to be greater than the gas time constant and the wall time constant to be much greater than either the gas time constant or transport delay. This is because the wall response is the controlling factor and the gas is always in thermal equilibrium with it. For the time constant calculations the design parameters allow estimates to be made of masses and flow rates. For the heat transfer coefficient it can be estimated from a number of correlations which center around the expression

$$N_u = .023 \, R_e^{.8} \, P_r^{.4} \tag{E-15}$$

where

N_u = Nusselt Number, hD/k

R_e = Reynolds Number, DG/μ

P_r = Prandtl Number, $C_p \mu/k$

and the heat transfer coefficient is

$$h = N_u \, k/D \tag{E-16}$$

SENSITIVITY

For the sensitivity of the sensor, define sensitivity as

$$S = \frac{d\rho/\rho}{dq/q} \tag{E-17}$$

(Note that if sensitivity with respect to source temperature is desired $q \sim T_s^4$ and $dq/q = 4 \, dT_s/T_s$)

First consider pressure from Eq (E-1), then

$$dP_2 = \left(\dot{m}/K_c\right) d\left(\sqrt{T_3}\right) = \frac{1}{2}\left(\frac{\dot{m}}{K}\right)\frac{dT_3}{\sqrt{T_3}}$$

or

$$\frac{dP_2}{P_2} = \frac{\frac{1}{2}\left(\dot{m}/K_c\right) dT_3/\sqrt{T_3}}{\left(\dot{m}/K_c\right)\sqrt{T_3}} = \frac{1}{2}\frac{dT_3}{T_3} \tag{E-18}$$

But from Eq   (E-1) and (E-8)

$$T_3 = T_1 + \frac{\Delta T}{1-\eta} = T_1 + \frac{q/\dot{m}C_p}{1-\eta}$$ (E-19)

or

$$\frac{dT_3}{T_3} = \frac{dq/\dot{m}C_p(1-\eta)}{T_1 + q/\dot{m}C_p(1-\eta)}$$ (E-20)

Now let $\Delta T = \Delta T_m \, q/q_m$ (E-21)

to give

$$\frac{dT_3}{T_3} = \frac{\left(\frac{\Delta T_m}{1-\eta}\right)\frac{dq}{q_m}}{T_1 + \frac{\Delta T_m}{1-\eta}\cdot\frac{q}{q_m}}$$ (E-22)

or

$$\frac{dT_3}{T_3} = \frac{q/q_m}{\frac{T_1(1-\eta)}{\Delta T_m} + q/q_m}\cdot\frac{dq}{q}$$

sensitivity is

$$S = \frac{d\rho/\rho}{dq/q} = \frac{1}{2}\frac{q/q_m}{\frac{T_1(1-\eta)}{\Delta T_m} + q/q_m}$$

where ΔT_m = temperature rise across radiation heat
exchanger at maximum energy input, q_m

GAMMA HEATING

The method of calculating gamma heating for the pneumatic probe is
similar to that used for the foil thermocouple. The same assumptions
were made. The material used for gamma heating calculations was
aluminum.

ROCKETDYNE • A DIVISION OF NORTH AMERICAN AVIATION, INC.

THIS PAGE IS UNCLASSIFIED

ERRATA

NASA Technical Report NASA CR-54306

FEASIBILITY STUDY OF RADIATION PYROMETER
FOR NUCLEAR ROCKET APPLICATION (U)

By J. Perow, B.E. Harper, P.A. Kenzie
31 October 1964

Insert Pages F-1, F-2 and F-3 at end of Report

Page vi: Add the first order heading "Distribution" and corresponding
Page "F-1" after the sub-heading "Gamma Heating".

Issue Date 24 June 1965

THIS PAGE IS UNCLASSIFIED

REPORT DISTRIBUTION LIST FOR
CONTRACT NO. NAS 3-5213

NASA-Lewis Research Center
21000 Brookpark Road
Cleveland, Ohio 44135
Attention: John J. Fackler
            AD&E Procurement
            Section   (1)

NASA-Lewis Research Center
Scientific & Technical
Information Facility
Box 5700
Bethesda, Md.   (7)

NASA-Lewis Research Center
21000 Brookpark Road
Cleveland, Ohio 44135
Attention: Report Control
            Office   (1)

NASA-Lewis Research Center
21000 Brookpark Road
Cleveland, Ohio 44135
Attention: Mr. Warshawsky   (1)

NASA-Lewis Research Center
21000 Brookpark Road
Cleveland, Ohio 44135
Attention: John E. Reardon   (5)

NASA-Lewis Research Center
21000 Brookpark Road
Cleveland, Ohio 44135
Attention: Miles O. Dustin   (1)

NASA-Lewis Research Center
21000 Brookpark Road
Cleveland, Ohio 44135
Attention: Technology Utiliza-
            tion Office   (1)

NASA-Lewis Research Center
21000 Brookpark Road
Cleveland, Ohio 44135
Attention: Office of Reliability
            and Quality Assurance
                               (1)

National Aeronautics & Space
Administration
Washington, D. C. 20546
Attention: NPO/ John Morrissey
                               (1)

NASA-Ames Research Center
Moffett Field, California 94035
Attention: Library   (1)

NASA-Lewis Research Center
21000 Brookpark Road
Cleveland, Ohio 44135
Attention: Library   (2)

NASA-Lewis Research Center
21000 Brookpark Road
Cleveland, Ohio 44135
Attention: Lewis Technical Informa-
            tion Division   (1)

NASA-Lewis Research Center
21000 Brookpark Road
Cleveland, Ohio 44135
Attention: R. C. Johnson   (1)

NASA-Lewis Research Center
21000 Brookpark Road
Cleveland, Ohio 44135
Attention: Sol Weiss, NRTO   (2)

NASA-Lewis Research Center
21000 Brookpark Road
Cleveland, Ohio 44135
Attention: Adolph Lovoff, SNPO (1)

National Aeronautics & Space
Administration
Washington, D. C. 20546
Attention: NPO/F. C. Schwenk (1)

Los Alamos Scientific Laboratory
Los Alamos, New Mexico
Attention: Dr. Joseph Perry, Jr.
            (Group N4)   (1)

NASA-Flight Research Center
P. O. Box 273
Edwards, California 93523   (2)

NASA-Goddard Space Flight Center
Greenbelt, Maryland 20771
Attention: Library   (1)

NASA-Langley Research Center
Langley Station
Hampton, Virginia 23365
Attention: Library   (1)

NASA-Marshall Space Flight Center
Huntsville, Alabama 35812
Attention: Library   (1)

NASA - Lewis Research Center
21000 Brookpark Road
Cleveland, Ohio 44135
Attention: J. R. Agee   (1)

U. S. Atomic Energy Commission
Technical Information Service
Extension
P.O. Box 62
Oak Ridge, Tennessee   (3)

Aerojet General Corporation
P. O. Box 1947
Sacramento, California 95809
Attention: T. F. McGrath   (1)

Bell Aerosystems Co.
P.O. Box 1
Buffalo 5, New York
Attention: J.V. Robinson   (1)

Barnes Engineering Co.
30 Commerce Road
Stamford, Connecticut
Attention: Jack Axelrod   (1)

Advanced Technology Laboratories
369 Whisman Road
Mountain View, California
Attention: John Chambers   (1)

Jet Propulsion Laboratory
4800 Oak Grove Drive
Pasadena, California 91103
Attention: Library   (1)

NASA-Manned Spacecraft Center
Houston, Texas 77001
Attention: Library   (1)

NASA-Western Operations
150 Pico Blvd.
Santa Monica, California 90406
Attention: Library   (1)

U. S. Atomic Energy Commission
Technical Reports Library
Washington, D. C.   (3)

Westinghouse Astronuclear Laboratory
P. O. Box 10864
Pittsburgh 36, Pennsylvania
Attention: R. L. Ramp   (3)

Parametrics Inc.
221 Crescent Street
Waltham 54, Massachusetts
Attention: E. H. Carnevale   (1)

General Electric Co.
Nuclear Materials Propulsion Operation
P.O. Box 15132
Cincinnati, Ohio 45215
Attention: George Pomeroy

Bendix Research Division
Southfield, Michigan
Attention: D. J. Niehaus   (1)

Wright-Patterson Air Force Base
Dayton, Ohio
Attention: Harry Snowball,
            AFFDL (FDCL)   (2)

NASA-Lewis Research Center
21000 Brookpark Road
Cleveland, Ohio 44135
Attention: Adam S. Hintze   (1)